Available online at www.sciencedirect.com
ScienceDirect
Comput. Methods Appl. Mech. Engrg. 402 (2022) 115240
Computer methods in applied mechanics and engineering
www.elsevier.com/locate/cma

A posteriori error estimates for Biot system using a mixed discretization for flow

Mary F. Wheeler[a], Vivette Girault[b], Hanyu Li[a,*]

[a] Center for Subsurface Modeling, Oden Institute, The University of Texas at Austin, United States of America
[b] Sorbonne-Université, CNRS, Université de Paris, Laboratoire Jacques-Louis Lions (LJLL), F-75005 Paris, France

Available online 4 July 2022

Abstract

We first derive convergence and a priori stability, and next reliability and efficiency of a posteriori error indicators for a Biot poroelastic model coupled with an elastic model in $\mathbb{R}^3$, solved by a continuous Galerkin scheme (CG) for the displacement and a mixed finite element scheme for the flow. The coupled system is decoupled by a fixed stress splitting algorithm. The numerical implementation of the residual based error indicators is simple, even for the mixed discretization, but at the expense of two suboptimal bounds. The scheme is tested on two benchmark problems via several numerical experiments.

Keywords: Biot system; Fixed stress algorithm; Mixed discretization; Residual a posteriori error indicators; Reliability; Efficiency

1. Introduction

Coupled multiphase flow, geochemistry, and geomechanics models are receiving growing research interests for applications in unconventional reservoirs that include geological CO_2 sequestration, geothermal and recently hydrogen storage. These multiphysics and multiscale simulations are computationally expensive and require preservation of physics, chemistry and biology across spatial and temporal scales, such as local mass conservation for flow. In addition, these algorithms must be able to handle efficiently high performance computing, adaptive mesh refinement and highly nonlinear algebraic systems with rough coefficients. Additional computational issues include data extraction, optimization, uncertainty quantification and machine learning. Solving monolithically these multiphysics and multinumerics problems is often too costly computationally, and decoupling algorithms such as iterative coupling are frequently applied. The latter, such as fixed-stress split algorithm, were first introduced by [1–3]. Later a contractive property of the scheme was established by [4]. In the fixed-stress split algorithm, the flow problem is solved first, followed by the mechanics problem, and a constant mean total stress is assumed during the flow solver. Additional references on stability and a priori convergence of fixed stress iterative coupling can be found in [5], a recent common publication on residual a posteriori error estimates for a poroelastic model discretized by an Enriched Galerkin method for the flow equation.

This work is dedicated to Professor J. Tinsley Oden. The authors wish to thank Professor J. Tinsley Oden for his many scientific contributions in engineering, applied mathematics, and computational science. Specifically we

* Corresponding author.
E-mail address: lihanyu234@oden.utexas.edu (H. Li).

https://doi.org/10.1016/j.cma.2022.115240
0045-7825/

acknowledge Professors Tinsley Oden and Mark Ainsworth [6] for their seminal work in the introduction of mesh adaptivity based on a posteriori estimation for numerical solution of partial differential equations. Their work has motivated the results obtained in this paper. Here, we introduce a high fidelity approach for unconventional reservoirs that shows promise for modeling reservoir energy production, namely a posteriori error estimation for coupling multiphase and geomechanics. A posteriori error estimates are derived for the poromechanics Biot system solved with a fixed-stress split where a mixed finite element (MFE) approximation for the flow equation, and a conforming Galerkin (CG) approximation for the mechanics equation are employed respectively. An upper bound is derived for the error equation, distinguishing different error indicators, namely the fixed-stress algorithmic error, the time error, the flow error and the errors arising from the mechanics equation. The residual a posteriori error analysis of mixed methods has been a standing concern of many authors over a long period of time, but so far no fully satisfying solution has emerged. The reason is that, in mixed formulations, the residual error equation for the velocity is set into a space ($H(\text{div})$) with very little regularity. Authors have tried to mitigate this deficiency by introducing a saturation assumption or by proposing error indicators computed by solving local problems as in [7,8], but these are too costly for many industrial applications. In the present work, the residual a posteriori error analysis is a simplified version of that applied to mixed discretizations by [9,10]. Here for deriving bounds a Helmholtz decomposition is utilized, but it does not involve computation of curls and tangential components as in [9,10]. No local problems need to solved but only a simple interpolation of the pressure is required at the vertices. These theoretical results are for general mixed method spaces provided such interpolation result is satisfied. The price to pay for this simplification is the loss of optimality of two velocity error indicators. This result is demonstrated by numerical experiments with RT_0 finite element spaces on hexahedra.

1.1. Notation

In this work, we shall use the following notation written in three dimensions in a bounded connected open set $\Omega \subset \mathbb{R}^3$. The scalar product of $L^2(\Omega)$ is denoted by $(\cdot,\cdot)_\Omega$

$$\forall f, g \in L^2(\Omega), \quad (f,g)_\Omega = \int_\Omega f(\boldsymbol{x}) g(\boldsymbol{x}) d\boldsymbol{x},$$

and the index Ω is omitted when the domain of integration is clear from the context. For any non-negative integer m, the classical Sobolev space $H^m(\Omega)$ is defined by (cf. [11] or [12]),

$$H^m(\Omega) = \{v \in L^2(\Omega) : \partial^k v \in L^2(\Omega) \,\forall\, |k| \le m\},$$

where

$$\partial^k v = \frac{\partial^{|k|} v}{\partial x_1^{k_1} \partial x_2^{k_2} \partial x_3^{k_3}},$$

equipped with the following seminorm and norm for which it is a Hilbert space:

$$|v|_{H^m(\Omega)} = \left[\sum_{|k|=m} \int_\Omega |\partial^k v|^2 \, d\boldsymbol{x} \right]^{\frac{1}{2}}, \quad \|v\|_{H^m(\Omega)} = \left[\sum_{0 \le |k| \le m} |v|^2_{H^k(\Omega)} \right]^{\frac{1}{2}}.$$

This definition is extended to any real number $s = m + s'$ for an integer $m \ge 0$ and $0 < s' < 1$ by defining in dimension d the fractional semi-norm and norm, see [13,14],

$$|v|_{H^s(\Omega)} = \left(\sum_{|k|=m} \int_\Omega \int_\Omega \frac{|\partial^k v(\boldsymbol{x}) - \partial^k v(\boldsymbol{y})|^2}{|\boldsymbol{x} - \boldsymbol{y}|^{d+2s'}} \, d\boldsymbol{x} \, d\boldsymbol{y} \right)^{\frac{1}{2}}, \quad \|v\|_{H^s(\Omega)} = \left(\|v\|^2_{H^m(\Omega)} + |v|^2_{H^s(\Omega)} \right)^{\frac{1}{2}}.$$

These fractional order spaces are often used for traces. The following trace property holds in a domain Ω with a Lipschitz continuous boundary $\partial\Omega$: If v belongs to $H^s(\Omega)$ for some $s \in]\frac{1}{2}, 1]$, then its trace on $\partial\Omega$ belongs to $H^{s-\frac{1}{2}}(\partial\Omega)$ and there exists a constant C_s such that

$$\forall v \in H^s(\Omega), \; \|v\|_{H^{s-\frac{1}{2}}(\partial\Omega)} \le C_s \|v\|_{H^s(\Omega)}. \tag{1.1}$$

In particular, $H^{\frac{1}{2}}(\partial\Omega)$ is the trace space of $H^1(\Omega)$, with norm

$$|v|_{H^{\frac{1}{2}}(\Gamma)} = \Big(\int_\Gamma\int_\Gamma \frac{|v(\boldsymbol{x}) - v(\boldsymbol{y})|^2}{|\boldsymbol{x}-\boldsymbol{y}|^d} d\boldsymbol{x}\, d\boldsymbol{y}\Big)^{\frac{1}{2}},$$

and $H^{-\frac{1}{2}}(\partial\Omega)$ is the dual space of $H^{\frac{1}{2}}(\partial\Omega)$. Finally, if Γ is a subset of $\partial\Omega$ with positive measure, $|\Gamma| > 0$, we say that a function g in $H^{\frac{1}{2}}(\Gamma)$ belongs to $H^{\frac{1}{2}}_{00}(\Gamma)$ if its extension by zero to $\partial\Omega$ belongs to $H^{\frac{1}{2}}(\partial\Omega)$. It is a proper subspace of $H^{\frac{1}{2}}(\Gamma)$, and is normed by

$$\|v\|_{H^{\frac{1}{2}}_{00}(\Gamma)} = \Big(|v|^2_{H^{\frac{1}{2}}(\Gamma)} + \int_\Gamma |v(\boldsymbol{x})|^2 \frac{d\boldsymbol{x}}{d(\boldsymbol{x},\Gamma)}\Big)^{\frac{1}{2}}, \tag{1.2}$$

where $d(\boldsymbol{x},\Gamma)$ denotes the distance to Γ.

The space $H(\mathrm{div},\Omega)$ is the Hilbert space

$$H(\mathrm{div},\Omega) = \{\boldsymbol{v} \in L^2(\Omega)^d \,:\, \mathrm{div}\,\boldsymbol{v} \in L^2(\Omega)\}, \tag{1.3}$$

equipped with the graph norm. Let $\boldsymbol{n}_\Omega$ denote the exterior unit normal vector to $\partial\Omega$. The normal trace $\boldsymbol{v}\cdot\boldsymbol{n}_\Omega$ of a function $\boldsymbol{v}$ of $H(\mathrm{div},\Omega)$ on $\partial\Omega$ belongs to $H^{-\frac{1}{2}}(\partial\Omega)$, the dual space of $H^{\frac{1}{2}}(\partial\Omega)$, see for instance [15]. This allows to define the subspace

$$H_0(\mathrm{div},\Omega) = \{\boldsymbol{v} \in H(\mathrm{div},\Omega) \,:\, \boldsymbol{v}\cdot\boldsymbol{n}_\Omega = 0 \text{ on } \partial\Omega\}. \tag{1.4}$$

Note that if $\boldsymbol{v}$ is in $H(\mathrm{div},\Omega)$ and if Γ is a portion of $\partial\Omega$ that is not a closed surface, then the restriction of $\boldsymbol{v}\cdot\boldsymbol{n}_\Omega$ to Γ belongs to the dual of $H^{\frac{1}{2}}_{00}(\Gamma)$.

We also recall Korn's and Poincaré's inequalities both valid for all functions $\boldsymbol{v}$ in $H^1(\Omega)^3$ that vanish on a portion Γ of $\partial\Omega$ with positive measure:

$$|\boldsymbol{v}|_{H^1(\Omega)} \le \mathcal{K}\|\boldsymbol{\varepsilon}(\boldsymbol{v})\|_{L^2(\Omega)}, \tag{1.5}$$

$$\|v\|_{L^2(\Omega)} \le \mathcal{P}|v|_{H^1(\Omega)}, \tag{1.6}$$

where $\boldsymbol{\varepsilon}(\boldsymbol{v})$ is the strain tensor, and $\mathcal{K}$ and $\mathcal{P}$ are constants depending only on Ω and Γ. We also recall a trace inequality on the complement of Γ on $\partial\Omega$, say $\tilde{\Gamma}$, assuming that $\tilde{\Gamma}$ has also positive measure:

$$\|v\|_{H^{\frac{1}{2}}_{00}(\tilde{\Gamma})} \le C_N |v|_{H^1(\Omega)}. \tag{1.7}$$

To understand this last inequality, recall that if v in $H^1(\Omega)$ vanishes on Γ, then its trace on $\tilde{\Gamma}$ belongs to $H^{\frac{1}{2}}_{00}(\tilde{\Gamma})$.

As usual, for handling time-dependent problems, it is convenient to consider measurable functions defined on a time interval $]a,b[$ with values in a functional space, say X (cf. [13]). More precisely, let $\|\cdot\|_X$ denote the norm of X; then for any number r, $1 \le r \le \infty$, we define

$$L^r(a,b;X) = \{f \text{ measurable in }]a,b[: \int_a^b \|f(t)\|_X^r dt < \infty\},$$

equipped with the norm

$$\|f\|_{L^r(a,b;X)} = \Big(\int_a^b \|f(t)\|_X^r dt\Big)^{\frac{1}{r}},$$

with the usual modification if $r = \infty$. It is a Banach space if X is a Banach space, and for $r = 2$, it is a Hilbert space if X is a Hilbert space. Derivatives with respect to time are denoted by ∂_t and we define for instance

$$H^1(a,b;X) = \{f \in L^2(a,b;X) \,:\, \partial_t f \in L^2(a,b;X)\}.$$

2. Domain and model formulations

Let Ω be a bounded, connected, Lipschitz domain in $\mathbb{R}^3$. We are interested in the situation where a poro-elastic model holds in a connected subset Ω_1 of Ω (the *pay-zone*), completely embedded into Ω, while an elastic model holds in Ω_2 (the *nonpay-zone*) where

$$\Omega_2 = \Omega \setminus \overline{\Omega_1}.$$

Let Γ_{12} denote the boundary of Ω_1, assumed to be Lipschitz, and let $\boldsymbol{n}_{12}$ be the unit normal on Γ_{12} exterior to Ω_1. In the examples we have in mind, Ω_1 is much smaller than Ω. This work extends readily to more general configurations, but for simplicity, we focus on this situation. Let the boundary of Ω, $\partial\Omega$, be partitioned into two disjoint open regions not necessarily connected, but with a finite number of connected components, each with Lipschitz-continuous boundaries,

$$\overline{\partial\Omega} = \overline{\Gamma_D} \cup \overline{\Gamma_N}.$$

To simplify, we assume that the measure of Γ_D is positive: $|\Gamma_D| > 0$.

Let $\boldsymbol{\sigma}$ be the effective linear elastic stress tensor,

$$\boldsymbol{\sigma}(\boldsymbol{u}) = 2G\boldsymbol{\varepsilon}(\boldsymbol{u}) + \lambda(\nabla\cdot\boldsymbol{u})\boldsymbol{I}, \tag{2.1}$$

where $\boldsymbol{\varepsilon}(\boldsymbol{u}) = \frac{1}{2}\big(\nabla\,\boldsymbol{u} + \nabla^t\boldsymbol{u}\big)$ is the symmetric gradient tensor, $\boldsymbol{I}$ the identity tensor, and $\lambda > 0$ and $G > 0$ are the Lamé coefficients. Let $\boldsymbol{\sigma}^{\text{por}}$ be the linear poro-elastic stress tensor

$$\boldsymbol{\sigma}^{\text{por}}(\boldsymbol{u}, p) = \boldsymbol{\sigma}(\boldsymbol{u}) - \alpha\, p\,\boldsymbol{I}, \tag{2.2}$$

where $\alpha > 0$ is the Biot–Willis coefficient. Let $\boldsymbol{f}$ be the body force in Ω. In the nonpay-zone, i.e., a.e. in $\Omega_2\times]0,T[$, the governing equations for the displacement $\boldsymbol{u}$ are those of linear elasticity. In the pay-zone Ω_1, the equations are those of Biot's consolidation model for a linear elastic, homogeneous, isotropic, porous solid saturated with a slightly compressible single-phase fluid. The unknowns are the solid's displacement $\boldsymbol{u}$ and the fluid's pressure p. This model is based on a *quasi-static* assumption, namely it assumes that the material deformation is much slower than the flow rate, and hence the second time derivative of the displacement (i.e., the acceleration) is zero. After linearization and simplifications, it leads to the following system of equations in $\Omega\times]0,T[$,

$$\begin{aligned}
-\nabla\cdot(\lambda(\nabla\cdot\boldsymbol{u})\boldsymbol{I} + 2G\boldsymbol{\varepsilon}(\boldsymbol{u}) - \alpha p\boldsymbol{I}) &= \boldsymbol{f} && \text{a.e. in } \Omega_1\times]0,T[,\\
-\nabla\cdot(\lambda(\nabla\cdot\boldsymbol{u})\boldsymbol{I} + 2G\boldsymbol{\varepsilon}(\boldsymbol{u})) &= \boldsymbol{f} && \text{a.e. in } \Omega_2\times]0,T[,\\
\partial_t\left(\frac{1}{M}p + \alpha\nabla\cdot\boldsymbol{u}\right) - \frac{1}{\mu_f}\nabla\cdot\big(\boldsymbol{\kappa}(\nabla p - \rho g\nabla\eta)\big) &= q && \text{a.e. in } \Omega_1\times]0,T[,\\
-\frac{1}{\mu_f}\boldsymbol{\kappa}(\nabla p - \rho g\nabla\eta)\cdot\boldsymbol{n}_{12} &= 0 && \text{a.e. on } \partial\Omega_1\times]0,T[,\\
[\boldsymbol{u}] &= \boldsymbol{0} && \text{a.e. on } \partial\Omega_1\times]0,T[,\\
[\boldsymbol{\sigma}(\boldsymbol{u})]\boldsymbol{n}_{12} &= \alpha\, p\,\boldsymbol{n}_{12} && \text{a.e. on } \partial\Omega_1\times]0,T[,\\
\boldsymbol{u} &= \boldsymbol{0} && \text{a.e. on } \Gamma_D\times]0,T[,\\
\boldsymbol{\sigma}\boldsymbol{n}_\Omega &= \boldsymbol{t}_N && \text{a.e. on } \Gamma_N\times]0,T[,\\
p(0) &= p_0 && \text{a.e. in } \Omega_1,
\end{aligned} \tag{2.3}$$

where $M > 0$ is the Biot modulus, μ_f the fluid's viscosity, $\boldsymbol{\kappa}$ the permeability tensor, g the gravity constant, ρ the reference density, η a signed distance in the vertical direction, q a given volumetric fluid source or sink term, and $\boldsymbol{t}_N$ a given normal traction.

The spaces for the primal formulation are

$$H^1_{0D}(\Omega) = \{v \in H^1(\Omega)\,:\, v|_{\Gamma_D} = 0\}, \quad \boldsymbol{W} = H^1_{0D}(\Omega)^d. \tag{2.4}$$

The equivalent primal variational formulation is:
Find $\boldsymbol{u} \in L^\infty(0,T;\boldsymbol{W})$ and $p \in L^\infty(0,T;L^2(\Omega_1)) \cap L^2(0,T;H^1(\Omega_1))$ solving a.e. in $]0,T[$

$$2G(\boldsymbol{\epsilon}(\boldsymbol{u}), \boldsymbol{\epsilon}(\boldsymbol{v}))_\Omega + \lambda(\nabla\cdot\boldsymbol{u}, \nabla\cdot\boldsymbol{v})_\Omega = (\boldsymbol{f}, \boldsymbol{v})_\Omega + \alpha(p, \nabla\cdot\boldsymbol{v})_{\Omega_1} + \langle\boldsymbol{t}_N, \boldsymbol{v}\rangle_{\Gamma_N}, \quad \forall\boldsymbol{v}\in\boldsymbol{W}, \tag{2.5}$$

$$\left(\partial_t\left(\frac{1}{M}p + \alpha\nabla\cdot\boldsymbol{u}\right), \theta\right)_{\Omega_1} + \frac{1}{\mu_f}\big(\boldsymbol{\kappa}(\nabla p - \rho\, g\nabla\eta), \nabla\theta\big)_{\Omega_1} = (q,\theta)_{\Omega_1}, \quad \forall\theta\in H^1(\Omega_1), \tag{2.6}$$

with the initial condition

$$p(0) = p_0 \quad \text{a.e. in } \Omega_1. \tag{2.7}$$

The assumptions on the data are $\boldsymbol{f} \in H^1(0, T; L^2(\Omega)^d)$, $q \in L^2(\Omega_1 \times]0, T[)$, $\boldsymbol{t}_N \in H^1(0, T; (H_{00}^{\frac{1}{2}}(\Gamma_N)^d)')$. It can be shown that, under these assumptions, problem (2.5)–(2.7) has a unique solution, see for instance [5].

2.1. Mixed variational formulation for the flow equation

Here, we use a mixed formulation for the flow because it leads to locally conservative discrete schemes.

For the mixed formulation, we introduce an auxiliary reservoir velocity z defined by

$$z = -\frac{\boldsymbol{\kappa}}{\mu_f}(\nabla p - \rho g \nabla \eta); \tag{2.8}$$

the space for the reservoir velocity is

$$\boldsymbol{Z} = \{\boldsymbol{q} \in H(\text{div}, \Omega_1) : \boldsymbol{q} \cdot \boldsymbol{n}_{12} = 0 \text{ on } \Gamma_{12}\} = H_0(\text{div}, \Omega_1). \tag{2.9}$$

With the same data regularity, the mixed variational formulation reads: Find $\boldsymbol{u} \in L^\infty(0, T; \boldsymbol{W})$, $p \in L^\infty(0, T; L^2(\Omega_1))$, and $z \in L^2(0, T; \boldsymbol{Z})$, such that a.e. in $]0, T[$,

$$\forall \boldsymbol{v} \in \boldsymbol{W},\ 2G\big(\boldsymbol{\varepsilon}(\boldsymbol{u}), \boldsymbol{\varepsilon}(\boldsymbol{v})\big)_\Omega + \lambda\big(\nabla \cdot \boldsymbol{u}, \nabla \cdot \boldsymbol{v}\big)_\Omega - \alpha\big(p, \nabla \cdot \boldsymbol{v}\big)_{\Omega_1} = \big(\boldsymbol{f}, \boldsymbol{v}\big)_\Omega + \langle \boldsymbol{t}_N, \boldsymbol{v}\rangle_{\Gamma_N}, \tag{2.10}$$

$$\forall \theta \in L^2(\Omega),\ \Big(\partial_t\big(\frac{1}{M}p + \alpha \nabla \cdot \boldsymbol{u}\big), \theta\Big)_{\Omega_1} + \big(\nabla \cdot z, \theta\big)_{\Omega_1} = \big(q, \theta\big)_{\Omega_1}, \tag{2.11}$$

$$\forall \boldsymbol{\zeta} \in \boldsymbol{Z},\ \big(\mu_f \boldsymbol{\kappa}^{-1} z, \boldsymbol{\zeta}\big)_{\Omega_1} = (p, \nabla \cdot \boldsymbol{\zeta})_{\Omega_1} + \big(\rho g \nabla \eta, \boldsymbol{\zeta}\big)_{\Omega_1}, \tag{2.12}$$

subject to the initial condition (2.7):

$$p(0) = p_0 \text{ a.e. in } \Omega_1.$$

The following equivalence result holds with the same assumptions on the data:

Proposition 1. *Let $\boldsymbol{f} \in H^1(0, T; L^2(\Omega)^d)$, $q \in L^2(\Omega_1 \times]0, T[)$, $\boldsymbol{t}_N \in H^1(0, T; (H_{00}^{\frac{1}{2}}(\Gamma_N)^d)')$. Suppose that problem (2.3) has a solution $\boldsymbol{u} \in L^\infty(0, T; \boldsymbol{W})$ and $p \in L^\infty(0, T; H^1(\Omega_1))$ such that*

$$\partial_t\big(\frac{1}{M}p + \alpha \nabla \cdot \boldsymbol{u}\big) \in L^2(\Omega \times]0, T[). \tag{2.13}$$

Then by defining z through (2.8), this solution also satisfies (2.10)–(2.12), and (2.7). Conversely, any solution of the mixed formulation (2.10)–(2.7) and *(2.12) also solves problem (2.3).*

Then by equivalence, problem (2.10)–(2.12), (2.7) has also a unique solution. In the sequel, we suppose that the assumptions of Proposition 1 hold.

3. Discretization and algorithm

We propose a finite element discretization of problem (2.10)–(2.12), (2.7), split by a fixed stress algorithm to reduce the memory load in the pay-zone.

3.1. Meshes and discrete spaces

From now on, we assume that the domain is a polygon or polyhedron according to the dimension d, and such that each part Γ_D and Γ_N has polygonal boundaries, when $d = 3$. For $h > 0$, let $\mathcal{T}_h$ be a regular family of conforming simplicial meshes of the domain $\overline{\Omega}$, with h the maximum element diameter. The family of meshes is regular in the sense of Ciarlet [16]: there exists a constant $\sigma > 0$, independent of h, such that

$$\frac{h_E}{\varrho_E} \le \sigma, \quad \forall E \in \mathcal{T}_h, \tag{3.1}$$

where h_E is the diameter of E and ϱ_E the diameter of the ball inscribed in E. We assume that

$$\mathcal{T}_h = \mathcal{T}_h^1 \cup \mathcal{T}_h^2,$$

where $\mathcal{T}_h^1$ (resp. $\mathcal{T}_h^2$) is a conforming simplicial mesh of Ω_1 (resp. Ω_2). We also assume that the trace of $\mathcal{T}_h^2$ on $\partial\Omega$ meshes completely Γ_D and Γ_N. Let $\mathcal{E}_h$ (resp. $\mathcal{E}_h^\partial$) denote the set of interior (resp. boundary) faces of $\mathcal{T}_h$. For any e in $\mathcal{E}_h$, ω_e denotes the union of the elements adjacent to e. We suppose that

$$\mathcal{E}_h^\partial = \mathcal{E}_h^{D,\partial} \cup \mathcal{E}_h^{N,\partial},$$

where $\mathcal{E}_h^{D,\partial}$ (resp. $\mathcal{E}_h^{N,\partial}$) is the set of all faces lying on Γ_D (resp. Γ_N). The set of faces interior to Ω_1 (resp. Ω_2) is $\mathcal{E}_h^1$ (resp. $\mathcal{E}_h^2$). Finally, the set of faces on Γ_{12} is $\mathcal{E}_h^{12}$. A unit normal vector $\boldsymbol{n}_e$ is attributed to each e in $\mathcal{E}_h$ and $\mathcal{E}_h^\partial$; its direction can be freely chosen. Here, the following rule is applied: if $e \in \mathcal{E}_h^\partial$, then $\boldsymbol{n}_e = \boldsymbol{n}_\Omega$, the exterior normal to Ω; if e is in $\mathcal{E}_h^1$ or $\mathcal{E}_h^2$, then $\boldsymbol{n}_e$ points from E_i to E_j, where E_i and E_j are the two elements of $\mathcal{T}_h$ adjacent to e and the number of E_i is smaller than that of E_j. Finally, if $e \in \mathcal{E}_h^{12}$, then $\boldsymbol{n}_e = \boldsymbol{n}_{12}$, the outward normal to Ω_1. The jumps and averages of any function f on $e \in \mathcal{E}_h$ (smooth enough to have a trace) are defined by

$$[f(\boldsymbol{x})]_e := f(\boldsymbol{x})|_{E_i} - f(\boldsymbol{x})|_{E_j}, \quad \text{when } \boldsymbol{n}_e \text{ points from } E_i \text{ to } E_j,$$

$$\{f(\boldsymbol{x})\}_e := \frac{1}{2}\big(f(\boldsymbol{x})|_{E_i} + f(\boldsymbol{x})|_{E_j}\big).$$

When $e \in \mathcal{E}_h^\partial$, the jump and average coincide with the trace on e.

Let $k \geq 0$ and $m \geq 1$ be two integers, $n = \max(1, k)$. On this mesh, we introduce first the following standard finite element spaces:

$$\boldsymbol{W}_h := \{\boldsymbol{v} \in \boldsymbol{W} \,:\, \boldsymbol{v}|_E \in \mathbb{P}_m(E)^d, \forall E \in \mathcal{T}_h\}, \tag{3.2}$$

$$\Theta_h = \{\theta \in H^1(\Omega_1) \,:\, \theta|_E \in \mathbb{P}_n(E), \forall E \in \mathcal{T}_h^1\}. \tag{3.3}$$

Next, we define the usual mixed finite element spaces such as for instance,

$$M_h = \{q \in L^2(\Omega_1) \,:\, q|_E \in \mathbb{P}_k(E), \forall E \in \mathcal{T}_h^1\}, \tag{3.4}$$

$$\boldsymbol{Z}_h = \{z \in \boldsymbol{Z} \,:\, z|_E \in \mathrm{RT}_k(E), \forall E \in \mathcal{T}_h^1\}, \tag{3.5}$$

where $\mathrm{RT}_k(E)$ is the Raviart–Thomas finite element space of order k (i.e., incomplete degree $k+1$). Recall that the pair $(\boldsymbol{Z}_h, M_h)$ satisfies the compatibility condition, see for instance [17],

$$\nabla \cdot \boldsymbol{Z}_h \subset M_h. \tag{3.6}$$

The displacement will be discretized in $\boldsymbol{W}_h$, the pressure in M_h, and the velocity in $\boldsymbol{Z}_h$.

In the sequel, we shall use the L^2 projection operator P_h from $L^2(\Omega)$ onto M_h in each element E, and the approximation operators of Scott & Zhang (see [18]),

$$S_h \in \mathcal{L}(\boldsymbol{W}, \boldsymbol{W}_h), \quad \tilde{S}_h \in \mathcal{L}(H^1(\Omega_1), \Theta_h). \tag{3.7}$$

Considering the degree of the polynomial functions in $\boldsymbol{W}_h$ and M_h, these interpolants have the following quasi-local optimal approximation errors:

$$\forall E \in \mathcal{T}_h, \forall \boldsymbol{v} \in H^s(\Omega)^d\,,\ |\boldsymbol{v} - S_h(\boldsymbol{v})|_{H^j(E)} \leq C\, h_E^{s-j} |\boldsymbol{v}|_{H^s(\Delta_E)}\,,\ 1 \leq s \leq m+1,\ 0 \leq j \leq s, \tag{3.8}$$

$$\forall E \in \mathcal{T}_h^1, \forall q \in H^s(\Omega)\,,\ |q - \tilde{S}_h(q)|_{H^j(E)} \leq C\, h_E^{s-j} |q|_{H^s(\Delta_E)}\,,\ 1 \leq s \leq k+1,\ 0 \leq j \leq s, \tag{3.9}$$

with constants C independent of E and h_E, where Δ_E is a small patch of elements including E containing the values used in computing the approximation.

Regarding approximation in time, the interval $[0, T]$ is divided into N equal subintervals with length Δt and endpoints $t_n = n\Delta t$. The choice of equal time steps is a simplification; the material below extends readily to variable time steps. The data is assumed to be continuous in time, and we set a.e. in Ω

$$\boldsymbol{f}^n(\boldsymbol{x}) = \boldsymbol{f}(\boldsymbol{x}, t_n),\ q^n(\boldsymbol{x}) = q(\boldsymbol{x}, t_n),\ \boldsymbol{t}_N^n(\boldsymbol{x}) = \boldsymbol{t}_N(\boldsymbol{x}, t_n). \tag{3.10}$$

Strictly speaking, the last equality should be understood in a dual sense.

3.2. Fixed stress algorithm

With the above discrete spaces, problem (2.10)–(2.12), (2.7) is discretized and split as follows by the fixed stress algorithm. Let K_b be the bulk modulus,

$$K_b = \lambda + \frac{2}{3}G, \tag{3.11}$$

and denote by n, $0 \le n \le N$, the time step, and for each n, by ℓ the iteration counter of the algorithm.
Initialization. Set

$$p_h^0 = \tilde{S}_h(p_0). \tag{3.12}$$

Compute $\boldsymbol{u}_h^0 \in \boldsymbol{W}_h$, $z_h^0 \in \boldsymbol{Z}_h$, and $\bar{\sigma}_h^0$ by solving

$$\forall \boldsymbol{v}_h \in \boldsymbol{W}_h\,,\ 2G\big(\boldsymbol{\varepsilon}(\boldsymbol{u}_h^0), \boldsymbol{\varepsilon}(\boldsymbol{v}_h)\big)_\Omega + \lambda\big(\nabla\cdot\boldsymbol{u}_h^0, \nabla\cdot\boldsymbol{v}_h\big)_\Omega = \alpha\left(p_h^0, \nabla\cdot\boldsymbol{v}_h\right)_{\Omega_1} + (\boldsymbol{f}^0, \boldsymbol{v}_h)_\Omega + \langle \boldsymbol{t}_N^0, \boldsymbol{v}_h\rangle_{\Gamma_N}, \tag{3.13}$$

$$\forall \boldsymbol{\zeta}_h \in \boldsymbol{Z}_h\,,\ \mu_f\big(\boldsymbol{\kappa}^{-1} z_h^0, \boldsymbol{\zeta}_h\big)_{\Omega_1} = \big(p_h^0, \nabla\cdot\boldsymbol{\zeta}_h\big)_{\Omega_1} + \big(\rho g \nabla\eta, \boldsymbol{\zeta}_h\big)_{\Omega_1} \tag{3.14}$$

and by setting

$$\bar{\sigma}_h^0 = K_b \nabla\cdot\boldsymbol{u}_h^0 - \alpha\, p_h^0. \tag{3.15}$$

Time step $n \ge 1$.

1. Set $p_h^{n,0} = p_h^{n-1}$, $\boldsymbol{u}_h^{n,0} = \boldsymbol{u}_h^{n-1}$, $z_h^{n,0} = z_h^{n-1}$ and $\bar{\sigma}_h^{n,0} = \bar{\sigma}_h^{n-1}$.
2. For $\ell \ge 1$, compute

   (a) the pair $\big(p_h^{n,\ell}, z_h^{n,\ell}\big) \in M_h \times \boldsymbol{Z}_h$ by solving for all $\big(\theta_h, \boldsymbol{\zeta}_h\big) \in M_h \times \boldsymbol{Z}_h$,

$$\Big(\frac{1}{M} + \frac{\alpha^2}{K_b}\Big)\frac{1}{\Delta t}\big(p_h^{n,\ell} - p_h^{n-1}, \theta_h\big)_{\Omega_1} + \big(\nabla\cdot z_h^{n,\ell}, \theta_h\big)_{\Omega_1} = -\frac{\alpha}{K_b}\frac{1}{\Delta t}\big(\bar{\sigma}_h^{n,l-1} - \bar{\sigma}_h^{n-1}, \theta_h\big)_{\Omega_1} + (q^n, \theta_h)_{\Omega_1}, \tag{3.16}$$

$$\mu_f\big(\boldsymbol{\kappa}^{-1} z_h^{n,\ell}, \boldsymbol{\zeta}_h\big)_{\Omega_1} = \big(p_h^{n,\ell}, \nabla\cdot\boldsymbol{\zeta}_h\big)_{\Omega_1} + \big(\rho g \nabla\eta, \boldsymbol{\zeta}_h\big)_{\Omega_1}, \tag{3.17}$$

   (b) the predictor of the difference in fluid content δ_ϕ^p by

$$\delta_\phi^p := \Big(\frac{1}{M} + \frac{\alpha^2}{K_b}\Big)\big(p_h^{n,\ell} - p_h^{n,\ell-1}\big), \tag{3.18}$$

   (c) $\boldsymbol{u}_h^{n,\ell} \in \boldsymbol{W}_h$ by solving for all $\boldsymbol{v}_h \in \boldsymbol{W}_h$,

$$2G\big(\boldsymbol{\varepsilon}(\boldsymbol{u}_h^{n,\ell}), \boldsymbol{\varepsilon}(\boldsymbol{v}_h)\big)_\Omega + \lambda\big(\nabla\cdot\boldsymbol{u}_h^{n,\ell}, \nabla\cdot\boldsymbol{v}_h\big)_\Omega = \alpha\big(p_h^{n,\ell}, \nabla\cdot\boldsymbol{v}_h\big)_{\Omega_1} + \big(\boldsymbol{f}^n, \boldsymbol{v}_h\big)_\Omega + \langle \boldsymbol{t}_N^n, \boldsymbol{v}_h\rangle_{\Gamma_N}, \tag{3.19}$$

   (d) $\bar{\sigma}_h^{n,\ell}$ by

$$\bar{\sigma}_h^{n,\ell} = K_b \nabla\cdot\boldsymbol{u}_h^{n,\ell} - \alpha p_h^{n,\ell}, \tag{3.20}$$

   (e) the corrector of the difference in fluid content δ_ϕ^c by

$$\delta_\phi^c := \alpha\nabla\cdot\big(\boldsymbol{u}_h^{n,\ell} - \boldsymbol{u}_h^{n,\ell-1}\big) + \frac{1}{M}\big(p_h^{n,\ell} - p_h^{n,\ell-1}\big). \tag{3.21}$$

   If

$$\left\|\delta_\phi^c - \delta_\phi^p\right\|_{L^\infty(\Omega_1)} > \varepsilon,$$

   set $\ell \leftarrow \ell + 1$ and return to (a);
   else, set

$$\ell_n := \ell, \quad p_h^n := p_h^{n,\ell_n}, \quad \boldsymbol{u}_h^n := \boldsymbol{u}_h^{n,\ell_n}, \quad z_h^n := z_h^{n,\ell_n}, \quad \bar{\sigma}_h^n := \bar{\sigma}_h^{n,\ell_n}, \tag{3.22}$$

   march in time $n \leftarrow n + 1$ and return to 1.

Note that at initial time, the given initial pressure is approximated by $\tilde{S}_h$, thus violating the space compatibility condition (3.6), but this property is not used at this stage since p_h^0 is known.

Owing to Korn's inequality (1.5), (3.13) and (3.19) are uniquely solvable. Clearly, (3.14) is uniquely solvable. The solvability of (3.16) and (3.17) for each $n \geq 1$ and $\ell \geq 1$ is given by the following proposition.

Proposition 2. *The system (3.16)–(3.17) has one and only one solution for each $n \geq 1$ and $\ell \geq 1$.*

Proof. Since (3.16)–(3.17) is a finite-dimensional linear square system it suffices to prove that if $p_h^{n-1} = q^n = \bar{\sigma}_h^{n,\ell-1} = \bar{\sigma}_h^{n-1} = 0$ and $\rho g \nabla \eta = \mathbf{0}$, then $p_h^{n,\ell} = 0$ and $z_h^{n,\ell} = \mathbf{0}$. Now, by testing (3.16) with $\theta_h = p_h^{n,\ell}$ and (3.17) with $\boldsymbol{\zeta} = z_h^{n,\ell}$, we obtain

$$\Big(\frac{1}{M} + \frac{\alpha^2}{K_b}\Big)\frac{1}{\Delta t}\|p_h^{n,\ell}\|^2_{L^2(\Omega_1)} + \mu_f\|\boldsymbol{\kappa}^{-\frac{1}{2}} z_h^{n,\ell}\|^2_{L^2(\Omega_1)} = 0,$$

whence $p_h^{n,\ell} = 0$ and $z_h^{n,\ell} = \mathbf{0}$. □

Therefore, as long as the iterative procedure with superscript ℓ converges, the algorithm (3.12)–(3.22) generates one and only one discrete sequence p_h^n, $\boldsymbol{u}_h^n$, z_h^n, for all time steps n.

The following theorem establishes convergence of the above algorithm with respect to ℓ. Beforehand, we define

$$\beta = \frac{1}{M\alpha^2} + \frac{1}{K_b}, \tag{3.23}$$

and denote the difference between two consecutive iterates by δ,

$$\forall \ell \geq 1, \quad \delta\xi^\ell = \xi^\ell - \xi^{\ell-1}. \tag{3.24}$$

Note that

$$\beta K_b > 1. \tag{3.25}$$

Note also that any vector valued function $\boldsymbol{v} : \mathbb{R}^3 \to \mathbb{R}^3$ satisfies formally

$$|\nabla \cdot \boldsymbol{v}|^2 \leq 3\boldsymbol{\varepsilon}(\boldsymbol{v}) : \boldsymbol{\varepsilon}(\boldsymbol{v}).$$

Theorem 1. *The algorithm (3.12)–(3.22) converges geometrically as ℓ tends to infinity.*

Proof. Following the ideas of Mikelic & Wheeler [4], it can be shown that

$$\begin{aligned}\|\delta\bar{\sigma}_h^{n,\ell}\|^2_{L^2(\Omega_1)} &+ \frac{2\Delta t}{\beta}\mu_f\|\boldsymbol{\kappa}^{-\frac{1}{2}}\delta z_h^{n,\ell}\|^2_{L^2(\Omega_1)} + 4G\Big(\frac{1}{3}G + \lambda\Big)\|\boldsymbol{\varepsilon}(\delta\boldsymbol{u}_h^{n,\ell})\|^2_{L^2(\Omega_1)} + \lambda^2\|\nabla\cdot\delta\boldsymbol{u}_h^{n,\ell}\|^2_{L^2(\Omega_1)} \\ &+ 4GK_b\|\boldsymbol{\varepsilon}(\delta\boldsymbol{u}_h^{n,\ell})\|^2_{L^2(\Omega_2)} + 2\lambda K_b\|\nabla\cdot\delta\boldsymbol{u}_h^{n,\ell}\|^2_{L^2(\Omega_2)} \leq \frac{1}{\beta^2 K_b^2}\|\delta\bar{\sigma}_h^{n,\ell-1}\|^2_{L^2(\Omega_1)}.\end{aligned} \tag{3.26}$$

This implies in particular that

$$\|\delta\bar{\sigma}_h^{n,\ell}\|_{L^2(\Omega_1)} \leq \frac{1}{\beta K_b}\|\delta\bar{\sigma}_h^{n,\ell-1}\|_{L^2(\Omega_1)},$$

hence

$$\|\delta\bar{\sigma}_h^{n,\ell}\|_{L^2(\Omega_1)} \le \Big(\frac{1}{\beta K_b}\Big)^{\ell-1}\|\delta\bar{\sigma}_h^{n,1}\|_{L^2(\Omega_1)}, \tag{3.27}$$

whence the unconditional geometric convergence of $\bar{\sigma}_h^{n,\ell}$, since $\beta K_b > 1$, unconditional in the sense that it does not depend on h, n and Δt. We also deduce that

$$\begin{aligned}
\|\boldsymbol{\varepsilon}(\delta\boldsymbol{u}_h^{n,\ell})\|_{L^2(\Omega)} &\le \frac{1}{2}\Big(\frac{1}{G(\frac{1}{3}G+\lambda)}\Big)^{\frac{1}{2}}\Big(\frac{1}{\beta K_b}\Big)^{\ell-1}\|\delta\bar{\sigma}_h^{n,1}\|_{L^2(\Omega_1)},\\
\|\nabla\cdot\delta\boldsymbol{u}_h^{n,\ell}\|_{L^2(\Omega)} &\le \frac{1}{\lambda}\Big(\frac{1}{\beta K_b}\Big)^{\ell-1}\|\delta\bar{\sigma}_h^{n,1}\|_{L^2(\Omega_1)},\\
(\Delta t)^{\frac{1}{2}}\|\boldsymbol{\kappa}^{-\frac{1}{2}}\delta\boldsymbol{z}_h^{n,\ell}\|_{L^2(\Omega_1)} &\le \Big(\frac{\beta}{2\mu_f}\Big)^{\frac{1}{2}}\Big(\frac{1}{\beta K_b}\Big)^{\ell-1}\|\delta\bar{\sigma}_h^{n,1}\|_{L^2(\Omega_1)},\\
\|\alpha\delta p_h^{n,\ell}\|_{L^2(\Omega_1)} &\le \Big(\frac{1}{\beta K_b}\Big)^{\ell-1}\|\delta\bar{\sigma}_h^{n,1}\|_{L^2(\Omega_1)}.
\end{aligned} \tag{3.28}$$

This proves the theorem. □

4. Stability of the discrete scheme

In this section, we show that the scheme issued from the fixed stress algorithm is stable when convergence is attained.

4.1. Basic stability estimates

Let us start with stability of the mean stress. It stems from (3.27) that the influence of the time-lagged term is determined by that of $\bar{\sigma}_h^{n,1}-\bar{\sigma}_h^{n-1}$. To simplify, we use the notation δ, see (3.24), and recall that at step n, $\ell=0$ corresponds to $n-1$, so that $\delta(\bar{\sigma}_h^{n,1})=\bar{\sigma}_h^{n,1}-\bar{\sigma}_h^{n-1}$.

We can derive a possibly sharper estimate for this quantity by proceeding as follows. We have

$$\begin{aligned}
\|\delta(\bar{\sigma}_h^{n,1})\|^2_{L^2(\Omega_1)} &= \|K_b\nabla\cdot\delta(\boldsymbol{u}_h^{n,1})-\alpha\delta(p_h^{n,1})\|^2_{L^2(\Omega_1)} = K_b^2\|\nabla\cdot\delta(\boldsymbol{u}_h^{n,1})\|^2_{L^2(\Omega_1)}+\alpha^2\|\delta(p_h^{n,1})\|^2_{L^2(\Omega_1)}\\
&\quad - 2\alpha K_b\big(\delta(p_h^{n,1}),\nabla\cdot\delta(\boldsymbol{u}_h^{n,1})\big)_{\Omega_1}.
\end{aligned}$$

This last term is evaluated by the difference in the elasticity equation (3.19) at step n with $\ell=1$ and at step $n-1$ tested with $\boldsymbol{v}_h=\delta(\boldsymbol{u}_h^{n,1})$,

$$\begin{aligned}
-2\alpha K_b\big(\delta(p_h^{n,1}),\nabla\cdot\delta(\boldsymbol{u}_h^{n,1})\big)_{\Omega_1} &= -4GK_b\|\boldsymbol{\varepsilon}(\delta(\boldsymbol{u}_h^{n,1}))\|^2_{L^2(\Omega)} - 2\lambda K_b\|\nabla\cdot\delta(\boldsymbol{u}_h^{n,1})\|^2_{L^2(\Omega)}\\
&\quad + 2K_b\big(\delta(\boldsymbol{f}^n),\delta(\boldsymbol{u}_h^{n,1})\big)_\Omega + 2K_b\big\langle\delta(\boldsymbol{t}_N^n),\delta(\boldsymbol{u}_h^{n,1})\big\rangle_{\Gamma_N}.
\end{aligned}$$

By substituting this equality into the preceding one, we obtain

$$\begin{aligned}
\|\delta(\bar{\sigma}_h^{n,1})\|^2_{L^2(\Omega_1)} &= -4GK_b\|\boldsymbol{\varepsilon}(\delta(\boldsymbol{u}_h^{n,1}))\|^2_{L^2(\Omega_1)} + (K_b^2-2\lambda K_b)\|\nabla\cdot\delta(\boldsymbol{u}_h^{n,1})\|^2_{L^2(\Omega_1)} + \alpha^2\|\delta(p_h^{n,1})\|^2_{L^2(\Omega_1)}\\
&+ 2K_b\big(\delta(\boldsymbol{f}^n),\delta(\boldsymbol{u}_h^{n,1})\big)_\Omega + 2K_b\big\langle\delta(\boldsymbol{t}_N^n),\delta(\boldsymbol{u}_h^{n,1})\big\rangle_{\Gamma_N} - 4GK_b\|\boldsymbol{\varepsilon}(\delta(\boldsymbol{u}_h^{n,1}))\|^2_{L^2(\Omega_2)} - 2\lambda K_b\|\nabla\cdot\delta(\boldsymbol{u}_h^{n,1})\|^2_{L^2(\Omega_2)}.
\end{aligned} \tag{4.1}$$

As

$$-4G\boldsymbol{\varepsilon}(\boldsymbol{v}):\boldsymbol{\varepsilon}(\boldsymbol{v}) \le -2G\boldsymbol{\varepsilon}(\boldsymbol{v}):\boldsymbol{\varepsilon}(\boldsymbol{v}) - \frac{2}{3}G|\nabla\cdot\boldsymbol{v}|^2,$$

the first line in the right-hand side of (4.1) is bounded above by

$$\begin{aligned}
&-2GK_b\,\|\boldsymbol{\varepsilon}(\delta(\boldsymbol{u}_h^{n,1}))\|^2_{L^2(\Omega_1)} + \Big(-\frac{2}{3}GK_b + K_b^2 - 2\lambda K_b\Big)\|\nabla\cdot\delta(\boldsymbol{u}_h^{n,1})\|^2_{L^2(\Omega_1)}\\
&\qquad = -2GK_b\|\boldsymbol{\varepsilon}(\delta(\boldsymbol{u}_h^{n,1}))\|^2_{L^2(\Omega_1)} - \lambda K_b\|\nabla\cdot\delta(\boldsymbol{u}_h^{n,1})\|^2_{L^2(\Omega_1)}.
\end{aligned}$$

This gives a first bound

$$\|\delta(\bar{\sigma}_h^{n,1})\|^2_{L^2(\Omega_1)} \le -2GK_b\|\boldsymbol{\varepsilon}(\delta(\boldsymbol{u}_h^{n,1}))\|^2_{L^2(\Omega_1)} - \lambda K_b\|\nabla\cdot\delta(\boldsymbol{u}_h^{n,1})\|^2_{L^2(\Omega_1)} + \alpha^2\|\delta(p_h^{n,1})\|^2_{L^2(\Omega_1)}$$
$$+ 2K_b\big(\delta(\boldsymbol{f}^n),\delta(\boldsymbol{u}_h^{n,1})\big)_\Omega + 2K_b\big\langle\delta(\boldsymbol{t}_N^n),\delta(\boldsymbol{u}_h^{n,1})\big\rangle_{\Gamma_N} - 4GK_b\|\boldsymbol{\varepsilon}(\delta(\boldsymbol{u}_h^{n,1}))\|^2_{L^2(\Omega_2)} - 2\lambda K_b\|\nabla\cdot\delta(\boldsymbol{u}_h^{n,1})\|^2_{L^2(\Omega_2)}. \tag{4.2}$$

By Young's inequality, we easily derive the next proposition.

Proposition 3. *Let $\boldsymbol{f}$ belong to $\mathcal{C}^0([0,T];L^2(\Omega)^d)$ and $\boldsymbol{t}_N$ to $\mathcal{C}^0([0,T];(H_{00}^{\frac12}(\Gamma_N)^d)')$. For all $n\ge 1$, we have*

$$\|\delta(\bar{\sigma}_h^{n,1})\|^2_{L^2(\Omega_1)} \le \alpha^2\|\delta(p_h^{n,1})\|^2_{L^2(\Omega_1)} - \lambda K_b\|\nabla\cdot\delta(\boldsymbol{u}_h^{n,1})\|^2_{L^2(\Omega_1)} - 2\lambda K_b\|\nabla\cdot\delta(\boldsymbol{u}_h^{n,1})\|^2_{L^2(\Omega_2)}$$
$$+ \frac{K_b}{2G}\mathcal{K}^2\big(\mathcal{P}^2\|\delta(\boldsymbol{f}^n)\|^2_{L^2(\Omega)} + C_N^2\|\delta(\boldsymbol{t}_N^n)\|^2_{(H_{00}^{\frac12}(\Gamma_N))'}\big). \tag{4.3}$$

This is done by splitting

$$\big(\delta(\boldsymbol{f}^n),\delta(\boldsymbol{u}_h^{n,1})\big)_\Omega = \big(\delta(\boldsymbol{f}^n),\delta(\boldsymbol{u}_h^{n,1})\big)_{\Omega_1} + \big(\delta(\boldsymbol{f}^n),\delta(\boldsymbol{u}_h^{n,1})\big)_{\Omega_2},$$

and applying Young's inequality to each term, with an analogous treatment of the boundary term after applying the trace inequality (1.7).

The next proposition gives a bound for the initial difference $\delta(p_h^{n,1})$.

Proposition 4. *Let q belong to $\mathcal{C}^0([0,T];L^2(\Omega_1))$. For all $n\ge 1$, we have*

$$\frac{1}{\Delta t}\|\delta p_h^{n,1}\|^2_{L^2(\Omega_1)} \le \frac12\mu_f\frac{1}{\alpha^2\beta}\|\boldsymbol{\kappa}^{-\frac12}\boldsymbol{z}_h^{n-1}\|^2_{L^2(\Omega_1)} + \Delta t\frac{1}{\alpha^4\beta^2}\|q^n\|^2_{L^2(\Omega_1)}. \tag{4.4}$$

Proof. The flow equation (3.16) at level $\ell=1$, tested with $\theta_h=\delta p_h^{n,1}$ gives

$$\Big(\frac{1}{M}+\frac{\alpha^2}{K_b}\Big)\frac{1}{\Delta t}\|\delta p_h^{n,1}\|^2_{L^2(\Omega_1)} + \big(\nabla\cdot\boldsymbol{z}_h^{n,1},\delta p_h^{n,1}\big)_{\Omega_1} = (q^n,\delta p_h^{n,1})_{\Omega_1}.$$

But the difference between (3.17) applied at level $(n,1)$ and $(n,0)$, i.e., $n-1$, tested with $\boldsymbol{\zeta}_h=\boldsymbol{z}_h^{n,1}$ yields

$$\big(\nabla\cdot\boldsymbol{z}_h^{n,1},\delta p_h^{n,1}\big)_{\Omega_1} = \mu_f\big(\boldsymbol{\kappa}^{-1}\delta\boldsymbol{z}_h^{n,1},\boldsymbol{z}_h^{n,1}\big)_{\Omega_1} = \mu_f\|\boldsymbol{\kappa}^{-\frac12}\delta\boldsymbol{z}_h^{n,1}\|^2_{L^2(\Omega_1)} + \mu_f\big(\boldsymbol{\kappa}^{-1}\delta\boldsymbol{z}_h^{n,1},\boldsymbol{z}_h^{n-1}\big)_{\Omega_1}.$$

Hence

$$\Big(\frac{1}{M}+\frac{\alpha^2}{K_b}\Big)\frac{1}{\Delta t}\|\delta p_h^{n,1}\|^2_{L^2(\Omega_1)} + \mu_f\|\boldsymbol{\kappa}^{-\frac12}\delta\boldsymbol{z}_h^{n,1}\|^2_{L^2(\Omega_1)} = -\mu_f\big(\boldsymbol{\kappa}^{-1}\delta\boldsymbol{z}_h^{n,1},\boldsymbol{z}_h^{n-1}\big)_{\Omega_1} + (q^n,\delta p_h^{n,1})_{\Omega_1}.$$

By Young's inequality, we infer

$$\Big(\frac{1}{M}+\frac{\alpha^2}{K_b}\Big)\frac{1}{\Delta t}\|\delta p_h^{n,1}\|^2_{L^2(\Omega_1)} \le \frac{\mu_f}{2}\|\boldsymbol{\kappa}^{-\frac12}\delta\boldsymbol{z}_h^{n-1}\|^2_{L^2(\Omega_1)} + \Delta t\Big(\frac{1}{M}+\frac{\alpha^2}{K_b}\Big)^{-1}\|q^n\|^2_{L^2(\Omega_1)},$$

and (4.4) follows by using the quantity β defined in (3.23). □

By substituting (4.4) into (4.3), we immediately deduce a further bound for $\delta\bar{\sigma}_h^{n,1}$.

Proposition 5. *Let $\boldsymbol{f}$ belong to $\mathcal{C}^0([0,T];L^2(\Omega)^d)$, q to $\mathcal{C}^0([0,T];L^2(\Omega_1))$, and $\boldsymbol{t}_N$ to $\mathcal{C}^0([0,T];(H_{00}^{\frac12}(\Gamma_N)^d)')$. For all $n\ge 1$, we have*

$$\frac{1}{\Delta t}\|\delta\bar{\sigma}_h^{n,1}\|^2_{L^2(\Omega_1)} \le \frac12\frac{\mu_f}{\beta}\|\boldsymbol{\kappa}^{-\frac12}\boldsymbol{z}_h^{n-1}\|^2_{L^2(\Omega_1)} + \Delta t\frac{1}{\alpha^2\beta^2}\|q^n\|^2_{L^2(\Omega_1)} - \lambda\frac{K_b}{\Delta t}\|\nabla\cdot\delta\boldsymbol{u}_h^{n,1}\|^2_{L^2(\Omega_1)}$$
$$- 2\lambda\frac{K_b}{\Delta t}\|\nabla\cdot\delta\boldsymbol{u}_h^{n,1}\|^2_{L^2(\Omega_2)}$$
$$+ \frac{K_b\mathcal{K}^2}{2G}\frac{1}{\Delta t}\Big(\mathcal{P}^2\|\delta\boldsymbol{f}^n\|^2_{L^2(\Omega)} + C_N^2\|\delta\boldsymbol{t}_N^n\|^2_{(H_{00}^{\frac12}(\Gamma_N)^d)'}\Big). \tag{4.5}$$

Therefore, a definite bound for $\delta\bar{\sigma}_h^{n,1}$ will follow from a standard proof of stability of the scheme. The next proposition establishes a partial stability result.

Proposition 6. *Under the assumptions of Proposition 5, the following bound holds for all n,* $1 \le n \le N$,

$$\begin{aligned}
&\frac{1}{M}\Big(\frac{1}{2}\|p_h^n\|^2_{L^2(\Omega_1)} + \sum_{m=1}^{n}\|\delta p_h^m\|^2_{L^2(\Omega_1)}\Big) + \mu_f \sum_{m=1}^{n} \Delta t \|\boldsymbol{\kappa}^{-\frac{1}{2}} \boldsymbol{z}_h^m\|^2_{L^2(\Omega_1)}\\
&+ G\Big(\|\boldsymbol{\varepsilon}(\boldsymbol{u}_h^n)\|^2_{L^2(\Omega)} + 2\sum_{m=1}^{n}\|\boldsymbol{\varepsilon}(\delta \boldsymbol{u}_h^m)\|^2_{L^2(\Omega)}\Big) + \lambda\Big(\|\nabla\cdot(\boldsymbol{u}_h^n)\|^2_{L^2(\Omega)} + \sum_{m=1}^{n}\|\nabla\cdot(\delta\boldsymbol{u}_h^m)\|^2_{L^2(\Omega)}\Big)\\
&\le \frac{1}{2M}\sum_{m=1}^{n-1}\Delta t\|p_h^m\|^2_{L^2(\Omega_1)} + G\sum_{m=1}^{n-1}\Delta t\|\boldsymbol{\varepsilon}(\boldsymbol{u}_h^m)\|^2_{L^2(\Omega)}\\
&+ 4M\frac{\alpha^2}{K_b^2}\Big(\|\bar{\sigma}_h^n - \bar{\sigma}_h^{n,\ell_n-1}\|^2_{L^2(\Omega_1)} + \sum_{m=1}^{n-1}\frac{1}{\Delta t}\|\bar{\sigma}_h^m - \bar{\sigma}_h^{m,\ell_m-1}\|^2_{L^2(\Omega_1)}\Big) + \mathcal{I}_h^0 + \mathcal{D}_h^n,
\end{aligned} \tag{4.6}$$

where $\mathcal{I}_h^0$ *and* $\mathcal{D}_h^n$ *are respectively contributions of the initial terms and data,*

$$\mathcal{I}_h^0 = \frac{1}{M}\|p_h^0\|^2_{L^2(\Omega_1)} + 3G\|\boldsymbol{\varepsilon}(\boldsymbol{u}_h^0)\|^2_{L^2(\Omega)} + \lambda\|\nabla\cdot\boldsymbol{u}_h^0\|^2_{L^2(\Omega)}, \tag{4.7}$$

$$\begin{aligned}
\mathcal{D}_h^n =& \frac{2}{G}(\mathcal{P}\mathcal{K})^2\Big(\|\boldsymbol{f}^1\|^2_{L^2(\Omega)} + \|\boldsymbol{f}^n\|^2_{L^2(\Omega)} + \sum_{m=1}^{n-1}\frac{1}{\Delta t}\|\delta \boldsymbol{f}^{m+1}\|^2_{L^2(\Omega)}\Big)\\
&+ \frac{2}{G}(C_N\mathcal{K})^2\Big(\|\boldsymbol{t}_N^1\|^2_{(H_{00}^{\frac{1}{2}}(\Gamma_N))'} + \|\boldsymbol{t}_N^n\|^2_{(H_{00}^{\frac{1}{2}}(\Gamma_N))'} + \sum_{m=1}^{n-1}\frac{1}{\Delta t}\|\delta \boldsymbol{t}_N^{m+1}\|^2_{(H_{00}^{\frac{1}{2}}(\Gamma_N))'}\Big)\\
&+ 4M\Big((\Delta t)^2\|q^n\|^2_{L^2(\Omega_1)} + \sum_{m=1}^{n-1}\Delta t\|q^m\|^2_{L^2(\Omega_1)}\Big) + \frac{1}{\mu_f}\sum_{m=1}^{n}\Delta t\|\boldsymbol{\kappa}^{\frac{1}{2}}(\rho g\nabla\eta)\|^2_{L^2(\Omega_1)},
\end{aligned} \tag{4.8}$$

with the constants $\mathcal{K}$, $\mathcal{P}$, *and* C_N *of (1.5)–(1.7). When* $n = 1$, *all sums ranging from* 1 *to* $n-1$ *in the right-hand sides of* (4.6) and (4.8) *are empty.*

Proof. At each time step n, we choose a suitable ℓ_n (that will correspond to a satisfactory level of iteration) and denote with the superscript n all unknowns at the level ℓ_n. First, we rewrite the flow equation (3.16) with a direct approximation of the exact equation in the left-hand side, as follows

$$\frac{1}{M\Delta t}\big(\delta(p_h^n), \theta_h\big)_{\Omega_1} + \frac{\alpha}{\Delta t}\big(\nabla\cdot\delta(\boldsymbol{u}_h^n), \theta_h\big)_{\Omega_1} + \big(\nabla\cdot \boldsymbol{z}_h^n, \theta_h\big)_{\Omega_1} = \frac{\alpha}{K_b}\frac{1}{\Delta t}\big(\bar{\sigma}_h^n - \bar{\sigma}_h^{n,\ell_n-1}, \theta_h\big)_{\Omega_1} + \big(q^n, \theta_h\big)_{\Omega_1}. \tag{4.9}$$

This equation is tested with $\theta_h = p_h^n$ and combined with the velocity equation (3.17) tested with z_h^n and the displacement equation (3.19) tested with $\boldsymbol{u}_h^n - \boldsymbol{u}_h^{n-1}$ divided by Δt. This gives

$$\begin{aligned}
&\frac{1}{2M\Delta t}\Big(\delta\big(\|p_h^n\|^2_{L^2(\Omega_1)}\big) + \|\delta(p_h^n)\|^2_{L^2(\Omega_1)}\Big) + \mu_f\|\boldsymbol{\kappa}^{-\frac{1}{2}}\boldsymbol{z}_h^n\|^2_{L^2(\Omega_1)} + \frac{G}{\Delta t}\Big(\delta\big(\|\boldsymbol{\varepsilon}(\boldsymbol{u}_h^n)\|^2_{L^2(\Omega)}\big) + \|\boldsymbol{\varepsilon}(\delta(\boldsymbol{u}_h^n))\|^2_{L^2(\Omega)}\Big)\\
&\quad + \frac{\lambda}{2\Delta t}\Big(\delta\big(\|\nabla\cdot(\boldsymbol{u}_h^n)\|^2_{L^2(\Omega)}\big) + \|\nabla\cdot\delta(\boldsymbol{u}_h^n)\|^2_{L^2(\Omega)}\Big) = \big(\rho g\nabla\eta, \boldsymbol{z}_h^n\big)_{\Omega_1} + \frac{\alpha}{K_b}\frac{1}{\Delta t}\big(\bar{\sigma}_h^n - \bar{\sigma}_h^{n,\ell_n-1}, p_h^n\big)_{\Omega_1}\\
&\quad + \big(q^n, p_h^n\big)_{\Omega_1} + \frac{1}{\Delta t}\big(\boldsymbol{f}^n, \delta(\boldsymbol{u}_h^n)\big)_{\Omega} + \frac{1}{\Delta t}\langle \boldsymbol{t}_N^n, \delta(\boldsymbol{u}_h^n)\rangle_{\Gamma_N}.
\end{aligned} \tag{4.10}$$

After multiplying both sides by $2\Delta t$ and summing, we proceed in three steps.

(1) As expected, the last two terms in the right-hand side of (4.10) are summed by parts because they cannot be controlled by the left-hand side. Owing to (1.5)–(1.7), we have

$$\begin{aligned}\Big|\sum_{m=1}^{n}(\boldsymbol{f}^m,\delta(\boldsymbol{u}_h^m))_\Omega\Big| &\le \mathcal{P}\mathcal{K}\Big(\sum_{m=1}^{n-1}\|\delta(\boldsymbol{f}^{m+1})\|_{L^2(\Omega)}\|\boldsymbol{\varepsilon}(\boldsymbol{u}_h^m)\|_{L^2(\Omega)}+\|\boldsymbol{f}^n\|_{L^2(\Omega)}\|\boldsymbol{\varepsilon}(\boldsymbol{u}_h^n)\|_{L^2(\Omega)}\\ &\quad+\|\boldsymbol{f}^1\|_{L^2(\Omega)}\|\boldsymbol{\varepsilon}(\boldsymbol{u}_h^0)\|_{L^2(\Omega)}\Big),\\ \Big|\sum_{m=1}^{n}\langle\boldsymbol{t}_N^m,\delta(\boldsymbol{u}_h^m)\rangle_{\Gamma_N}\Big| &\le C_N\mathcal{K}\Big(\sum_{m=1}^{n-1}\|\delta(\boldsymbol{t}_N^{m+1})\|_{(H_{00}^{\frac12}(\Gamma_N))'}\|\boldsymbol{\varepsilon}(\boldsymbol{u}_h^m)\|_{L^2(\Omega)}+\|\boldsymbol{t}_N^n\|_{(H_{00}^{\frac12}(\Gamma_N))'}\|\boldsymbol{\varepsilon}(\boldsymbol{u}_h^n)\|_{L^2(\Omega)}\\ &\quad+\|\boldsymbol{t}_N^1\|_{(H_{00}^{\frac12}(\Gamma_N))'}\|\boldsymbol{\varepsilon}(\boldsymbol{u}_h^0)\|_{L^2(\Omega)}\Big).\end{aligned}\tag{4.11}$$

Then, by Young's inequality, we infer

$$\begin{aligned}2\sum_{m=1}^{n}\Big[\big|(\boldsymbol{f}^m,\delta(\boldsymbol{u}_h^m))_\Omega\big|+\big|\langle\boldsymbol{t}_N^m,\delta(\boldsymbol{u}_h^m)\rangle_{\Gamma_N}\big|\Big] &\le G\Big(\|\boldsymbol{\varepsilon}(\boldsymbol{u}_h^n)\|^2_{L^2(\Omega)}+\Delta t\sum_{m=1}^{n-1}\|\boldsymbol{\varepsilon}(\boldsymbol{u}_h^m)\|^2_{L^2(\Omega)}+\|\boldsymbol{\varepsilon}(\boldsymbol{u}_h^0)\|^2_{L^2(\Omega)}\Big)\\ &\quad+\frac{2}{G}\Big[\mathcal{P}^2\mathcal{K}^2\Big(\|\boldsymbol{f}^1\|^2_{L^2(\Omega)}+\|\boldsymbol{f}^n\|^2_{L^2(\Omega)}+\frac{1}{\Delta t}\sum_{m=1}^{n-1}\|\delta(\boldsymbol{f}^{m+1})\|^2_{L^2(\Omega)}\Big)\\ &\quad+C_N^2\mathcal{K}^2\Big(\|\boldsymbol{t}_N^1\|^2_{(H_{00}^{\frac12}(\Gamma_N))'}+\|\boldsymbol{t}_N^n\|^2_{(H_{00}^{\frac12}(\Gamma_N))'}+\frac{1}{\Delta t}\sum_{m=1}^{n-1}\|\delta(\boldsymbol{t}_N^{m+1})\|^2_{(H_{00}^{\frac12}(\Gamma_N))'}\Big)\Big].\end{aligned}\tag{4.12}$$

(2) To apply Gronwall's Lemma, the terms involving p_h^n in the right-hand side of (4.10) cannot be left as such. There are several ways to deal with them. The simplest, but perhaps not the sharpest way, is to write for the term at time t_n,

$$\begin{aligned}2\frac{\alpha}{K_b}\big|(\bar\sigma_h^n-\bar\sigma_h^{n,\ell_n-1},p_h^n)_{\Omega_1}\big|+2\Delta t\big|(q^n,p_h^n)_{\Omega_1}\big| &\le \frac{1}{2M}\|p_h^n\|^2_{L^2(\Omega_1)}\\ &\quad+4M\frac{\alpha^2}{K_b^2}\|\bar\sigma_h^n-\bar\sigma_h^{n,\ell_n-1}\|^2_{L^2(\Omega_1)}+4M(\Delta t)^2\|q^n\|^2_{L^2(\Omega_1)},\end{aligned}\tag{4.13}$$

and for the sum of terms at the preceding times

$$\begin{aligned}\sum_{m=1}^{n-1}\Big(2\frac{\alpha}{K_b}\big|(\bar\sigma_h^m-\bar\sigma_h^{m,\ell_m-1},p_h^m)_{\Omega_1}\big|+2\Delta t\big|(q^m,p_h^m)_{\Omega_1}\big|\Big) &\le \frac{1}{2M}\sum_{m=1}^{n-1}\Delta t\|p_h^m\|^2_{L^2(\Omega_1)}\\ &\quad+4M\frac{\alpha^2}{K_b^2}\sum_{m=1}^{n-1}\frac{1}{\Delta t}\|\bar\sigma_h^m-\bar\sigma_h^{m,\ell_m-1}\|^2_{L^2(\Omega_1)}+4M\sum_{m=1}^{n-1}\Delta t\|q^m\|^2_{L^2(\Omega_1)}.\end{aligned}\tag{4.14}$$

(3) The treatment of the flow velocity is straightforward,

$$2\sum_{m=1}^{n}\Delta t\big|\big(\rho g\nabla\eta,\boldsymbol{z}_h^m\big)_{\Omega_1}\big|\le\mu_f\sum_{m=1}^{n}\Delta t\|\boldsymbol{\kappa}^{-\frac12}\boldsymbol{z}_h^m\|^2_{L^2(\Omega_1)}+\frac{1}{\mu_f}\sum_{m=1}^{n}\Delta t\|\boldsymbol{\kappa}^{\frac12}\rho g\nabla\eta\|^2_{L^2(\Omega_1)}.\tag{4.15}$$

Finally, (4.6) follows by collecting (4.12)–(4.15). □

From here, stability of the scheme is derived by taking ℓ_n sufficiently large at each time step, and applying (3.27) and (4.5).

Proposition 7. *Under the assumptions of Proposition 5, if $\Delta t \le 1$ and if for each m, $1 \le m \le N$, the number of iterations ℓ_m satisfies*

$$\Big(\frac{1}{\beta K_b}\Big)^{2\ell_m-1}\le\frac{\Delta t}{2}(\beta K_b-1),\tag{4.16}$$

then the following bound holds for all n, $1 \leq n \leq N$,

$$\frac{1}{M}\Big(\frac{1}{2}\|p_h^n\|^2_{L^2(\Omega_1)} + \sum_{m=1}^{n}\|\delta p_h^m\|^2_{L^2(\Omega_1)}\Big) + \mu_f \Delta t \|\boldsymbol{\kappa}^{-\frac{1}{2}}\boldsymbol{z}_h^n\|^2_{L^2(\Omega_1)}$$
$$+ G\Big(\|\boldsymbol{\varepsilon}(\boldsymbol{u}_h^n)\|^2_{L^2(\Omega)} + 2\sum_{m=1}^{n}\|\boldsymbol{\varepsilon}(\delta\boldsymbol{u}_h^m)\|^2_{L^2(\Omega)}\Big) + \lambda\Big(\|\nabla\cdot(\boldsymbol{u}_h^n)\|^2_{L^2(\Omega)} + \sum_{m=1}^{n}\|\nabla\cdot(\delta\boldsymbol{u}_h^m)\|^2_{L^2(\Omega)}\Big) \tag{4.17}$$
$$\leq \frac{1}{2M}\sum_{m=1}^{n-1}\Delta t\|p_h^m\|^2_{L^2(\Omega_1)} + G\sum_{m=1}^{n-1}\Delta t\|\boldsymbol{\varepsilon}(\boldsymbol{u}_h^m)\|^2_{L^2(\Omega)} + \mathcal{I}_h^0 + \mathcal{I}_h^{\sigma,0} + \mathcal{D}_h^n + \mathcal{D}_h^{\sigma,n},$$

where $\mathcal{I}_h^0$, $\mathcal{I}_h^{\sigma,0}$, $\mathcal{D}_h^n$, *and* $\mathcal{D}_h^{\sigma,n}$ *are defined respectively by* (4.7), (4.20) *below,* (4.8), *and* (4.19) *below. When* $n = 1$, *all sums ranging from* 1 *to* $n-1$ *are empty.*

Proof. By substituting (4.5) into (3.27) and neglecting the negative terms in its right-hand side, we obtain

$$\|\bar{\sigma}_h^{n,\ell_n} - \bar{\sigma}_h^{n,\ell_n-1}\|^2_{L^2(\Omega_1)} \leq \Big(\frac{1}{\beta K_b}\Big)^{2(\ell_n-1)}\Delta t\Big[\frac{1}{2}\frac{\mu_f}{\beta}\|\boldsymbol{\kappa}^{-\frac{1}{2}}\boldsymbol{z}_h^{n-1}\|^2_{L^2(\Omega_1)} + \Delta t\frac{1}{\alpha^2\beta^2}\|q^n\|^2_{L^2(\Omega_1)}$$
$$+ \frac{K_b\mathcal{K}^2}{2G}\frac{1}{\Delta t}\Big(\mathcal{P}^2\|\delta\boldsymbol{f}^n\|^2_{L^2(\Omega)} + C_N^2\|\delta\boldsymbol{t}_N^n\|^2_{(H_{00}^{\frac{1}{2}}(\Gamma_N))'}\Big)\Big], \tag{4.18}$$

with a similar inequality (without the first factor Δt) for the sum of $\frac{1}{\Delta t}\|\bar{\sigma}_h^{m,\ell_m} - \bar{\sigma}_h^{m,\ell_m-1}\|^2_{L^2(\Omega_1)}$ running from $m = 1$ to $m = n-1$. By inspecting the right-hand side of (4.18) multiplied by the factor $4M\frac{\alpha^2}{K_b^2}$, we see that the upper bound for the sum of all these terms involves a sum of terms $\|\boldsymbol{\kappa}^{-\frac{1}{2}}\boldsymbol{z}_h^m\|^2_{L^2(\Omega_1)}$ with m running from 0 to $n-1$. Except for the first term, that will be addressed further on, this sum can be controlled by the left-hand side of (4.6) provided the fixed-stress algorithm is iterated a sufficiently large number of times. More precisely, we assume on the one hand that ℓ_n is large enough so that

$$4M\frac{\alpha^2}{K_b^2}\frac{1}{2}\frac{\mu_f}{\beta}\Delta t\Big(\frac{1}{\beta K_b}\Big)^{2(\ell_n-1)} \leq \mu_f\Delta t,$$

i.e.,

$$\Big(\frac{1}{\beta K_b}\Big)^{2\ell_n-1} \leq \frac{1}{2}(\beta K_b - 1).$$

On the other hand, we assume that for $1 \leq m \leq n-1$, ℓ_m is large enough so that

$$4M\frac{\alpha^2}{K_b^2}\frac{1}{2}\frac{\mu_f}{\beta}\Big(\frac{1}{\beta K_b}\Big)^{2(\ell_m-1)} \leq \mu_f\Delta t,$$

i.e. we recover (4.16). As we can reasonably suppose that $\Delta t \leq 1$, this is the stronger assumption and therefore we assume that at each time step m, the number of iterations ℓ_m of the fixed-stress algorithm is chosen so that (4.16) holds.

Of course, (4.18) also brings a data term; under hypothesis (4.16), this data term becomes

$$\mathcal{D}_h^{\sigma,n} = M\alpha^2\beta\frac{\mathcal{K}^2}{G}(\beta K_b - 1)\Big[\mathcal{P}^2\big(\Delta t\|\delta\boldsymbol{f}^n\|^2_{L^2(\Omega)} + \sum_{m=1}^{n-1}\|\delta\boldsymbol{f}^m\|^2_{L^2(\Omega)}\big)$$
$$+ C_N^2\big(\Delta t\|\delta\boldsymbol{t}_N^n\|^2_{(H_{00}^{\frac{1}{2}}(\Gamma_N))'} + \sum_{m=1}^{n-1}\|\delta\boldsymbol{t}_N^m\|^2_{(H_{00}^{\frac{1}{2}}(\Gamma_N))'}\big)\Big] + 2\frac{M}{\beta K_b}(\beta K_b - 1)\Delta t \tag{4.19}$$
$$\times \Big((\Delta t)^2\|q^n\|^2_{L^2(\Omega_1)} + \sum_{m=1}^{n-1}\Delta t\|q^m\|^2_{L^2(\Omega_1)}\Big).$$

Finally, (4.18) brings an additional initial term when $m = 1$; under hypothesis (4.16), this term reads

$$\mathcal{I}_h^{\sigma,0} = \frac{M\alpha^2}{K_b}\Delta t\, \mu_f\big(\beta K_b - 1\big)\|\boldsymbol{\kappa}^{-\frac{1}{2}}\boldsymbol{z}_h^0\|^2_{L^2(\Omega_1)}. \tag{4.20}$$

Then (4.17) follows by collecting these results. □

Regarding the initial data, $\boldsymbol{\varepsilon}(\boldsymbol{u}_h^0)$ and $\nabla\cdot\boldsymbol{u}_h^0$ are computed by solving (3.13). An easy application of Young's inequality shows that

$$G\|\boldsymbol{\varepsilon}(\boldsymbol{u}_h^0)\|^2_{L^2(\Omega)} + \frac{\lambda}{2}\|\nabla\cdot\boldsymbol{u}_h^0\|^2_{L^2(\Omega)} \le \frac{\alpha^2}{2\lambda}\|p_h^0\|^2_{L^2(\Omega_1)} + \frac{1}{2}\frac{\mathcal{K}^2}{G}\big(\mathcal{P}^2\|\boldsymbol{f}^0\|^2_{L^2(\Omega)} + C_N^2\|\boldsymbol{t}_N^0\|^2_{(H_{00}^{\frac{1}{2}}(\Gamma_N)^d)'}\big). \tag{4.21}$$

The control of $\boldsymbol{z}_h^0$ is more problematic because it is defined by (3.14) that involves its divergence. However, since $\tilde{S}_h(p_0)$ is a continuous approximation of p_0, we have

$$\big(p_h^0, \nabla\cdot\boldsymbol{z}_h^0\big)_{\Omega_1} = -\big(\nabla\,\tilde{S}_h(p_0), \boldsymbol{z}_h^0\big)_{\Omega_1},$$

thus implying that

$$\mu_f\|\boldsymbol{\kappa}^{-\frac{1}{2}}\boldsymbol{z}_h^0\|_{L^2(\Omega_1)} \le \|\boldsymbol{\kappa}^{\frac{1}{2}}\big(\rho g\nabla\eta - \nabla\,\tilde{S}_h(p_0)\big)\|_{L^2(\Omega_1)}.$$

Consequently

$$\mathcal{I}_h^{\sigma,0} \le \frac{M\alpha^2}{\mu_f K_b}\Delta t\,\big(\beta K_b - 1\big)\|\boldsymbol{\kappa}^{\frac{1}{2}}\big(\rho g\nabla\eta - \nabla\,\tilde{S}_h(p_0)\big)\|^2_{L^2(\Omega_1)}. \tag{4.22}$$

Finally, regarding the data terms in $\mathcal{D}_h^n$, and $\mathcal{D}_h^{\sigma,n}$, it is easy to see that they are bounded uniformly with respect to h, n, and Δt provided $\boldsymbol{f}$ belongs to $H^1(0,T;L^2(\Omega)^d)$ and $\boldsymbol{t}_N$ to $H^1(0,T;(H_{00}^{\frac{1}{2}}(\Gamma_N)^d)')$. Summing up, by applying Gronwall's Lemma, we obtain the stability of p_h and $\boldsymbol{u}_h$.

Lemma 1. *We retain the assumptions of Proposition 7. Then the following bound holds for all n, $1 \le n \le N$,*

$$\frac{1}{2M}\|p_h^n\|^2_{L^2(\Omega_1)} + G\|\boldsymbol{\varepsilon}(\boldsymbol{u}_h^n)\|^2_{L^2(\Omega)} + \lambda\|\nabla\cdot(\boldsymbol{u}_h^n)\|^2_{L^2(\Omega)} \le C\,\exp(t_n), \tag{4.23}$$

where C depends only on $\mathcal{I}_h^0$, $\mathcal{I}_h^{\sigma,0}$, $\mathcal{D}_h^n$, and $\mathcal{D}_h^{\sigma,n}$. Moreover, if in addition $\boldsymbol{f}$ belongs to $H^1(0,T;L^2(\Omega)^d)$ and $\boldsymbol{t}_N$ to $H^1(0,T;(H_{00}^{\frac{1}{2}}(\Gamma_N)^d)')$, then (4.23) holds with a constant C independent of h, n, and Δt.

It remains to establish stability of the discrete velocity $\boldsymbol{z}_h^n$. For this, we revisit the contribution of the velocity to the right-hand side of (4.10) when it is multiplied by $2\Delta t$ and summed. It occurs in two terms. The first term is

$$2\Delta t\sum_{m=1}^n\big(\rho g\nabla\eta, \boldsymbol{z}_h^m\big)_{\Omega_1} \le \mu_f\sum_{m=1}^n\Delta t\|\boldsymbol{\kappa}^{-\frac{1}{2}}\boldsymbol{z}_h^m\|^2_{L^2(\Omega_1)} + \frac{1}{\mu_f}\sum_{m=1}^n\Delta t\|\boldsymbol{\kappa}^{\frac{1}{2}}\rho g\nabla\eta\|^2_{L^2(\Omega_1)}.$$

This will leave $\mu_f\sum_{m=1}^n\Delta t\|\boldsymbol{\kappa}^{-\frac{1}{2}}\boldsymbol{z}_h^m\|^2_{L^2(\Omega_1)}$ in the left-hand side of the new formulation of (4.10). The second term is

$$\sum_{m=1}^n\frac{2\alpha}{K_b}\big(\bar{\sigma}_h^m - \bar{\sigma}_h^{m,\ell_m-1}, p_h^m\big)_{\Omega_1} \le \frac{2\alpha}{K_b}\Big(\sum_{m=1}^n\Delta t\|p_h^m\|^2_{L^2(\Omega_1)}\Big)^{\frac{1}{2}}\Big(\sum_{m=1}^n\frac{1}{\Delta t}\|\bar{\sigma}_h^m - \bar{\sigma}_h^{m,\ell_m-1}\|^2_{L^2(\Omega_1)}\Big)^{\frac{1}{2}}.$$

As we now know that $\Big(\sum_{m=1}^n\Delta t\|p_h^m\|^2_{L^2(\Omega_1)}\Big)^{\frac{1}{2}}$ is bounded uniformly with respect to h, n, and Δt, we can use Young's inequality with whatever parameter is convenient to control the occurrence of the velocity in the upper bound of the second sum (in view of (4.5), the other terms are bounded by the data). Thus the relevant term in the sum is

$$\frac{1}{2}\frac{\mu_f}{\beta}\Big(\frac{1}{\beta K_b}\Big)^{2(\ell_m-1)}\|\boldsymbol{\kappa}^{-\frac{1}{2}}\boldsymbol{z}_h^{m-1}\|^2_{L^2(\Omega_1)} \le \frac{1}{4}\Delta t K_b\big(\beta K_b - 1\big)\mu_f\|\boldsymbol{\kappa}^{-\frac{1}{2}}\boldsymbol{z}_h^{m-1}\|^2_{L^2(\Omega_1)},$$

owing to (4.18) and (4.16). Therefore, by Young's inequality, we can write

$$\sum_{m=1}^{n} \frac{2\alpha}{K_b}\big(\bar{\sigma}_h^m - \bar{\sigma}_h^{m,\ell_m-1}, p_h^m\big)_{\Omega_1} \le \frac{1}{2}\mu_f \sum_{m=1}^{n} \Delta t \|\boldsymbol{\kappa}^{-\frac{1}{2}} \boldsymbol{z}_h^{m-1}\|^2_{L^2(\Omega_1)} + \frac{1}{2}\frac{\alpha^2}{K_b}\big(\beta K_b - 1\big)\sum_{m=1}^{n} \Delta t \|p_h^m\|^2_{L^2(\Omega_1)} \\ + \text{ bounded data terms.} \tag{4.24}$$

Hence by combining (4.24) with the second part of Lemma 1 we deduce that under all its assumptions,

$$\frac{1}{2}\mu_f \sum_{m=1}^{n} \Delta t \|\boldsymbol{\kappa}^{-\frac{1}{2}} \boldsymbol{z}_h^{m-1}\|^2_{L^2(\Omega_1)} \le C \exp(t_n), \tag{4.25}$$

with a constant C independent of h, n, and Δt. With (4.25) and the previous arguments (see (4.18)), we readily derive that

$$\sum_{m=1}^{n} \frac{1}{\Delta t}\|\bar{\sigma}_h^m - \bar{\sigma}_h^{m,\ell_m-1}\|^2_{L^2(\Omega_1)} \le C \exp(t_n). \tag{4.26}$$

Of course, the sum of differences

$$\frac{1}{M}\sum_{m=1}^{n}\|\delta(p_h^m)\|^2_{L^2(\Omega_1)}, \quad 2G\sum_{m=1}^{n}\|\boldsymbol{\varepsilon}(\delta(\boldsymbol{u}_h^m))\|^2_{L^2(\Omega)}, \quad \lambda\sum_{m=1}^{n}\|\nabla\cdot\delta(\boldsymbol{u}_h^m)\|^2_{L^2(\Omega)},$$

are also bounded independently of h, n, and Δt.

4.2. Additional stability of the discrete scheme

Neither (4.23) nor (4.25) address stability of the velocity's divergence. We can interpret the velocity equation as a constraint on the pressure equation and it is well known that in this case, a bound for this divergence requires a bound on the time derivatives of the pressure.

Proposition 8. *If q belongs to $\mathcal{C}^0([0,T]; L^2(\Omega_1))$, then*

$$\frac{1}{2}\sum_{m=1}^{n}\Delta t\|\nabla\cdot\boldsymbol{z}_h^n\|^2_{L^2(\Omega_1)} \le \frac{2}{M^2}\sum_{m=1}^{n}\frac{1}{\Delta t}\|\delta(p_h^m)\|^2_{L^2(\Omega_1)} + 2\alpha^2\sum_{m=1}^{n}\frac{1}{\Delta t}\|\nabla\cdot\delta(\boldsymbol{u}_h^m)\|^2_{L^2(\Omega_1)} \\ + 2\frac{\alpha^2}{K_b^2}\sum_{m=1}^{n}\frac{1}{\Delta t}\|\bar{\sigma}_h^m - \bar{\sigma}_h^{m,\ell_m-1}\|^2_{L^2(\Omega_1)} + 2\sum_{m=1}^{n}\Delta t\|q^m\|^2_{L^2(\Omega_1)}. \tag{4.27}$$

Proof. Owing to the compatibility condition (3.6), (4.9) can be tested with $\theta_h = \nabla\cdot\boldsymbol{z}_h^n$, for $n \ge 1$,

$$\Delta t\|\nabla\cdot\boldsymbol{z}_h^n\|^2_{L^2(\Omega_1)} = -\frac{1}{M}\big(\delta(p_h^n),\nabla\cdot\boldsymbol{z}_h^n\big)_{\Omega_1} - \alpha\big(\nabla\cdot\delta(\boldsymbol{u}_h^n),\nabla\cdot\boldsymbol{z}_h^n\big)_{\Omega_1} + \frac{\alpha}{K_b}\big(\bar{\sigma}_h^n - \bar{\sigma}_h^{n,\ell_n-1},\nabla\cdot\boldsymbol{z}_h^n\big)_{\Omega_1} + \Delta t\big(q^n,\nabla\cdot\boldsymbol{z}_h^n\big)_{\Omega_1}.$$

From this, we easily derive (4.27) by Young's inequality. □

Hence a uniform (L^2 in time) bound for the divergence of the velocity requires a uniform bound (L^2 in time) for the time derivative of the pressure and divergence of the displacement. This is the object of the next lemma.

Lemma 2. *Under the assumptions of Proposition 5, we have*

$$\frac{1}{2M}\sum_{m=1}^{n}\frac{1}{\Delta t}\|\delta(p_h^m)\|^2_{L^2(\Omega_1)} + G\sum_{m=1}^{n}\frac{1}{\Delta t}\|\boldsymbol{\varepsilon}(\delta(\boldsymbol{u}_h^m))\|^2_{L^2(\Omega)} + \lambda\sum_{m=1}^{n}\frac{1}{\Delta t}\|\nabla\cdot\delta(\boldsymbol{u}_h^m)\|^2_{L^2(\Omega)} \\ + \frac{\mu_f}{2}\Big(\|\boldsymbol{\kappa}^{-\frac{1}{2}}\boldsymbol{z}_h^n\|^2_{L^2(\Omega_1)} + \|\boldsymbol{\kappa}^{-\frac{1}{2}}\boldsymbol{z}_h^1\|^2_{L^2(\Omega_1)} + \sum_{m=1}^{n-1}\|\boldsymbol{\kappa}^{-\frac{1}{2}}\delta(\boldsymbol{z}_h^{m+1})\|^2_{L^2(\Omega_1)}\Big)$$

$$\le \mu_f\big(\boldsymbol{\kappa}^{-1}\boldsymbol{z}_h^0, \boldsymbol{z}_h^1\big)_{\Omega_1} + M\sum_{m=1}^{n}\Delta t\|q^m\|^2_{L^2(\Omega_1)} + \frac{\mathcal{K}^2}{4G}\sum_{m=1}^{n}\frac{1}{\Delta t}\big(\mathcal{P}\|\delta(\boldsymbol{f}^m)\|_{L^2(\Omega)} + C_N\|\delta(\boldsymbol{t}_N^m)\|_{(H_{00}^{\frac12}(\Gamma_N))'}\big)^2 + \Big(\frac{\alpha}{K_b}\Big)^2 M\sum_{m=1}^{n}\frac{1}{\Delta t}\|\bar\sigma_h^m - \bar\sigma_h^{m,\ell_m-1}\|^2_{L^2(\Omega_1)}. \tag{4.28}$$

Proof. To derive a bound for the time derivative of the pressure, (4.9) is tested with $\theta_h = \delta(p_h^n)$,

$$\frac{1}{M\Delta t}\|\delta(p_h^n)\|^2_{L^2(\Omega_1)} + \frac{\alpha}{\Delta t}\big(\nabla\cdot\delta(\boldsymbol{u}_h^n), \delta(p_h^n)\big)_{\Omega_1} + \big(\nabla\cdot \boldsymbol{z}_h^n, \delta(p_h^n)\big)_{\Omega_1} = \frac{\alpha}{K_b}\frac{1}{\Delta t}\big(\bar\sigma_h^n - \bar\sigma_h^{n,\ell_n-1}, \delta(p_h^n)\big)_{\Omega_1} + \big(q^n, \delta(p_h^n)\big)_{\Omega_1}.$$

The displacement equation (3.19) at times t_n and t_{n-1} gives

$$\alpha\big(\delta(p_h^n), \nabla\cdot\boldsymbol{v}_h\big)_{\Omega_1} = 2G\big(\boldsymbol{\varepsilon}(\delta(\boldsymbol{u}_h^n)), \boldsymbol{\varepsilon}(\boldsymbol{v}_h)\big)_{\Omega} + \lambda\big(\nabla\cdot\delta(\boldsymbol{u}_h^n), \nabla\cdot\boldsymbol{v}_h\big)_{\Omega} - \big(\delta(\boldsymbol{f}^n), \boldsymbol{v}_h\big)_{\Omega} - \big\langle\delta(\boldsymbol{t}_N^n), \boldsymbol{v}_h\big\rangle_{\Gamma_N}.$$

By combining these two equalities, summing, and applying Poincaré's and Korn's inequalities and a trace, inequality, we deduce

$$\begin{aligned}
&\frac{1}{M}\sum_{m=1}^{n}\frac{1}{\Delta t}\|\delta(p_h^m)\|^2_{L^2(\Omega_1)} + 2G\sum_{m=1}^{n}\frac{1}{\Delta t}\|\boldsymbol{\varepsilon}(\delta(\boldsymbol{u}_h^m))\|^2_{L^2(\Omega)} + \lambda\sum_{m=1}^{n}\frac{1}{\Delta t}\|\nabla\cdot\delta(\boldsymbol{u}_h^m)\|^2_{L^2(\Omega)}\\
&\qquad\le \sum_{m=1}^{n}\|q^m\|_{L^2(\Omega_1)}\|\delta(p_h^m)\|_{L^2(\Omega_1)}\\
&\qquad+ \mathcal{K}\sum_{m=1}^{n}\frac{1}{\Delta t}\big(\mathcal{P}\|\delta(\boldsymbol{f}^m)\|_{L^2(\Omega)} + C_N\|\delta(\boldsymbol{t}_N^m)\|_{(H_{00}^{\frac12}(\Gamma_N))'}\big)\|\boldsymbol{\varepsilon}(\delta(\boldsymbol{u}_h^m))\|_{L^2(\Omega)}\\
&\qquad+ \frac{\alpha}{K_b}\sum_{m=1}^{n}\frac{1}{\Delta t}\|\bar\sigma_h^m - \bar\sigma_h^{m,\ell_m-1}\|_{L^2(\Omega_1)}\|\delta(p_h^m)\|_{L^2(\Omega_1)} - \sum_{m=1}^{n}\big(\nabla\cdot\boldsymbol{z}_h^m, \delta(p_h^m)\big)_{\Omega_1}.
\end{aligned} \tag{4.29}$$

Of course, the last term cannot be left as such. Let us sum it by parts,

$$-\sum_{m=1}^{n}\big(\nabla\cdot\boldsymbol{z}_h^m, \delta(p_h^m)\big)_{\Omega_1} = \sum_{m=1}^{n-1}\big(\nabla\cdot\delta(\boldsymbol{z}_h^{m+1}), p_h^m\big)_{\Omega_1} - \big(\nabla\cdot\boldsymbol{z}_h^n, p_h^n\big)_{\Omega_1} + \big(\nabla\cdot\boldsymbol{z}_h^1, p_h^0\big)_{\Omega_1}.$$

For the sum, we test the velocity equation (3.17), first with $\boldsymbol{z}_h^{m+1}$, next with $\boldsymbol{z}_h^m$, and for the last and first terms, we test it with $\boldsymbol{z}_h^n$ and with $\boldsymbol{z}_h^1$. By collecting these equalities, the gravity terms cancel, we obtain

$$\begin{aligned}
-\sum_{m=1}^{n}\big(\nabla\cdot\boldsymbol{z}_h^m, \delta(p_h^m)\big)_{\Omega_1} &= \frac{\mu_f}{2}\Big(\|\boldsymbol{\kappa}^{-\frac12}\boldsymbol{z}_h^n\|^2_{L^2(\Omega_1)} - \|\boldsymbol{\kappa}^{-\frac12}\boldsymbol{z}_h^1\|^2_{L^2(\Omega_1)} - \sum_{m=1}^{n-1}\|\boldsymbol{\kappa}^{-\frac12}\delta(\boldsymbol{z}_h^{m+1})\|^2_{L^2(\Omega_1)}\Big)\\
&\quad - \mu_f\|\boldsymbol{\kappa}^{-\frac12}\boldsymbol{z}_h^n\|^2_{L^2(\Omega_1)} + \mu_f\big(\boldsymbol{\kappa}^{-1}\boldsymbol{z}_h^0, \boldsymbol{z}_h^1\big)_{\Omega_1}.
\end{aligned} \tag{4.30}$$

When (4.30) is substituted into (4.29), we find

$$\begin{aligned}
&\frac{1}{M}\sum_{m=1}^{n}\frac{1}{\Delta t}\|\delta(p_h^m)\|^2_{L^2(\Omega_1)} + 2G\sum_{m=1}^{n}\frac{1}{\Delta t}\|\boldsymbol{\varepsilon}(\delta(\boldsymbol{u}_h^m))\|^2_{L^2(\Omega)} + \lambda\sum_{m=1}^{n}\frac{1}{\Delta t}\|\nabla\cdot\delta(\boldsymbol{u}_h^m)\|^2_{L^2(\Omega)}\\
&\qquad+ \frac{\mu_f}{2}\Big(\|\boldsymbol{\kappa}^{-\frac12}\boldsymbol{z}_h^n\|^2_{L^2(\Omega_1)} + \|\boldsymbol{\kappa}^{-\frac12}\boldsymbol{z}_h^1\|^2_{L^2(\Omega_1)} + \sum_{m=1}^{n-1}\|\boldsymbol{\kappa}^{-\frac12}\delta(\boldsymbol{z}_h^{m+1})\|^2_{L^2(\Omega_1)}\Big)\\
&\qquad\le \mu_f\big(\boldsymbol{\kappa}^{-1}\boldsymbol{z}_h^0, \boldsymbol{z}_h^1\big)_{\Omega_1} + \sum_{m=1}^{n}\|q^m\|_{L^2(\Omega_1)}\|\delta(p_h^m)\|_{L^2(\Omega_1)}
\end{aligned}$$

$$+ \mathcal{K}\sum_{m=1}^{n} \frac{1}{\Delta t}\big(\mathcal{P}\|\delta(\boldsymbol{f}^m)\|_{L^2(\Omega)} + C_N\|\delta(\boldsymbol{t}_N^m)\|_{(H_{00}^{\frac{1}{2}}(\Gamma_N))'}\big)\|\boldsymbol{\varepsilon}(\delta(\boldsymbol{u}_h^m))\|_{L^2(\Omega)}$$
$$+ \frac{\alpha}{K_b}\sum_{m=1}^{n} \frac{1}{\Delta t}\|\bar{\sigma}_h^m - \bar{\sigma}_h^{m,\ell_m-1}\|_{L^2(\Omega_1)}\|\delta(p_h^m)\|_{L^2(\Omega_1)},$$

and (4.28) follows by suitable applications of Young's inequality. □

Then (4.26) leads to the stability for all n of

$$\frac{1}{M}\sum_{m=1}^{n}\frac{1}{\Delta t}\|\delta(p_h^m)\|^2_{L^2(\Omega_1)},\quad 2G\sum_{m=1}^{n}\frac{1}{\Delta t}\|\boldsymbol{\varepsilon}(\delta(\boldsymbol{u}_h^m))\|^2_{L^2(\Omega)},\quad \lambda\sum_{m=1}^{n}\frac{1}{\Delta t}\|\nabla\cdot\delta(\boldsymbol{u}_h^m)\|^2_{L^2(\Omega)},\quad \|\boldsymbol{\kappa}^{-\frac{1}{2}}\boldsymbol{z}_h^n\|^2_{L^2(\Omega_1)}.$$

In view of (4.27), this in turn leads to the stability of

$$\frac{1}{2}\sum_{m=1}^{n}\Delta t\|\nabla\cdot\boldsymbol{z}_h^n\|^2_{L^2(\Omega_1)}.$$

5. First a posteriori analysis

To simplify, all a posteriori analysis will be done under the assumption that the exact solution is smooth enough.

In contrast to Enriched Galerkin or Discontinuous Galerkin discretizations of the flow equation, as is done in [5], a posteriori estimates for a mixed discretization of the flow equation are not derived by the two consecutive steps used in establishing stability in Section 4. Indeed, the velocity's divergence is eliminated in the a priori estimates of Section 4.1, so that all other terms can be bounded. As we shall see below, this is not the case of a posteriori estimates, and although we shall still proceed in two steps, the first step will not produce an independent estimate; this will be closed in the second step.

As is usual in time dependent problems, we need to interpolate the discrete sequences in time. As the time discretization is first order, for any discrete function in time v^n, we define the affine, globally continuous function in each interval $[t_{n-1}, t_n]$, for $1 \le n \le N$,

$$v_\tau^n = v^{n-1} + \frac{t - t_{n-1}}{\Delta t}(v^n - v^{n-1}), \quad t \in [t_{n-1}, t_n]. \tag{5.1}$$

5.1. First basic error equation

The discrete flow equation (3.16) reads in each interval $]t_{n-1}, t_n]$

$$\forall\theta_h \in M_h,\quad \Big(\frac{1}{M} + \frac{\alpha^2}{K_b}\Big)\big(\partial_t p_{h\tau}^{n,\ell}, \theta_h\big)_{\Omega_1} + \big(\nabla\cdot\boldsymbol{z}_h^{n,\ell}, \theta_h\big)_{\Omega_1} = -\frac{\alpha}{K_b}\big(\partial_t\bar{\sigma}_{h\tau}^{n,\ell-1}, \theta_h\big)_{\Omega_1} + (q^n, \theta_h)_{\Omega_1}. \tag{5.2}$$

Hence, assuming that $\partial_t p$, $\nabla\cdot(\partial_t\boldsymbol{u})$, and $\nabla\cdot\boldsymbol{z}$ are sufficiently smooth in each interval $]t_{n-1}, t_n]$, the flow's error equation, tested with θ_h, is

$$\forall\theta_h \in M_h,\quad \Big(\frac{1}{M} + \frac{\alpha^2}{K_b}\Big)\big(\partial_t(p - p_{h\tau}^{n,\ell}), \theta_h\big)_{\Omega_1} + \big(\nabla\cdot(\boldsymbol{z} - \boldsymbol{z}_h^{n,\ell}), \theta_h\big)_{\Omega_1} + \frac{\alpha}{K_b}\big(\partial_t(\bar{\sigma} - \bar{\sigma}_{h\tau}^{n,\ell-1}), \theta_h\big)_{\Omega_1} = (q - q^n, \theta_h)_{\Omega_1}. \tag{5.3}$$

Let θ be an arbitrary function in $L^2(\Omega_1)$. The exact flow equation (2.6) tested with $\theta - \theta_h$ reads in each interval $]t_{n-1}, t_n]$,

$$\forall\theta_h \in M_h,\quad \Big(\frac{1}{M} + \frac{\alpha^2}{K_b}\Big)(\partial_t p, \theta - \theta_h)_{\Omega_1} + \big(\nabla\cdot\boldsymbol{z}, \theta - \theta_h\big)_{\Omega_1} = -\frac{\alpha}{K_b}\big(\partial_t\bar{\sigma}, \theta - \theta_h\big)_{\Omega_1} + (q, \theta - \theta_h)_{\Omega_1}. \tag{5.4}$$

Therefore, by writing $\theta = \theta - \theta_h + \theta_h$ and using (5.3) and (5.4), the flow error tested with any $\theta \in L^2(\Omega_1)$, becomes for all $\theta_h \in M_h$, in each interval $]t_{n-1}, t_n]$,

$$\begin{aligned}&\Big(\frac{1}{M} + \frac{\alpha^2}{K_b}\Big)\big(\partial_t(p - p_{h\tau}^{n,\ell}), \theta\big)_{\Omega_1} + \big(\nabla\cdot(z - z_h^{n,\ell}), \theta\big)_{\Omega_1} + \frac{\alpha}{K_b}\big(\partial_t(\bar\sigma - \bar\sigma_{h\tau}^{n,l-1}), \theta\big)_{\Omega_1}\\&= (q, \theta - \theta_h)_{\Omega_1} - \Big[\Big(\frac{1}{M} + \frac{\alpha^2}{K_b}\Big)(\partial_t p_{h\tau}^{n,\ell}, \theta - \theta_h)_{\Omega_1} + \big(\nabla\cdot z_h^{n,\ell}, \theta - \theta_h\big)_{\Omega_1} + \frac{\alpha}{K_b}\big(\partial_t \bar\sigma_{h\tau}^{n,l-1}, \theta - \theta_h\big)_{\Omega_1}\Big]\\&+ (q - q^n, \theta_h)_{\Omega_1}.\end{aligned} \tag{5.5}$$

By observing that

$$(q^n, \theta_h)_{\Omega_1} = (q_h^n, \theta_h)_{\Omega_1} \text{ and } (q, \theta - \theta_h)_{\Omega_1} + (q - q_h^n, \theta_h)_{\Omega_1} = (q - q_h^n, \theta)_{\Omega_1} + (q_h^n, \theta - \theta_h)_{\Omega_1},$$

where q_h denotes the L^2 projection on $\mathbb{P}_k$ in each cell E, (5.5) becomes for all $\theta \in L^2(\Omega_1)$, all $\theta_h \in M_h$, and in each interval $]t_{n-1}, t_n]$,

$$\begin{aligned}&\Big(\frac{1}{M} + \frac{\alpha^2}{K_b}\Big)(\partial_t(p - p_{h\tau}^{n,\ell}), \theta)_{\Omega_1} + \big(\nabla\cdot(z - z_h^{n,\ell}), \theta\big)_{\Omega_1} + \frac{\alpha}{K_b}\big(\partial_t(\bar\sigma - \bar\sigma_{h\tau}^{n,l-1}), \theta\big)_{\Omega_1}\\&= (q - q_h^n, \theta)_{\Omega_1} + \sum_{E\subset\overline{\Omega}_1}\Big(q_h^n - \Big(\frac{1}{M} + \frac{\alpha^2}{K_b}\Big)\partial_t p_{h\tau}^{n,\ell} - \nabla\cdot z_h^{n,\ell} - \frac{\alpha}{K_b}\partial_t\bar\sigma_{h\tau}^{n,\ell-1}, \theta - \theta_h\Big)_E.\end{aligned} \tag{5.6}$$

The time error is exhibited by replacing $z_h^{n,\ell}$ by $z_{h\tau}^{n,\ell}$ in the left-hand side of (5.6), and the algorithmic error by collecting all terms involving $\frac{\alpha^2}{K_b}$; this gives the following intermediate flow error equality for all $\theta \in L^2(\Omega_1)$, all $\theta_h \in M_h$, in each interval $]t_{n-1}, t_n]$:

$$\begin{aligned}&\Big(\partial_t\Big(\frac{1}{M}(p - p_{h\tau}^{n,\ell}) + \alpha\nabla\cdot(\boldsymbol{u} - \boldsymbol{u}_{h\tau}^{n,\ell})\Big), \theta\Big)_{\Omega_1} + \big(\nabla\cdot(z - z_{h\tau}^{n,\ell}), \theta\big)_{\Omega_1}\\&\qquad= (q - q_h^n, \theta)_{\Omega_1} + \sum_{E\subset\overline{\Omega}_1}\Big(q_h^n - \partial_t\Big(\frac{1}{M}p_{h\tau}^{n,\ell} + \alpha\nabla\cdot\boldsymbol{u}_{h\tau}^{n,\ell}\Big) - \nabla\cdot z_h^{n,\ell}, \theta - \theta_h\Big)_E\\&\qquad+ \big(\nabla\cdot(z_h^{n,\ell} - z_{h\tau}^{n,\ell}), \theta\big)_{\Omega_1} - \frac{\alpha}{K_b}\big(\partial_t(\bar\sigma_{h\tau}^{n,\ell} - \bar\sigma_{h\tau}^{n,\ell-1}), \theta_h\big)_{\Omega_1}.\end{aligned} \tag{5.7}$$

By the assumption (3.6) on the spaces, we have

$$q_h^n - \frac{1}{M}\partial_t p_{h\tau}^{n,\ell} - \nabla\cdot z_h^{n,\ell} \in M_h.$$

Therefore, by choosing $\theta_h = P_h(\theta)$, the L^2 projection of θ on M_h in each element E, the second sum in the above right-hand side reduces to

$$-\sum_{E\subset\overline{\Omega}_1}\big(\alpha\partial_t\nabla\cdot\boldsymbol{u}_{h\tau}^{n,\ell}, \theta - P_h(\theta)\big)_E.$$

With this choice, we have the flow error equality for all $\theta \in L^2(\Omega_1)$, in each interval $]t_{n-1}, t_n]$:

$$\begin{aligned}&\Big(\partial_t\Big(\frac{1}{M}(p - p_{h\tau}^{n,\ell}) + \alpha\nabla\cdot(\boldsymbol{u} - \boldsymbol{u}_{h\tau}^{n,\ell})\Big), \theta\Big)_{\Omega_1} + \big(\nabla\cdot(z - z_{h\tau}^{n,\ell}), \theta\big)_{\Omega_1} = (q - q_h^n, \theta)_{\Omega_1}\\&- \sum_{E\subset\overline{\Omega}_1}\big(\alpha\partial_t\nabla\cdot\boldsymbol{u}_{h\tau}^{n,\ell}, \theta - P_h(\theta)\big)_E + \big(\nabla\cdot(z_h^{n,\ell} - z_{h\tau}^{n,\ell}), \theta\big)_{\Omega_1} - \frac{\alpha}{K_b}\big(\partial_t(\bar\sigma_{h\tau}^{n,\ell} - \bar\sigma_{h\tau}^{n,\ell-1}), P_h(\theta)\big)_{\Omega_1}.\end{aligned} \tag{5.8}$$

As Eq. (5.8) will be tested below with $\theta = p - p_{h\tau}^{n,\ell}$, we must examine the cross terms

$$\alpha\big(\nabla\cdot\partial_t(\boldsymbol{u} - \boldsymbol{u}_{h\tau}^{n,\ell}), p - p_{h\tau}^{n,\ell}\big)_{\Omega_1} \quad\text{and}\quad \big(\nabla\cdot(z - z_{h\tau}^{n,\ell}), p - p_{h\tau}^{n,\ell}\big)_{\Omega_1}.$$

The first term is obtained by means of the elasticity error equation. By arguing as above, it reads in each interval $]t_{n-1}, t_n]$, for all $\boldsymbol{v}$ in $\boldsymbol{W}$

$$\begin{aligned}\forall \boldsymbol{v}_h \in \boldsymbol{W}_h,\quad & 2G(\boldsymbol{\varepsilon}(\boldsymbol{u}-\boldsymbol{u}_{h\tau}^{n,\ell}), \boldsymbol{\varepsilon}(\boldsymbol{v}))_\Omega + \lambda(\nabla\cdot(\boldsymbol{u}-\boldsymbol{u}_{h\tau}^{n,\ell}), \nabla\cdot\boldsymbol{v})_\Omega - \alpha(p-p_{h\tau}^{n,\ell}, \nabla\cdot\boldsymbol{v})_{\Omega_1}\\ &= (\boldsymbol{f}-\boldsymbol{f}_{h\tau}^n, \boldsymbol{v})_\Omega + \big\langle \boldsymbol{t}_N - \boldsymbol{t}_{N,h\tau}^n, \boldsymbol{v}\big\rangle_{\Gamma_N}\\ &+ \sum_{E\subset\overline{\Omega}_1}(\boldsymbol{f}_{h\tau}^n + \nabla\cdot\boldsymbol{\sigma}(\boldsymbol{u}_{h\tau}^{n,\ell}) - \alpha\nabla p_{h\tau}^{n,\ell}, \boldsymbol{v}-\boldsymbol{v}_h)_E + \sum_{E\subset\overline{\Omega}_2}(\boldsymbol{f}_{h\tau}^n + \nabla\cdot\boldsymbol{\sigma}(\boldsymbol{u}_{h\tau}^{n,\ell}), \boldsymbol{v}-\boldsymbol{v}_h)_E\\ &- \sum_{e\in\mathcal{E}_h^1\cup\mathcal{E}_h^{12}}\big([\boldsymbol{\sigma}(\boldsymbol{u}_{h\tau}^{n,\ell}) - \alpha p_{h\tau}^{n,\ell}\boldsymbol{I}]_e\boldsymbol{n}_e, \boldsymbol{v}-\boldsymbol{v}_h\big)_e - \sum_{e\in\mathcal{E}_h^2}\big([\boldsymbol{\sigma}(\boldsymbol{u}_{h\tau}^{n,\ell})]_e\boldsymbol{n}_e, \boldsymbol{v}-\boldsymbol{v}_h\big)_e\\ &- \big\langle \boldsymbol{\sigma}(\boldsymbol{u}_{h\tau}^{n,\ell})\boldsymbol{n}_\Omega - \boldsymbol{t}_{N,h\tau}^n, \boldsymbol{v}-\boldsymbol{v}_h\big\rangle_{\Gamma_N}.\end{aligned}\tag{5.9}$$

Note that (5.9) is valid at initial time (i.e. when $n=0$). Note also that when the data and solution are smooth enough, (5.9) can be differentiated with respect to time,

$$\begin{aligned}&2G\big(\boldsymbol{\varepsilon}(\partial_t(\boldsymbol{u}-\boldsymbol{u}_{h\tau}^{n,\ell})), \boldsymbol{\varepsilon}(\boldsymbol{v})\big)_\Omega + \lambda\big(\nabla\cdot(\partial_t(\boldsymbol{u}-\boldsymbol{u}_{h\tau}^{n,\ell})), \nabla\cdot\boldsymbol{v}\big)_\Omega - \alpha\big(\partial_t(p-p_{h\tau}^{n,\ell}), \nabla\cdot\boldsymbol{v}\big)_{\Omega_1}\\ &= \big(\partial_t(\boldsymbol{f}-\boldsymbol{f}_{h\tau}^n), \boldsymbol{v}\big)_\Omega + \big\langle \partial_t(\boldsymbol{t}_N - \boldsymbol{t}_{N,h\tau}^n), \boldsymbol{v}\big\rangle_{\Gamma_N} - \big\langle \boldsymbol{\sigma}(\partial_t\boldsymbol{u}_{h\tau}^{n,\ell})\boldsymbol{n}_\Omega - \partial_t\boldsymbol{t}_{N,h\tau}^n, \boldsymbol{v}-\boldsymbol{v}_h\big\rangle_{\Gamma_N}\\ &+ \sum_{E\subset\overline{\Omega}_1}\Big(\partial_t\boldsymbol{f}_{h\tau}^n + \nabla\cdot\boldsymbol{\sigma}(\partial_t\boldsymbol{u}_{h\tau}^{n,\ell}) - \alpha\nabla\partial_t p_{h\tau}^{n,\ell}, \boldsymbol{v}-\boldsymbol{v}_h\Big)_E + \sum_{E\subset\overline{\Omega}_2}\Big(\partial_t\boldsymbol{f}_{h\tau}^n + \nabla\cdot\boldsymbol{\sigma}(\partial_t\boldsymbol{u}_{h\tau}^{n,\ell}), \boldsymbol{v}-\boldsymbol{v}_h\Big)_E\\ &- \sum_{e\in\mathcal{E}_h^1\cup\mathcal{E}_h^{12}}\big([\boldsymbol{\sigma}(\partial_t\boldsymbol{u}_{h\tau}^{n,\ell}) - \alpha\partial_t p_{h\tau}^{n,\ell}\boldsymbol{I}]_e\boldsymbol{n}_e, \boldsymbol{v}-\boldsymbol{v}_h\big)_e - \sum_{e\in\mathcal{E}_h^2}\big([\boldsymbol{\sigma}(\partial_t\boldsymbol{u}_{h\tau}^{n,\ell})]_e\boldsymbol{n}_e, \boldsymbol{v}-\boldsymbol{v}_h\big)_e.\end{aligned}\tag{5.10}$$

It stems from (5.9) tested with $\boldsymbol{v} = \partial_t(\boldsymbol{u}-\boldsymbol{u}_{h\tau}^{n,\ell})$ that

$$\begin{aligned}&\alpha\big(\nabla\cdot\partial_t(\boldsymbol{u}-\boldsymbol{u}_{h\tau}^{n,\ell}), p-p_{h\tau}^{n,\ell}\big)_{\Omega_1} = G\frac{d}{dt}\|\boldsymbol{\varepsilon}(\boldsymbol{u}-\boldsymbol{u}_{h\tau}^{n,\ell})\|_{L^2(\Omega)}^2 + \frac{\lambda}{2}\frac{d}{dt}\|\nabla\cdot(\boldsymbol{u}-\boldsymbol{u}_{h\tau}^{n,\ell})\|_{L^2(\Omega)}^2\\ &- \big(\boldsymbol{f}-\boldsymbol{f}_{h\tau}^n, \partial_t(\boldsymbol{u}-\boldsymbol{u}_{h\tau}^{n,\ell})\big)_\Omega - \big\langle \boldsymbol{t}_N - \boldsymbol{t}_{N,h\tau}^n, \partial_t(\boldsymbol{u}-\boldsymbol{u}_{h\tau}^{n,\ell})\big\rangle_{\Gamma_N}\\ &- \sum_{E\subset\overline{\Omega}_1}\Big(\boldsymbol{f}_{h\tau}^n + \nabla\cdot\boldsymbol{\sigma}(\boldsymbol{u}_{h\tau}^{n,\ell}) - \alpha\nabla p_{h\tau}^{n,\ell}, \partial_t(\boldsymbol{u}-\boldsymbol{u}_{h\tau}^{n,\ell}) - \partial_t\boldsymbol{v}_h\Big)_E\\ &- \sum_{E\subset\overline{\Omega}_2}\Big(\boldsymbol{f}_{h\tau}^n + \nabla\cdot\boldsymbol{\sigma}(\boldsymbol{u}_{h\tau}^{n,\ell}), \partial_t(\boldsymbol{u}-\boldsymbol{u}_{h\tau}^{n,\ell}) - \partial_t\boldsymbol{v}_h\Big)_E\\ &+ \sum_{e\in\mathcal{E}_h^1\cup\mathcal{E}_h^{12}}\big([\boldsymbol{\sigma}(\boldsymbol{u}_{h\tau}^{n,\ell}) - \alpha p_{h\tau}^{n,\ell}\boldsymbol{I}]_e\boldsymbol{n}_e, \partial_t(\boldsymbol{u}-\boldsymbol{u}_{h\tau}^{n,\ell}) - \partial_t\boldsymbol{v}_h\big)_e + \sum_{e\in\mathcal{E}_h^2}\big([\boldsymbol{\sigma}(\boldsymbol{u}_{h\tau}^{n,\ell})]_e\boldsymbol{n}_e, \partial_t(\boldsymbol{u}-\boldsymbol{u}_{h\tau}^{n,\ell}) - \partial_t\boldsymbol{v}_h\big)_e\\ &+ \big\langle \boldsymbol{\sigma}(\boldsymbol{u}_{h\tau}^{n,\ell})\boldsymbol{n}_\Omega - \boldsymbol{t}_{N,h\tau}^n, \partial_t(\boldsymbol{u}-\boldsymbol{u}_{h\tau}^{n,\ell}) - \partial_t\boldsymbol{v}_h\big\rangle_{\Gamma_N}.\end{aligned}\tag{5.11}$$

This gives a first basic error equation.

Lemma 3. *Let the solution be smooth enough so that all terms below are meaningful. Then, the following error equality holds in each interval* $]t_{n-1}, t_n]$, $1 \le n \le N$*:*

$$\begin{aligned}&\frac{d}{dt}\Big(\frac{1}{2M}\|p-p_{h\tau}^{n,\ell}\|_{L^2(\Omega_1)}^2 + G\|\boldsymbol{\varepsilon}(\boldsymbol{u}-\boldsymbol{u}_{h\tau}^{n,\ell})\|_{L^2(\Omega)}^2 + \frac{\lambda}{2}\|\nabla\cdot(\boldsymbol{u}-\boldsymbol{u}_{h\tau}^{n,\ell})\|_{L^2(\Omega)}^2\Big)\\ &= -\big(\nabla\cdot(\boldsymbol{z}-\boldsymbol{z}_{h\tau}^{n,\ell}), p-p_{h\tau}^{n,\ell}\big)_{\Omega_1} + \big(\nabla\cdot(\boldsymbol{z}_h^{n,\ell}-\boldsymbol{z}_{h\tau}^{n,\ell}), p-p_{h\tau}^{n,\ell}\big)_{\Omega_1} + (q-q_h^n, p-p_{h\tau}^{n,\ell})_{\Omega_1}\\ &- \sum_{E\subset\overline{\Omega}_1}\big(\alpha\partial_t\nabla\cdot\boldsymbol{u}_{h\tau}^{n,\ell}, p-p_{h\tau}^{n,\ell} - P_h(p-p_{h\tau}^{n,\ell})\big)_E - \frac{\alpha}{K_b}\big(\partial_t(\bar{\sigma}_{h\tau}^{n,\ell} - \bar{\sigma}_{h\tau}^{n,\ell-1}), P_h(p-p_{h\tau}^{n,\ell})\big)_{\Omega_1}\end{aligned}$$

$$
\begin{aligned}
&+ \big(\boldsymbol{f} - \boldsymbol{f}^n_{h\tau}, \partial_t(\boldsymbol{u} - \boldsymbol{u}^{n,\ell}_{h\tau})\big)_\Omega + \big\langle \boldsymbol{t}_N - \boldsymbol{t}^n_{N,h\tau}, \partial_t(\boldsymbol{u} - \boldsymbol{u}^{n,\ell}_{h\tau})\big\rangle_{\Gamma_N} \\
&+ \sum_{E\subset\overline{\Omega}_1} \Big(\boldsymbol{f}^n_{h\tau} + \nabla\cdot\boldsymbol{\sigma}(\boldsymbol{u}^{n,\ell}_{h\tau}) - \alpha\nabla p^{n,\ell}_{h\tau}, \partial_t(\boldsymbol{u} - \boldsymbol{u}^{n,\ell}_{h\tau}) - \partial_t\boldsymbol{v}_h\Big)_E \\
&+ \sum_{E\subset\overline{\Omega}_2} \Big(\boldsymbol{f}^n_{h\tau} + \nabla\cdot\boldsymbol{\sigma}(\boldsymbol{u}^{n,\ell}_{h\tau}), \partial_t(\boldsymbol{u} - \boldsymbol{u}^{n,\ell}_{h\tau}) - \partial_t\boldsymbol{v}_h\Big)_E \\
&- \sum_{e\in\mathcal{E}^1_h\cup\mathcal{E}^{12}_h} \big([\boldsymbol{\sigma}(\boldsymbol{u}^{n,\ell}_{h\tau}) - \alpha p^{n,\ell}_{h\tau}\boldsymbol{I}]_e\boldsymbol{n}_e, \partial_t(\boldsymbol{u} - \boldsymbol{u}^{n,\ell}_{h\tau}) - \partial_t\boldsymbol{v}_h\big)_e - \sum_{e\in\mathcal{E}^2_h} \big([\boldsymbol{\sigma}(\boldsymbol{u}^{n,\ell}_{h\tau})]_e\boldsymbol{n}_e, \partial_t(\boldsymbol{u} - \boldsymbol{u}^{n,\ell}_{h\tau}) - \partial_t\boldsymbol{v}_h\big)_e \\
&- \big\langle \boldsymbol{\sigma}(\boldsymbol{u}^{n,\ell}_{h\tau})\boldsymbol{n}_\Omega - \boldsymbol{t}^n_{N,h\tau}, \partial_t(\boldsymbol{u} - \boldsymbol{u}^{n,\ell}_{h\tau}) - \partial_t\boldsymbol{v}_h\big\rangle_{\Gamma_N}.
\end{aligned}
\tag{5.12}
$$

Remark 1. *The degree m of the discrete displacements is frequently chosen as* $m = \max(1, k)$*; when the elements are simplices, then* $\alpha\partial_t\nabla\cdot\boldsymbol{u}^{n,\ell}_{h\tau}$ *is also in* M_h*. As a result,*

$$q^n_h - \partial_t(\frac{1}{M}p^{n,\ell}_{h\tau} + \alpha\nabla\cdot\boldsymbol{u}^{n,\ell}_{h\tau}) - \nabla\cdot\boldsymbol{z}^{n,\ell}_h \in M_h,$$

and this term vanishes when tested by $\theta_h = P_h(\theta)$*.*

5.2. The velocity cross term

The velocity error equation yields a first error equality for the second cross term. Indeed we deduce from (2.12) and (3.17) for all $\boldsymbol{\zeta} \in \boldsymbol{Z}$ and $\boldsymbol{\zeta}_h \in \boldsymbol{Z}_h$,

$$\big(\mu_f\boldsymbol{\kappa}^{-1}(z - z^{n,\ell}_{h\tau}), \boldsymbol{\zeta}\big)_{\Omega_1} - (p - p^{n,\ell}_{h\tau}, \nabla\cdot\boldsymbol{\zeta})_{\Omega_1} = \big(-\mu_f\boldsymbol{\kappa}^{-1}z^{n,\ell}_{h\tau} + \rho g\nabla\eta, \boldsymbol{\zeta} - \boldsymbol{\zeta}_h\big)_{\Omega_1} + \big(p^{n,\ell}_{h\tau}, \nabla\cdot(\boldsymbol{\zeta} - \boldsymbol{\zeta}_h)\big)_{\Omega_1}. \tag{5.13}$$

The difficulty with this equality is that little can be gained from approximating $\boldsymbol{\zeta}$ because it is only in $H(\text{div}, \Omega_1)$. As a remedy, first [9] and next [10] proposed to replace $\boldsymbol{\zeta}$ by the following Helmholtz decomposition:

Lemma 4. *Let* Ω_1 *be a Lipschitz domain of* $\mathbb{R}^3$*. For any* $\boldsymbol{\zeta} \in H_0(\text{div}, \Omega_1)$*, there exist* $\boldsymbol{\lambda}$ *and* $\boldsymbol{\psi}$ *both in* $H^1_0(\Omega_1)^3$ *and constants C depending only on the domain, such that*

$$\boldsymbol{\zeta} = \boldsymbol{\lambda} + \mathbf{curl}\,\boldsymbol{\psi},$$

and

$$\|\boldsymbol{\lambda}\|_{H^1(\Omega_1)} \le C\|\nabla\cdot\boldsymbol{\zeta}\|_{L^2(\Omega_1)}, \quad \|\boldsymbol{\psi}\|_{H^1(\Omega_1)} \le C\big(\|\boldsymbol{\zeta}\|_{L^2(\Omega_1)} + \|\nabla\cdot\boldsymbol{\zeta}\|_{L^2(\Omega_1)}\big). \tag{5.14}$$

It can be obtained by first lifting the divergence with a function in $H^1_0(\Omega_1)^3$ and next writing the difference as the curl of a function in $H^1_0(\Omega_1)^3$.

To approximate $\boldsymbol{\zeta}$, we can take

$$\boldsymbol{\zeta}_h = \Pi_h(\boldsymbol{\lambda}) + \mathbf{curl}\,S_h(\boldsymbol{\psi}),$$

where Π_h is the standard Raviart–Thomas interpolant which is well-defined since $\boldsymbol{\lambda}$ is now smooth enough, and S_h is the regularizing Scott–Zhang operator of order $k+1$ such that $\mathbf{curl}\,R_h(\boldsymbol{\psi})$ belongs to $\boldsymbol{Z}_h$ (recall that $S_h(\boldsymbol{\psi})$ belongs to $H^1_0(\Omega_1)^3$ owing that $\boldsymbol{\psi} \in H^1_0(\Omega_1)^3$). To simplify, we drop for the moment the superscripts n, ℓ. By applying Green's formula in each element E,

$$\big(p_{h\tau}, \nabla\cdot(\boldsymbol{\zeta} - \boldsymbol{\zeta}_h)\big)_{\Omega_1} = \big(p_{h\tau}, \nabla\cdot(\boldsymbol{\lambda} - \Pi_h(\boldsymbol{\lambda}))\big)_{\Omega_1} = -\sum_{E\in\overline{\Omega}_1}\big(\nabla p_{h\tau}, \boldsymbol{\lambda} - \Pi_h(\boldsymbol{\lambda})\big)_E + \sum_{e\in\mathcal{E}^1_h}\int_e [p_{h\tau}]_e(\boldsymbol{\lambda} - \Pi_h(\boldsymbol{\lambda}))\cdot\boldsymbol{n}_e.$$

Therefore

$$
\begin{aligned}
\big(\mu_f\boldsymbol{\kappa}^{-1}(z - z_{h\tau}), \boldsymbol{\zeta}\big)_{\Omega_1} - (p - p_{h\tau}, \nabla\cdot\boldsymbol{\zeta})_{\Omega_1} &= \sum_{E\in\overline{\Omega}_1}\big(-\mu_f\boldsymbol{\kappa}^{-1}z_{h\tau} + \rho g\nabla\eta - \nabla p_{h\tau}, \boldsymbol{\lambda} - \Pi_h(\boldsymbol{\lambda})\big)_E \\
&+ \sum_{E\in\overline{\Omega}_1}\big(-\mu_f\boldsymbol{\kappa}^{-1}z_{h\tau} + \rho g\nabla\eta, \mathbf{curl}(\boldsymbol{\psi} - S_h(\boldsymbol{\psi}))\big)_E + \sum_{e\in\mathcal{E}^1_h}\int_e [p_{h\tau}]_e(\boldsymbol{\lambda} - \Pi_h(\boldsymbol{\lambda}))\cdot\boldsymbol{n}_e.
\end{aligned}
\tag{5.15}
$$

Note that

$$\forall r \in H^1(\Omega_1), \quad \sum_{E\in\overline{\Omega}_1} \big(-\mu_f \boldsymbol{\kappa}^{-1} \boldsymbol{z}_{h\tau} + \rho g \nabla \eta, \mathbf{curl}(\boldsymbol{\psi} - S_h(\boldsymbol{\psi}))\big)_E$$
$$= \sum_{E\in\overline{\Omega}_1} \big(-\mu_f \boldsymbol{\kappa}^{-1} \boldsymbol{z}_{h\tau} + \rho g \nabla \eta - \nabla r, \mathbf{curl}(\boldsymbol{\psi} - R_h(\boldsymbol{\psi}))\big)_E.$$

In [9,10], Green's formula is also applied to this sum. But the computing load of the resulting terms (that will be error indicators) is high, and we prefer to keep this sum unchanged. Then, we have the following velocity error equality for all $r \in H^1(\Omega_1)$:

$$\big(\mu_f \boldsymbol{\kappa}^{-1}(\boldsymbol{z} - \boldsymbol{z}_{h\tau}^{n,\ell}), \boldsymbol{\zeta}\big)_{\Omega_1} - (p - p_{h\tau}^{n,\ell}, \nabla\cdot\boldsymbol{\zeta})_{\Omega_1} = \sum_{E\in\overline{\Omega}_1} \big(-\mu_f \boldsymbol{\kappa}^{-1} \boldsymbol{z}_{h\tau}^{n,\ell} + \rho g \nabla \eta - \nabla p_{h\tau}^{n,\ell}, \boldsymbol{\lambda} - \Pi_h(\boldsymbol{\lambda})\big)_E$$
$$+ \sum_{E\in\overline{\Omega}_1} \big(-\mu_f \boldsymbol{\kappa}^{-1} \boldsymbol{z}_{h\tau}^{n,\ell} + \rho g \nabla \eta - \nabla r, \mathbf{curl}(\boldsymbol{\psi} - S_h(\boldsymbol{\psi}))\big)_E + \sum_{e\in\mathcal{E}_h^1} \int_e [p_{h\tau}^{n,\ell}]_e (\boldsymbol{\lambda} - \Pi_h(\boldsymbol{\lambda}))\cdot\boldsymbol{n}_e. \tag{5.16}$$

Let us bound the terms in the right-hand side of (5.16). In view of (5.14), the first and last sums give

$$\Big|\sum_{E\in\overline{\Omega}_1} \big(-\mu_f \boldsymbol{\kappa}^{-1} \boldsymbol{z}_{h\tau} + \rho g \nabla \eta - \nabla p_{h\tau}, \boldsymbol{\lambda} - \Pi_h(\boldsymbol{\lambda})\big)_E\Big|$$
$$\le C\Big(\sum_{E\in\overline{\Omega}_1} h_E^2 \|-\mu_f \boldsymbol{\kappa}^{-1} \boldsymbol{z}_{h\tau} + \rho g \nabla \eta - \nabla p_{h\tau}\|_{L^2(E)}^2\Big)^{\frac12} \|\nabla\cdot\boldsymbol{\zeta}\|_{L^2(\Omega_1)}, \tag{5.17}$$

and

$$\Big|\sum_{e\in\mathcal{E}_h^1} \int_e [p_{h\tau}]_e (\boldsymbol{\lambda} - \Pi_h(\boldsymbol{\lambda}))\cdot\boldsymbol{n}_e\Big| \le C\Big(\sum_{e\in\mathcal{E}_h^1} h_e \|[p_{h\tau}]_e\|_{L^2(E)}^2\Big)^{\frac12} \|\nabla\cdot\boldsymbol{\zeta}\|_{L^2(\Omega_1)}. \tag{5.18}$$

There remains the middle sum,

$$\Big|\sum_{E\in\overline{\Omega}_1} \big(-\mu_f \boldsymbol{\kappa}^{-1} \boldsymbol{z}_{h\tau} + \rho g \nabla \eta, \mathbf{curl}(\boldsymbol{\psi} - P_h(\boldsymbol{\psi}))\big)_E\Big|$$
$$\le C \inf_{r\in H^1(\Omega_1)} \Big(\sum_{E\in\overline{\Omega}_1} \|-\mu_f \boldsymbol{\kappa}^{-1} \boldsymbol{z}_{h\tau} + \rho g \nabla \eta - \nabla r\|_{L^2(E)}^2\Big)^{1/2} \big(\|\boldsymbol{\zeta}\|_{L^2(\Omega_1)} + \|\nabla\cdot\boldsymbol{\zeta}\|_{L^2(\Omega_1)}\big). \tag{5.19}$$

A possible candidate for r is $R_h(p_{h\tau}^{n,\ell})$, where R_h is a regularization operator of the Scott–Zhang type that will be described in Section 5.4 ; with this choice, by substituting (5.17)–(5.19) into (5.15) tested with $\boldsymbol{\zeta} = \boldsymbol{z} - \boldsymbol{z}_{h\tau}^{n,\ell}$, we obtain

$$\big(p - p_{h\tau}^{n,\ell}, \nabla\cdot(\boldsymbol{z} - \boldsymbol{z}_{h\tau}^{n,\ell})\big)_{\Omega_1} = \mu_f \|\boldsymbol{\kappa}^{-\frac12}(\boldsymbol{z} - \boldsymbol{z}_{h\tau}^{n,\ell})\|_{L^2(\Omega_1)}^2 - B, \tag{5.20}$$

where

$$|B| \le C\Big[\Big(\sum_{E\subset\overline{\Omega}_1} h_E^2 \|-\mu_f \boldsymbol{\kappa}^{-1} \boldsymbol{z}_{h\tau}^{n,\ell} + \rho g \nabla \eta - \nabla p_{h\tau}^{n,\ell}\|_{L^2(E)}^2\Big)^{\frac12} + \Big(\sum_{e\in\mathcal{E}_h^1} h_e \|[p_{h\tau}]_e\|_{L^2(E)}^2\Big)^{\frac12}\Big]$$
$$\times \|\nabla\cdot(\boldsymbol{z} - \boldsymbol{z}_{h\tau}^{n,\ell})\|_{L^2(\Omega_1)}$$
$$+ C\Big(\sum_{E\in\overline{\Omega}_1} \|-\mu_f \boldsymbol{\kappa}^{-1} \boldsymbol{z}_{h\tau} + \rho g \nabla \eta - \nabla R_h(p_{h\tau}^{n,\ell})\|_{L^2(E)}^2\Big)^{\frac12} \big(\|\boldsymbol{z} - \boldsymbol{z}_{h\tau}^{n,\ell}\|_{L^2(\Omega_1)} + \|\nabla\cdot(\boldsymbol{z} - \boldsymbol{z}_{h\tau}^{n,\ell})\|_{L^2(\Omega_1)}\big). \tag{5.21}$$

Remark 2. *Since $\boldsymbol{\psi}$ is only in $H^1(\Omega)^3$, no positive power of h_E can be gained from $\mathbf{curl}(\boldsymbol{\psi} - S_h(\boldsymbol{\psi}))$; for this reason, the corresponding indicator will not be optimal, see Section 7.5. Optimality can be recovered by means of Green's formula as in [9,10], but the computer implementation of the resulting indicator is expensive.*

5.3. Second basic error equation

From now on, to alleviate notation, it is convenient to extend the pressure by zero in the nonpay-zone. Let us introduce the following residuals that are not the definite error indicators, but are related to the error indicators:

$$R_{\text{time}}^{n,\ell} = \nabla\cdot(z_h^{n,\ell} - z_{h\tau}^{n,\ell}),\quad R_{\text{alg}}^{n,\ell} = \partial_t(\bar{\sigma}_{h\tau}^{n,\ell} - \bar{\sigma}_{h\tau}^{n,\ell-1}),\quad R_{\text{flow}}^{n,\ell} = \alpha\partial_t\nabla\cdot \boldsymbol{u}_{h\tau}^{n,\ell},$$

$$R_{E,\text{vel}}^{n,\ell} = \mu_f\boldsymbol{\kappa}^{-1}z_{h\tau}^{n,\ell} - \rho g\nabla\eta + \nabla p_{h\tau}^{n,\ell},$$

$$\overline{R}_{E,\text{vel}}^{n,\ell} = \mu_f\boldsymbol{\kappa}^{-1}z_{h\tau}^{n,\ell} - \rho g\nabla\eta + \nabla R_h(p_{h\tau}^{n,\ell}),$$

$$R_{e,\text{p}}^{n,\ell} = [p_{h\tau}^{n,\ell}]_e,$$

$$R_{E,\text{displ}}^{n,\ell} = \boldsymbol{f}_{h\tau}^n + \nabla\cdot\boldsymbol{\sigma}(\boldsymbol{u}_{h\tau}^{n,\ell}) - \alpha\nabla p_{h\tau}^{n,\ell},$$

$$R_{J,\boldsymbol{\sigma}}^{n,\ell} = [\boldsymbol{\sigma}(\boldsymbol{u}_{h\tau}^{n,\ell}) - \alpha p_{h\tau}^{n,\ell}\boldsymbol{I}]_e\boldsymbol{n}_e,\quad R_{\text{tract}}^{n,\ell} = \boldsymbol{\sigma}(\boldsymbol{u}_{h\tau}^{n,\ell})\boldsymbol{n}_\Omega - \boldsymbol{t}_{N,h\tau}^n.$$

Then, by substituting (5.20) into (5.12) and using the above residual notation, we derive a preliminary basic error equality, in each interval $]t_{n-1}, t_n]$,

$$\begin{aligned}
&\frac{d}{dt}\Big(\frac{1}{2M}\|p - p_{h\tau}^{n,\ell}\|^2_{L^2(\Omega_1)} + G\|\boldsymbol{\varepsilon}(\boldsymbol{u} - \boldsymbol{u}_{h\tau}^{n,\ell})\|^2_{L^2(\Omega)} + \frac{\lambda}{2}\|\nabla\cdot(\boldsymbol{u} - \boldsymbol{u}_{h\tau}^{n,\ell})\|^2_{L^2(\Omega)}\Big) + \mu_f\|\boldsymbol{\kappa}^{-\frac12}(z - z_{h\tau}^{n,\ell})\|^2_{L^2(\Omega_1)}\\
&= (q - q_h^n, p - p_{h\tau}^{n,\ell})_{\Omega_1} + \big(R_{\text{time}}^{n,\ell}, p - p_{h\tau}^{n,\ell}\big)_{\Omega_1} - \frac{\alpha}{K_b}\big(R_{\text{alg}}^{n,\ell}, P_h(p - p_{h\tau}^{n,\ell})\big)_{\Omega_1} + B\\
&- \sum_{E\subset\overline{\Omega}_1}\big(R_{\text{flow}}^{n,\ell}, p - p_{h\tau}^{n,\ell} - P_h(p - p_{h\tau}^{n,\ell})\big)_E + \big(\boldsymbol{f} - \boldsymbol{f}_{h\tau}^n, \partial_t(\boldsymbol{u} - \boldsymbol{u}_{h\tau}^{n,\ell})\big)_\Omega + \big\langle \boldsymbol{t}_N - \boldsymbol{t}_{N,h\tau}^n, \partial_t(\boldsymbol{u} - \boldsymbol{u}_{h\tau}^{n,\ell})\big\rangle_{\Gamma_N}\\
&+ \sum_{E\subset\overline{\Omega}}\big(R_{E,\text{displ}}^{n,\ell}, \partial_t(\boldsymbol{u} - \boldsymbol{u}_{h\tau}^{n,\ell} - \boldsymbol{v}_h)\big)_E - \sum_{e\in\mathcal{E}_h}\big(R_{J,\boldsymbol{\sigma}}^{n,\ell}, \partial_t(\boldsymbol{u} - \boldsymbol{u}_{h\tau}^{n,\ell} - \boldsymbol{v}_h)\big)_e - \big\langle R_{\text{tract}}^{n,\ell}, \partial_t(\boldsymbol{u} - \boldsymbol{u}_{h\tau}^{n,\ell} - \boldsymbol{v}_h)\big\rangle_{\Gamma_N},
\end{aligned}\tag{5.22}$$

where B is bounded by (5.21) that with this notation reads

$$\begin{aligned}
|B| \le\, & C\|\nabla\cdot(z - z_{h\tau}^{n,\ell})\|_{L^2(\Omega_1)}\Big[\Big(\sum_{E\subset\overline{\Omega}_1} h_E^2\|R_{E,\text{vel}}^{n,\ell}\|^2_{L^2(E)}\Big)^{\frac12} + \Big(\sum_{e\in\mathcal{E}_h^1} h_e\|R_{e,\text{p}}^{n,\ell}\|^2_{L^2(E)}\Big)^{\frac12} + \Big(\sum_{E\in\overline{\Omega}_1}\|\overline{R}_{E,\text{vel}}^{n,\ell}\|^2_{L^2(E)}\Big)^{\frac12}\Big]\\
&+ C\|z - z_{h\tau}^{n,\ell}\|_{L^2(\Omega_1)}\Big(\sum_{E\in\overline{\Omega}_1}\|\overline{R}_{E,\text{vel}}^{n,\ell}\|^2_{L^2(E)}\Big)^{\frac12}.
\end{aligned}\tag{5.23}$$

In (5.22), we can pick at each time t

$$\boldsymbol{v}_h = S_h(\boldsymbol{u} - \boldsymbol{u}_{h\tau}^{n,\ell}).$$

Finally, at each time step n, we choose the smallest iteration counter ℓ that achieves convergence of the algorithm and, for this value of ℓ, we integrate the error equality (5.22) in time over the interval $]0, t[$, say with $t_{n-1} < t \le t_n$. But in doing so, we integrate by parts the terms in the right-hand side of (5.22) that involve the time derivative of the errors to be bounded, because these are not controlled by its left-hand side. This gives another preliminary basic error equation, as stated in the next proposition.

Proposition 9. *The following error equality holds for $t_{n-1} < t \le t_n$, $1 \le n \le N$, with n, ℓ replaced by n and ℓ suppressed everywhere except in the algorithmic residual*

$$\begin{aligned}
&\frac{1}{2M}\|(p - p_{h\tau})(t)\|^2_{L^2(\Omega_1)} + G\|\boldsymbol{\varepsilon}(\boldsymbol{u} - \boldsymbol{u}_{h\tau})(t)\|^2_{L^2(\Omega)} + \frac{\lambda}{2}\|\nabla\cdot(\boldsymbol{u} - \boldsymbol{u}_{h\tau})(t)\|^2_{L^2(\Omega)}\\
&+ \mu_f\|\boldsymbol{\kappa}^{-\frac12}(z - z_{h\tau})\|^2_{L^2(\Omega_1\times]0,t[)}
\end{aligned}$$

$$
\begin{aligned}
&= \int_0^t (q-q_h, p-p_{h\tau})_{\Omega_1} + \int_0^t \big(R_{\text{time}}, p-p_{h\tau}\big)_{\Omega_1} - \frac{\alpha}{K_b}\int_0^t \big(R_{\text{alg}}^{\ell}, P_h(p-p_{h\tau})\big)_{\Omega_1} + \int_0^t B \\
&- \int_0^t \big(\partial_t(\boldsymbol{f}-\boldsymbol{f}_{h\tau}), \boldsymbol{u}-\boldsymbol{u}_{h\tau}\big)_{\Omega} - \int_0^t \big\langle \partial_t(\boldsymbol{t}_N - \boldsymbol{t}_{N,h\tau}), \boldsymbol{u}-\boldsymbol{u}_{h\tau}\big\rangle_{\Gamma_N} \\
&- \sum_{E\subset\overline{\Omega}} \int_0^t \big(\partial_t R_{E,\text{displ}}, \boldsymbol{u}-\boldsymbol{u}_{h\tau}-\boldsymbol{v}_h\big)_E + \sum_{e\in\mathcal{E}_h}\int_0^t \big(\partial_t R_{J,\boldsymbol{\sigma}}, \boldsymbol{u}-\boldsymbol{u}_{h\tau}-\boldsymbol{v}_h\big)_e - \int_0^t \sum_{E\subset\overline{\Omega}_1} \big(R_{\text{flow}}, p-p_{h\tau}-\theta_h\big)_E \\
&+ \int_0^t \big(\partial_t R_{\text{tract}}, \boldsymbol{u}-\boldsymbol{u}_{h\tau}-\boldsymbol{v}_h\big)_{\Gamma_N} + \text{Init} + \text{Ip}(t) - \text{Ip}(0),
\end{aligned}
\tag{5.24}
$$

where the piecewise constant functions in time are denoted without subscript, B is bounded by (5.23), $\boldsymbol{v}_h = S_h(\boldsymbol{u}-\boldsymbol{u}_{h\tau})$, $\theta_h = P_h(p-p_{h\tau})$, and

$$
\text{Init} := \frac{1}{2M}\|p_0 - p_h^0\|^2_{L^2(\Omega_1)} + G\|\boldsymbol{\varepsilon}(\boldsymbol{u}(0)-\boldsymbol{u}_h^0)\|^2_{L^2(\Omega)} + \frac{\lambda}{2}\|\nabla\cdot(\boldsymbol{u}(0)-\boldsymbol{u}_h^0)\|^2_{L^2(\Omega)},
\tag{5.25}
$$

$$
\begin{aligned}
\text{IP}(t) &= \sum_{E\subset\overline{\Omega}} \big(R_{E,\text{displ}}(t), (\boldsymbol{u}-\boldsymbol{u}_{h\tau}-\boldsymbol{v}_h)(t)\big)_E - \sum_{e\in\mathcal{E}_h}\big(R_{J,\boldsymbol{\sigma}}(t), (\boldsymbol{u}-\boldsymbol{u}_{h\tau}-\boldsymbol{v}_h)(t)\big)_e \\
&- \big(R_{\text{tract}}(t), (\boldsymbol{u}-\boldsymbol{u}_{h\tau}-\boldsymbol{v}_h)(t)\big)_{\Gamma_N} \\
&+ \big((\boldsymbol{f}-\boldsymbol{f}_{h\tau})(t), (\boldsymbol{u}-\boldsymbol{u}_{h\tau})(t)\big)_{\Omega} + \big\langle(\boldsymbol{t}_N-\boldsymbol{t}_{N,h\tau})(t), (\boldsymbol{u}-\boldsymbol{u}_{h\tau})(t)\big\rangle_{\Gamma_N}.
\end{aligned}
\tag{5.26}
$$

5.4. Error indicators

Let us make precise the choice of R_h; this operator acts on M_h and takes its values in Θ_h. For theoretical purposes, here is a construction in the spirit of Scott–Zhang; a different implementation will be found in Section 8. Take any node $\boldsymbol{a}$ of $\mathcal{T}_h^1$; then $\boldsymbol{a}$ belongs to some element $E \subset \overline{\Omega}_1$ (the elements are closed) and is a member of the principal lattice of order n on E, recall that $n = \max(k, 1)$ (the maximum is only used when $k = 0$, i.e., in regularizing piecewise constant functions). We associate with $\boldsymbol{a}$ a suitable element $E_{\boldsymbol{a}} \subset \overline{\Omega}_1$ containing $\boldsymbol{a}$; repetitions are allowed. Then, for any q in M_h, we define

$$
\big(R_h(q)\big)(\boldsymbol{a}) = q|_{E_{\boldsymbol{a}}}(\boldsymbol{a}).
\tag{5.27}
$$

This defines $R_h(q)$ at all nodes of the triangulation and it suffices to interpolate these values by the interpolant of Θ_h to define $R_h(q)$ in $\overline{\Omega}_1$. Clearly, as the functions of Θ_h are continuous, we have

$$
\forall q \in \Theta_h, \quad R_h(q) = q.
$$

Regarding the bounds, it follows from the projection's properties that

$$
\forall E \subset \overline{\Omega}_1, \quad \|p - p_{h\tau} - P_h(p-p_{h\tau})\|_{L^2(E)} = \|p-p_{h\tau}\|_{L^2(E)/\mathbb{P}_k} \le \|p-p_{h\tau}\|_{L^2(E)},
$$

and from (3.8) and Korn's inequality (1.5), that there exists a constant C independent of h, such that

$$
\forall E \subset \overline{\Omega}, \quad \|\boldsymbol{u}-\boldsymbol{u}_{h\tau}-\boldsymbol{v}_h\|_{L^2(E)} \le C h_E \|\boldsymbol{\varepsilon}(\boldsymbol{u}-\boldsymbol{u}_{h\tau})\|_{L^2(\Delta_E)},
$$

and in addition from a trace inequality,

$$
\forall e \in \mathcal{E}_h, \quad \|\boldsymbol{u}-\boldsymbol{u}_{h\tau}-\boldsymbol{v}_h\|_{L^2(e)} \le C h_e^{\frac{1}{2}} \|\boldsymbol{\varepsilon}(\boldsymbol{u}-\boldsymbol{u}_{h\tau})\|_{L^2(\Delta_E)},
$$

where Δ_E is a small patch of elements including E. Then, these estimates applied to the right-hand side of (5.24), suggest the following error indicators (to be very precise, we retain here the superscript ℓ):

- the velocity's error in time,

$$
\eta_{\text{time}}^{n,\ell} := \frac{\sqrt{3}}{2}\|R_{\text{time}}^{n,\ell}\|_{L^2(\Omega_1\times]t_{n-1},t_n[)} = \frac{1}{2}\big(\Delta t\big)^{\frac{1}{2}}\big\|\nabla\cdot(\boldsymbol{z}_h^{n,\ell} - \boldsymbol{z}_h^{n-1})\big\|_{L^2(\Omega_1)},
\tag{5.28}
$$

- the algorithmic error,

$$\eta_{\mathrm{fs}}^{n,\ell} := \big(\Delta t\big)^{\frac{1}{2}} \big\| R_{\mathrm{alg}}^{n,\ell} \big\|_{L^2(\Omega_1)} = \big(\Delta t\big)^{\frac{1}{2}} \big\| \frac{1}{\Delta t} \big(\bar{\sigma}_h^{n,\ell} - \bar{\sigma}_h^{n,\ell-1}\big) \big\|_{L^2(\Omega_1)}, \tag{5.29}$$

- the flow error in space on each element $E \subset \overline{\Omega}_1$,

$$\eta_{E,\mathrm{flow}}^{n,\ell} := \big(\Delta t\big)^{\frac{1}{2}} \big\| R_{E,\mathrm{flow}}^{n,\ell} \big\|_{L^2(E)/\mathbb{P}_k} = \big(\Delta t\big)^{\frac{1}{2}} \big\| \alpha \partial_t \nabla \cdot \boldsymbol{u}_{h\tau}^{n,\ell} \big\|_{L^2(E)/\mathbb{P}_k}, \tag{5.30}$$

- the first velocity error in space on each element $E \subset \overline{\Omega}_1$,

$$\eta_{E,\mathrm{vel}}^{n,\ell} := \big(\Delta t\big)^{\frac{1}{2}} h_E \big\| R_{E,\mathrm{vel}}^{n,\ell} \big\|_{L^2(E)} = \big(\Delta t\big)^{\frac{1}{2}} h_E \big\| \mu_f \boldsymbol{\kappa}^{-1} \boldsymbol{z}_{h\tau}^{n,\ell} - \rho g \nabla \eta + \nabla p_{h\tau}^{n,\ell} \big\|_{L^2(E)}, \tag{5.31}$$

- the second velocity error in space on each element $E \subset \overline{\Omega}_1$,

$$\overline{\eta}_{E,\mathrm{vel}}^{n,\ell} := \big(\Delta t\big)^{\frac{1}{2}} \big\| \overline{R}_{E,\mathrm{vel}}^{n,\ell} \big\|_{L^2(E)} = \big(\Delta t\big)^{\frac{1}{2}} \big\| \mu_f \boldsymbol{\kappa}^{-1} \boldsymbol{z}_{h\tau}^{n,\ell} - \rho g \nabla \eta + \nabla R_h(p_{h\tau}^{n,\ell}) \big\|_{L^2(E)}, \tag{5.32}$$

- the pressure's interface jump at each face $e \in \mathcal{E}_h^1$,

$$\eta_{e,\mathrm{p}}^{n,\ell} := \big(\Delta t\big)^{\frac{1}{2}} h_e^{\frac{1}{2}} \big\| [p_{h\tau}^{n,\ell}] \big\|_{L^2(e)}, \tag{5.33}$$

- the displacement error on each element $E \subset \overline{\Omega}$,

$$\eta_{E,\boldsymbol{u}}^{n,\ell} := h_E \| \boldsymbol{f}_h^n + \nabla \cdot \boldsymbol{\sigma}(\boldsymbol{u}_h^{n,\ell}) - \alpha \nabla p_h^{n,\ell} \|_{L^2(E)}, \tag{5.34}$$

recall that p_h is set to zero in the nonpay-zone,

- the stress tensor's jump at all interior interfaces i.e., all $e \in \mathcal{E}_h$

$$\eta_{e,\boldsymbol{\sigma}}^{n,\ell} := h_e^{\frac{1}{2}} \| [\boldsymbol{\sigma}(\boldsymbol{u}_h^{n,\ell}) - \alpha p_h^{n,\ell} \boldsymbol{I}]_e \boldsymbol{n}_e \|_{L^2(e)}, \tag{5.35}$$

- the stress tensor's error on $e \subset \Gamma_N$,

$$\eta_{e,\boldsymbol{\sigma},N}^{n,\ell} := h_e^{\frac{1}{2}} \| \boldsymbol{\sigma}(\boldsymbol{u}_h^{n,\ell}) \boldsymbol{n}_\Omega - \boldsymbol{t}_{N,h}^n \|_{L^2(e)}, \tag{5.36}$$

- the time derivative of the displacement error on each element $E \subset \overline{\Omega}$,

$$\eta_{E,\partial\boldsymbol{u}}^{n,\ell} := h_E \big(\Delta t\big)^{\frac{1}{2}} \| \frac{1}{\Delta t} \big(\boldsymbol{f}_h^n - \boldsymbol{f}_h^{n-1} + \nabla \cdot \boldsymbol{\sigma}(\boldsymbol{u}_h^{n,\ell} - \boldsymbol{u}_h^{n-1}) - \alpha \nabla (p_h^{n,\ell} - p_h^{n-1}) \big) \|_{L^2(E)}, \tag{5.37}$$

- the time derivative of the stress tensor's jump at all interior interfaces i.e., all $e \in \mathcal{E}_h$,

$$\eta_{e,\partial\boldsymbol{\sigma}}^{n,\ell} := h_e^{\frac{1}{2}} \big(\Delta t\big)^{\frac{1}{2}} \| \frac{1}{\Delta t} [\boldsymbol{\sigma}(\boldsymbol{u}_h^{n,\ell} - \boldsymbol{u}_h^{n-1}) - \alpha (p_h^{n,\ell} - p_h^{n-1}) \boldsymbol{I}]_e \boldsymbol{n}_e \|_{L^2(e)}, \tag{5.38}$$

- the time derivative of the stress tensor error on $e \subset \Gamma_N$,

$$\eta_{e,\partial\boldsymbol{\sigma},N}^{n,\ell} := h_e^{\frac{1}{2}} \big(\Delta t\big)^{\frac{1}{2}} \| \frac{1}{\Delta t} \big(\boldsymbol{\sigma}(\boldsymbol{u}_h^{n,\ell} - \boldsymbol{u}_h^{n-1}) \boldsymbol{n}_\Omega - (\boldsymbol{t}_{N,h}^n - \boldsymbol{t}_{N,h}^{n-1}) \big) \|_{L^2(e)}. \tag{5.39}$$

5.5. Basic upper bounds

Recall that $t_{n-1} < t \leq t_n$. Let us estimate each term of (5.24); recall that ℓ is omitted except in the algorithmic error indicator. The terms involving the time integral of the error on the pressure or displacement are bounded in time by an $L^\infty - L^1$ inequality in order to avoid an exponential constant factor arising from Gronwall's Lemma. For instance,

$$\Big| \int_0^t \big(R_{\mathrm{time}}, p - p_{h\tau} \big)_{\Omega_1} \Big| \leq \| p - p_{h\tau} \|_{L^\infty(0,t;L^2(\Omega_1))} \frac{2}{\sqrt{3}} \sum_{m=1}^n \big(\Delta t\big)^{\frac{1}{2}} \eta_{\mathrm{time}}^m,$$

and

$$\Big| \frac{\alpha}{K_b} \int_0^t \big(R_{\mathrm{alg}}^\ell, \theta_h \big)_{\Omega_1} \Big| \leq \frac{\alpha}{K_b} \| p - p_{h\tau} \|_{L^\infty(0,t;L^2(\Omega_1))} \sum_{m=1}^n \big(\Delta t\big)^{\frac{1}{2}} \eta_{\mathrm{fs}}^{m,\ell}.$$

In contrast, the terms involving the velocity error are bounded by the Cauchy–Schwarz inequality. For instance, regarding B and considering that $\boldsymbol{\kappa}$ and $\rho g \nabla \eta$ are independent of time, we note that

$$R^n_{E,\text{vel}}(t) = \frac{1}{\Delta t}(t_n - t)R_{E,\text{vel}}(t_{n-1}) + \frac{1}{\Delta t}(t - t_{n-1})R_{E,\text{vel}}(t_n),$$

hence

$$\Big| \int_0^t \sum_{E \subset \overline{\Omega}_1} \big(R_{E,\text{vel}}(t), \nabla \cdot (\boldsymbol{z} - \boldsymbol{z}_{h\tau})(t)\big)_E \Big| \le \sqrt{\frac{2}{3}} \Big(\sum_{m=1}^n \sum_{E \subset \overline{\Omega}_1} (\eta^m_{E,\text{vel}})^2 \Big)^{\frac{1}{2}} \|\nabla \cdot (\boldsymbol{z} - \boldsymbol{z}_{h\tau})\|_{L^2(\Omega_1 \times]0,t[)},$$

with similar expressions for $\overline{R}_{E,\text{vel}}(t)$, and $R_{e,\text{p}}(t)$. Thus (5.23) now reads

$$\begin{aligned} \int_0^t |B| \le & C\|\nabla \cdot (\boldsymbol{z} - \boldsymbol{z}_{h\tau})\|_{L^2(\Omega_1 \times]0,t[)} \Big[\Big(\sum_{m=1}^n \sum_{E \subset \overline{\Omega}_1} (\eta^m_{E,\text{vel}})^2 \Big)^{\frac{1}{2}} + \Big(\sum_{m=1}^n \sum_{e \in \mathcal{E}_h^1} (\eta^m_{e,\text{p}})^2 \Big)^{\frac{1}{2}} + \Big(\sum_{m=1}^n \sum_{E \in \overline{\Omega}_1} (\overline{\eta}^m_{E,\text{vel}})^2 \Big)^{\frac{1}{2}} \Big] \\ & + C\|\boldsymbol{z} - \boldsymbol{z}_{h\tau}\|_{L^2(\Omega_1 \times]0,t[)} \Big(\sum_{m=1}^n \sum_{E \in \overline{\Omega}_1} (\overline{\eta}^m_{E,\text{vel}})^2 \Big)^{\frac{1}{2}}. \end{aligned} \tag{5.40}$$

Reverting to the flow, we have with $\theta_h = P_h(p - p_{h\tau})$,

$$\int_0^t \sum_{E \subset \overline{\Omega}_1} \big(R_{E,\text{flow}}, p - p_{h\tau} - \theta_h\big)_E \le \|p - p_{h\tau}\|_{L^\infty(0,t;L^2(\Omega_1))} \sum_{m=1}^n (\Delta t)^{\frac{1}{2}} \Big(\sum_{E \subset \overline{\Omega}_1} \big(\eta_{E,\text{flow}}\big)^2 \Big)^{\frac{1}{2}}.$$

For the terms involving the displacement, recall that p_h is extended by zero in Ω_2. Note that by Poincaré's and Korn's inequalities (1.5) and (1.6), we have

$$\Big| \int_0^t \big(\partial_t(\boldsymbol{f} - \boldsymbol{f}_{h\tau}), \boldsymbol{u} - \boldsymbol{u}_{h\tau}\big)_\Omega \Big| \le \mathcal{P}\mathcal{K}\|\boldsymbol{\varepsilon}(\boldsymbol{u} - \boldsymbol{u}_{h\tau})\|_{L^\infty(0,t;L^2(\Omega))} \|\partial_t(\boldsymbol{f} - \boldsymbol{f}_{h\tau})\|_{L^1(0,t;L^2(\Omega))}.$$

Likewise, the trace inequality (1.7) gives

$$\Big| \int_0^t \big\langle \partial_t(\boldsymbol{t}_N - \boldsymbol{t}_{N,h\tau}), \boldsymbol{u} - \boldsymbol{u}_{h\tau} \big\rangle_{\Gamma_N} \Big| \le C_N \mathcal{K}\|\boldsymbol{\varepsilon}(\boldsymbol{u} - \boldsymbol{u}_{h\tau})\|_{L^\infty(0,t;L^2(\Omega))} \|\partial_t(\boldsymbol{t}_N - \boldsymbol{t}_{N,h\tau})\|_{L^1(0,t;(H^{\frac{1}{2}}_{00}(\Gamma_N))')}.$$

Next by the approximation properties (3.8) of S_h, we have (to simplify, the number of repetitions of an element is not specified and is incorporated in the constant $\hat{C}$),

$$\Big| \int_0^t \sum_{E \subset \overline{\Omega}} \big(\partial_t R_{E,\text{displ}}, \boldsymbol{u} - \boldsymbol{u}_{h\tau} - \boldsymbol{v}_h\big)_E \Big| \le \hat{C}\mathcal{K}\|\boldsymbol{\varepsilon}(\boldsymbol{u} - \boldsymbol{u}_{h\tau})\|_{L^\infty(0,t;L^2(\Omega))} \sum_{m=1}^n (\Delta t)^{\frac{1}{2}} \Big(\sum_{E \subset \overline{\Omega}} \big(\eta^m_{E,\partial \boldsymbol{u}}\big)^2 \Big)^{\frac{1}{2}},$$

where we have used that by Korn's inequality (1.5) with $\Gamma = \Gamma_D$

$$\|\nabla(\boldsymbol{u} - \boldsymbol{u}_{h\tau})\|_{L^2(\Omega)} \le \mathcal{K}\|\boldsymbol{\varepsilon}(\boldsymbol{u} - \boldsymbol{u}_{h\tau})\|_{L^2(\Omega)}.$$

A similar argument leads to the following bound for the displacement errors on interfaces,

$$\Big| \int_0^t \sum_{e \in \mathcal{E}_h} \big(\partial_t R_{J,\boldsymbol{\sigma}}, \boldsymbol{u} - \boldsymbol{u}_{h\tau} - \boldsymbol{v}_h\big)_e \Big| \le \hat{C}\mathcal{K}\|\boldsymbol{\varepsilon}(\boldsymbol{u} - \boldsymbol{u}_{h\tau})\|_{L^\infty(0,t;L^2(\Omega))} \sum_{m=1}^n (\Delta t)^{\frac{1}{2}} \Big(\sum_{e \in \mathcal{E}_h} \big(\eta^m_{e,\partial \boldsymbol{\sigma}}\big)^2 \Big)^{\frac{1}{2}},$$

and for the traction error on Γ_N

$$\Big| \int_0^t \big(\partial_t R_{\text{tract}}, \boldsymbol{u} - \boldsymbol{u}_{h\tau} - \boldsymbol{v}_h\big)_{\Gamma_N} \Big| \le \hat{C}\mathcal{K}\|\boldsymbol{\varepsilon}(\boldsymbol{u} - \boldsymbol{u}_{h\tau})\|_{L^\infty(0,t;L^2(\Omega))} \sum_{m=1}^n (\Delta t)^{\frac{1}{2}} \Big(\sum_{e \subset \Gamma_N} \big(\eta^m_{e,\partial \boldsymbol{\sigma},N}\big)^2 \Big)^{\frac{1}{2}}.$$

Next, we evaluate the first three terms of IP at time t, $t_{n-1} \le t \le t_n$. We have,

$$\|R_{E,\text{displ}}(t)\|_{L^2(E)} \le (1 - s)\eta^{n-1}_{E,\boldsymbol{u}} + s\eta^n_{E,\boldsymbol{u}}, \tag{5.41}$$

where $s = \frac{t-t_{n-1}}{\Delta t}$, $0 \le s \le 1$. Hence

$$\Big| \sum_{E \subset \overline{\Omega}} \big(R_{E,\text{displ}}(t), (\boldsymbol{u} - \boldsymbol{u}_{h\tau} - \boldsymbol{v}_h)(t)\big)_E \Big| \le \hat{C}\mathcal{K} \|\boldsymbol{\varepsilon}(\boldsymbol{u} - \boldsymbol{u}_{h\tau})(t)\|_{L^2(\Omega)} \times \Big(\sum_{E \subset \overline{\Omega}} \Big((1-s)\big(\eta_{E,\boldsymbol{u}}^{n-1}\big)^2 + s\big(\eta_{E,\boldsymbol{u}}^{n}\big)^2 \Big)\Big)^{\frac{1}{2}},$$

with analogous inequalities for the other two terms. More simply, we have

$$\Big|\big((\boldsymbol{f} - \boldsymbol{f}_{h\tau})(t), (\boldsymbol{u} - \boldsymbol{u}_{h\tau})(t)\big)_\Omega\Big| \le \mathcal{P}\mathcal{K}\|\boldsymbol{\varepsilon}(\boldsymbol{u} - \boldsymbol{u}_{h\tau})(t)\|_{L^2(\Omega)} \|(\boldsymbol{f} - \boldsymbol{f}_{h\tau})(t)\|_{L^2(\Omega)},$$

$$\Big|\big((\boldsymbol{t}_N - \boldsymbol{t}_{N,h\tau})(t), (\boldsymbol{u} - \boldsymbol{u}_{h\tau})(t)\big)_{\Gamma_N}\Big| \le C_N\mathcal{K}\|\boldsymbol{\varepsilon}(\boldsymbol{u} - \boldsymbol{u}_{h\tau})(t)\|_{L^2(\Omega)} \|(\boldsymbol{t}_N - \boldsymbol{t}_{N,h\tau})(t)\|_{(H_{00}^{\frac{1}{2}}(\Gamma_N))'}.$$

Of course, these estimates simplify when $t = 0$. For instance we have

$$\Big| \sum_{E \subset \overline{\Omega}} \big(R_{E,\text{displ}}(0), (\boldsymbol{u} - \boldsymbol{u}_{h\tau} - \boldsymbol{v}_h)(0)\big)_E \Big| \le \hat{C}\mathcal{K} \|\boldsymbol{\varepsilon}(\boldsymbol{u}(0) - \boldsymbol{u}_h^0)\|_{L^2(\Omega)} \Big(\sum_{E \subset \overline{\Omega}} \big(\eta_{E,\boldsymbol{u}}^{0}\big)^2\Big)^{\frac{1}{2}},$$

with similar inequalities for the other terms.

Remark 3. *The extra factor $(\Delta t)^{\frac{1}{2}}$ in the time derivative of the mechanics residual comes from a discrete L^1 norm in time. At this stage, it could have been included in the indicator.*

Now, by collecting these estimates, we derive another intermediate upper bound. Beforehand, to simplify, we set

$$\eta_{\text{displ}}^n = \Big(\sum_{E \subset \overline{\Omega}} \big(\eta_{E,\boldsymbol{u}}^n\big)^2 \Big)^{\frac{1}{2}} + \Big(\sum_{e \subset \mathcal{E}_h} \big(\eta_{e,\boldsymbol{\sigma}}^n\big)^2 \Big)^{\frac{1}{2}} + \Big(\sum_{e \subset \Gamma_N} \big(\eta_{e,\boldsymbol{\sigma},N}^n\big)^2 \Big)^{\frac{1}{2}}, \tag{5.42}$$

$$\eta_{\partial(\text{displ})}^n = \Big(\sum_{E \subset \overline{\Omega}} \big(\eta_{E,\partial\boldsymbol{u}}^n\big)^2 \Big)^{\frac{1}{2}} + \Big(\sum_{e \subset \mathcal{E}_h} \big(\eta_{e,\partial\boldsymbol{\sigma}}^n\big)^2 \Big)^{\frac{1}{2}} + \Big(\sum_{e \subset \Gamma_N} \big(\eta_{e,\partial\boldsymbol{\sigma},N}^n\big)^2 \Big)^{\frac{1}{2}}, \tag{5.43}$$

$$\eta_{\text{vel}}^n = \Big(\sum_{m=1}^{n} \sum_{E \subset \overline{\Omega}_1} (\eta_{E,\text{vel}}^m)^2 \Big)^{\frac{1}{2}}, \quad \overline{\eta}_{\text{vel}}^n = \Big(\sum_{m=1}^{n} \sum_{E \subset \overline{\Omega}_1} (\overline{\eta}_{E,\text{vel}}^m)^2 \Big)^{\frac{1}{2}}, \quad \eta_{J,\text{p}}^n = \Big(\sum_{m=1}^{n} \sum_{e \in \mathcal{E}_h^1} (\eta_{e,\text{p}}^m)^2 \Big)^{\frac{1}{2}}, \tag{5.44}$$

$$\eta_{\text{flow}}^n = \Big(\sum_{E \subset \overline{\Omega}_1} (\eta_{E,\text{flow}}^n)^2 \Big)^{\frac{1}{2}}. \tag{5.45}$$

Proposition 10. *For $1 \le n \le N$ and $t_{n-1} < t \le t_n$, we have*

$$\begin{aligned}
&\frac{1}{2M}\|(p - p_{h\tau})(t)\|_{L^2(\Omega_1)}^2 + G\|\boldsymbol{\varepsilon}(\boldsymbol{u} - \boldsymbol{u}_{h\tau})(t)\|_{L^2(\Omega)}^2 + \frac{\lambda}{2}\|\nabla\cdot(\boldsymbol{u} - \boldsymbol{u}_{h\tau})(t)\|_{L^2(\Omega)}^2 \\
&+ \mu_f\|\boldsymbol{\kappa}^{-\frac{1}{2}}(\boldsymbol{z} - \boldsymbol{z}_{h\tau})\|_{L^2(\Omega_1\times]0,t[)}^2 \\
&\le \mathcal{K}\|\boldsymbol{\varepsilon}(\boldsymbol{u} - \boldsymbol{u}_{h\tau})(t)\|_{L^2(\Omega)}\Big[\hat{C}\Big(\sum_{E \subset \overline{\Omega}} \Big((1-s)\big(\eta_{E,\boldsymbol{u}}^{n-1}\big)^2 + s\big(\eta_{E,\boldsymbol{u}}^{n}\big)^2 \Big)\Big)^{\frac{1}{2}} + \hat{C}\Big(\sum_{e \in \mathcal{E}_h} \Big((1-s)\big(\eta_{e,\boldsymbol{\sigma}}^{n-1}\big)^2 + s\big(\eta_{e,\boldsymbol{\sigma}}^{n}\big)^2 \Big)\Big)^{\frac{1}{2}} \\
&+ \hat{C}C_N\Big(\sum_{e \subset \Gamma_N} \Big((1-s)\big(\eta_{e,\boldsymbol{\sigma},N}^{n-1}\big)^2 + s\big(\eta_{e,\boldsymbol{\sigma},N}^{n}\big)^2 \Big)\Big)^{\frac{1}{2}} + \mathcal{P}\|(\boldsymbol{f} - \boldsymbol{f}_{h\tau})(t)\|_{L^2(\Omega)} + C_N\|(\boldsymbol{t}_N - \boldsymbol{t}_{N,h\tau})(t)\|_{(H_{00}^{\frac{1}{2}}(\Gamma_N))'}\Big]
\end{aligned}$$

$$
\begin{aligned}
&+\ \hat{C}\|\boldsymbol{\kappa}^{-\frac{1}{2}}(\boldsymbol{z}-\boldsymbol{z}_{h\tau})\|_{L^2(\Omega_1\times]0,t[)}\|\boldsymbol{\kappa}^{\frac{1}{2}}\|_{L^\infty(\Omega_1)}\overline{\eta}^n_{\mathrm{vel}}+\hat{C}\|\nabla\cdot(\boldsymbol{z}-\boldsymbol{z}_{h\tau})\|_{L^2(\Omega_1\times]0,t[)}\Big(\overline{\eta}^n_{\mathrm{vel}}+\overline{\eta}^n_{e,\mathrm{p}}+\overline{\eta}^n_{\mathrm{vel}}\Big)\\
&+\ \|p-p_{h\tau}\|_{L^\infty(0,t;L^2(\Omega_1))}\Big[\|q-q_h\|_{L^1(0,t;L^2(\Omega_1))}+\sum_{m=1}^{n}(\Delta t)^{\frac{1}{2}}\Big(\frac{2}{\sqrt{3}}\eta^m_{\mathrm{time}}+\frac{\alpha}{K_b}\eta^{m,\ell}_{\mathrm{fs}}+\overline{\eta}^m_{\mathrm{flow}}\Big)\Big]\\
&+\ \mathcal{K}\|\boldsymbol{\varepsilon}(\boldsymbol{u}-\boldsymbol{u}_{h\tau})\|_{L^\infty(0,t;L^2(\Omega))}\Big[\mathcal{P}\|\partial_t(\boldsymbol{f}-\boldsymbol{f}_{h\tau})\|_{L^1(0,t;L^2(\Omega))}+C_N\|\partial_t(\boldsymbol{t}_N-\boldsymbol{t}_{N,h\tau})\|_{L^1(0,t;(H^{\frac{1}{2}}_{00}(\Gamma_N))')}\\
&+\ \hat{C}\sum_{m=1}^{n}(\Delta t)^{\frac{1}{2}}\eta_{\partial(\mathrm{displ})}\Big]\\
&+\ \frac{1}{2M}\|p_0-p_h^0\|^2_{L^2(\Omega_1)}+G\|\boldsymbol{\varepsilon}(\boldsymbol{u}(0)-\boldsymbol{u}_h^0)\|^2_{L^2(\Omega)}+\frac{\lambda}{2}\|\nabla\cdot(\boldsymbol{u}(0)-\boldsymbol{u}_h^0)\|^2_{L^2(\Omega)}\\
&+\ \mathcal{K}\|\boldsymbol{\varepsilon}(\boldsymbol{u}(0)-\boldsymbol{u}_h^0)\|_{L^2(\Omega)}\Big[\hat{C}\Big(\sum_{E\in\overline{\Omega}}(\eta^0_{E,\boldsymbol{u}})^2\Big)^{\frac{1}{2}}+\hat{C}\Big(\sum_{e\in\mathcal{E}_h}(\eta^0_{e,\boldsymbol{\sigma}})^2\Big)^{\frac{1}{2}}\\
&+\hat{C}C_N\Big(\sum_{e\subset\Gamma_N}(\eta^0_{e,\boldsymbol{\sigma},N})^2\Big)^{\frac{1}{2}}+\mathcal{P}\|(\boldsymbol{f}-\boldsymbol{f}_h)(0)\|_{L^2(\Omega)}+C_N\|(\boldsymbol{t}_N-\boldsymbol{t}_{N,h})(0)\|_{(H^{\frac{1}{2}}_{00}(\Gamma_N))'}\Big].
\end{aligned}
\tag{5.46}
$$

The notation $\hat{C}$ stands for different constants that depend only on the regularity of the mesh and degree of the polynomials.

Let us simplify (5.46). By absorbing some errors by corresponding terms in the left-hand side and expressing the displacement in terms of the pressure, we arrive at the following upper bound.

Lemma 5. *There exists a constant C, independent of h, n, and Δt, such that for $1 \le n \le N$, and $t_{n-1} < t \le t_n$, we have*

$$
\begin{aligned}
&\frac{1}{4M}\|(p-p_{h\tau})(t)\|^2_{L^2(\Omega_1)}+\frac{G}{2}\|\boldsymbol{\varepsilon}(\boldsymbol{u}-\boldsymbol{u}_{h\tau})(t)\|^2_{L^2(\Omega)}+\frac{\lambda}{2}\|\nabla\cdot(\boldsymbol{u}-\boldsymbol{u}_{h\tau})(t)\|^2_{L^2(\Omega)}\\
&+\frac{\mu_f}{2}\|\boldsymbol{\kappa}^{-\frac{1}{2}}(\boldsymbol{z}-\boldsymbol{z}_{h\tau})\|^2_{L^2(\Omega_1\times]0,t[)}\\
&\le C\Big[\|\boldsymbol{f}-\boldsymbol{f}_{h\tau}\|^2_{L^\infty(0,t;L^2(\Omega))}+\|\boldsymbol{t}_N-\boldsymbol{t}_{N,h\tau}\|^2_{L^\infty(0,t;(H^{\frac{1}{2}}_{00}(\Gamma_N))')}\\
&+\ \|\partial_t(\boldsymbol{f}-\boldsymbol{f}_{h\tau})\|^2_{L^1(0,t;L^2(\Omega))}+\|\partial_t(\boldsymbol{t}_N-\boldsymbol{t}_{N,h\tau})\|^2_{L^1(0,t;(H^{\frac{1}{2}}_{00}(\Gamma_N))')}+\|q-q_h\|^2_{L^1(0,t;L^2(\Omega_1))}\\
&+\ \sup_{m\le n}\big(\eta^m_{\mathrm{displ}}\big)^2+\big(\overline{\eta}^n_{\mathrm{vel}}\big)^2+\Big(\sum_{m=1}^{n}(\Delta t)^{\frac{1}{2}}\eta^m_{\mathrm{flow}}\Big)^2+\Big(\sum_{m=1}^{n}(\Delta t)^{\frac{1}{2}}\eta^m_{\partial(\mathrm{displ})}\Big)^2+\Big(\sum_{m=1}^{n}(\Delta t)^{\frac{1}{2}}\eta^m_{\mathrm{time}}\Big)^2+\Big(\sum_{m=1}^{n}(\Delta t)^{\frac{1}{2}}\eta^{m,\ell}_{\mathrm{fs}}\Big)^2\\
&+\ \|\nabla\cdot(\boldsymbol{z}-\boldsymbol{z}_{h\tau})\|_{L^2(\Omega_1\times]0,t[)}\big(\eta^n_{\mathrm{vel}}+\overline{\eta}^n_{\mathrm{vel}}+\eta^n_{J,p}\big)\Big]\\
&+\ \frac{1}{2M}\|p_0-p_h^0\|^2_{L^2(\Omega_1)}+\frac{3G}{2}\|\boldsymbol{\varepsilon}(\boldsymbol{u}(0)-\boldsymbol{u}_h^0)\|^2_{L^2(\Omega)}+\frac{\lambda}{2}\|\nabla\cdot(\boldsymbol{u}(0)-\boldsymbol{u}_h^0)\|^2_{L^2(\Omega)}.
\end{aligned}
\tag{5.47}
$$

Proof. The argument proceeds in three steps.

(1) By Young's inequality, the contribution of $\|\boldsymbol{\varepsilon}(\boldsymbol{u}-\boldsymbol{u}_{h\tau})(t)\|_{L^2(\Omega_1)}$ and $\|\boldsymbol{\kappa}^{-\frac{1}{2}}(\boldsymbol{z}-\boldsymbol{z}_{h\tau})\|_{L^2(\Omega_1\times]0,t[)}$ can be absorbed by the corresponding terms in the left-hand side that is now replaced by:

$$
\frac{1}{2M}\|(p-p_{h\tau})(t)\|^2_{L^2(\Omega_1)}+\frac{G}{2}\|\boldsymbol{\varepsilon}(\boldsymbol{u}-\boldsymbol{u}_{h\tau})(t)\|^2_{L^2(\Omega)}+\frac{\lambda}{2}\|\nabla\cdot(\boldsymbol{u}-\boldsymbol{u}_{h\tau})(t)\|^2_{L^2(\Omega)}+\frac{\mu_f}{2}\|\boldsymbol{\kappa}^{-\frac{1}{2}}(\boldsymbol{z}-\boldsymbol{z}_{h\tau})\|^2_{L^2(\Omega_1\times]0,t[)}.
\tag{5.48}
$$

The sum of the first two terms in the right-hand side of (5.46) is replaced by

$$
\begin{aligned}
A^n := & \frac{\hat{C}}{2\mu_f}\|\boldsymbol{\kappa}^{\frac{1}{2}}\|^2_{L^\infty(\Omega_1)}\big(\overline{\eta}^n_{\mathrm{vel}}\big)^2 + \frac{\mathcal{K}^2}{2G}\Big[\hat{C}\Big(\sum_{E\subset\overline{\Omega}}\big((1-s)\big(\eta^{n-1}_{E,\boldsymbol{u}}\big)^2 + s\big(\eta^n_{E,\boldsymbol{u}}\big)^2\big)\Big)^{\frac{1}{2}} \\
& + \hat{C}\Big(\sum_{e\in\mathcal{E}_h}\big((1-s)\big(\eta^{n-1}_{e,\boldsymbol{\sigma}}\big)^2 + s\big(\eta^n_{e,\boldsymbol{\sigma}}\big)^2\big)\Big)^{\frac{1}{2}} + \hat{C}C_N\Big(\sum_{e\subset\Gamma_N}\big((1-s)\big(\eta^{n-1}_{e,\boldsymbol{\sigma},N}\big)^2 + s\big(\eta^n_{e,\boldsymbol{\sigma},N}\big)^2\big)\Big)^{\frac{1}{2}} \\
& + \mathcal{P}\|(\boldsymbol{f}-\boldsymbol{f}_{h\tau})(t)\|_{L^2(\Omega)} + C_N\|(\boldsymbol{t}_N-\boldsymbol{t}_{N,h\tau})(t)\|_{(H^{\frac{1}{2}}_{00}(\Gamma_N))'}\Big]^2.
\end{aligned}
$$

Recalling that $0 \le s \le 1$, and denoting by C various constants that are independent of h, n, Δt, A^n has the bound

$$
A^n \le C\Big[\sup_{m\le n}\big(\eta^m_{\mathrm{displ}}\big)^2 + \big(\overline{\eta}^n_{\mathrm{vel}}\big)^2 + \|\boldsymbol{f}-\boldsymbol{f}_{h\tau}\|^2_{L^\infty(0,t;L^2(\Omega)^d)} + \|\boldsymbol{t}_N-\boldsymbol{t}_{N,h\tau}\|^2_{L^\infty(0,t;(H^{\frac{1}{2}}_{00}(\Gamma_N)^d)')}\Big]. \tag{5.49}
$$

(2) Next, it is convenient to express the contribution of $\|\boldsymbol{\varepsilon}(\boldsymbol{u}-\boldsymbol{u}_{h\tau})\|_{L^\infty(0,t;L^2(\Omega))}$ in terms of the pressure by means of (5.9) tested with $\boldsymbol{u}-\boldsymbol{u}_{h\tau}$ at time t, $t_{n-1} < t \le t_n$. By applying (1.6)–(1.7), the definition of the indicators, and (5.41), we infer

$$
\begin{aligned}
2G\,\|\boldsymbol{\varepsilon}(\boldsymbol{u}-\boldsymbol{u}_{h\tau})(t)\|^2_{L^2(\Omega)} + \lambda\|\nabla\cdot(\boldsymbol{u}-\boldsymbol{u}_{h\tau})(t)\|^2_{L^2(\Omega)} \le & \ \alpha\|(p-p_{h\tau})(t)\|_{L^2(\Omega_1)}\|\nabla\cdot(\boldsymbol{u}-\boldsymbol{u}_{h\tau})(t)\|_{L^2(\Omega_1)} \\
& + \mathcal{K}\|\boldsymbol{\varepsilon}(\boldsymbol{u}-\boldsymbol{u}_{h\tau})(t)\|_{L^2(\Omega)}\Big[\mathcal{P}\|(\boldsymbol{f}-\boldsymbol{f}_{h\tau})(t)\|_{L^2(\Omega)} + C_N\|(\boldsymbol{t}_N-\boldsymbol{t}_{N,h\tau})(t)\|_{(H^{\frac{1}{2}}_{00}(\Gamma_N))'} \\
& + C\Big(\sum_{E\subset\overline{\Omega}}\big((1-s)\big(\eta^{n-1}_{E,\boldsymbol{u}}\big)^2 + s\big(\eta^n_{E,\boldsymbol{u}}\big)^2\big)\Big)^{\frac{1}{2}} + C\Big(\sum_{e\in\mathcal{E}_h}\big((1-s)\big(\eta^{n-1}_{e,\boldsymbol{\sigma}}\big)^2 + s\big(\eta^n_{e,\boldsymbol{\sigma}}\big)^2\big)\Big)^{\frac{1}{2}} \\
& + CC_N\Big(\sum_{e\subset\Gamma_N}\big((1-s)\big(\eta^{n-1}_{e,\boldsymbol{\sigma},N}\big)^2 + s\big(\eta^n_{e,\boldsymbol{\sigma},N}\big)^2\big)\Big)^{\frac{1}{2}}\Big].
\end{aligned} \tag{5.50}
$$

This gives an inequality that is valid for any t and implies

$$
\begin{aligned}
G\,\|\boldsymbol{\varepsilon}(\boldsymbol{u}-\boldsymbol{u}_{h\tau})\|^2_{L^\infty(0,t;L^2(\Omega))} \le & \frac{\alpha^2}{4\lambda}\|p-p_{h\tau}\|^2_{L^\infty(0,t;L^2(\Omega_1))} \\
& + C\Big[\sup_{m\le n}\big(\eta^m_{\mathrm{displ}}\big)^2 + \|\boldsymbol{f}-\boldsymbol{f}_{h\tau}\|^2_{L^\infty(0,t;L^2(\Omega)^d)} + \|\boldsymbol{t}_N-\boldsymbol{t}_{N,h\tau}\|^2_{L^\infty(0,t;(H^{\frac{1}{2}}_{00}(\Gamma_N)^d)')}\Big].
\end{aligned} \tag{5.51}
$$

(3) Let X^n denote the factor of $\mathcal{K}\|\boldsymbol{\varepsilon}(\boldsymbol{u}-\boldsymbol{u}_{h\tau})\|_{L^\infty(0,t;L^2(\Omega))}$ in the right-hand side of (5.46),

$$
X^n = \mathcal{P}\|\partial_t(\boldsymbol{f}-\boldsymbol{f}_{h\tau})\|_{L^1(0,t;L^2(\Omega))} + C_N\|\partial_t(\boldsymbol{t}_N-\boldsymbol{t}_{N,h\tau})\|_{L^1(0,t;(H^{\frac{1}{2}}_{00}(\Gamma_N))')} + \hat{C}\sum_{m=1}^n(\Delta t)^{\frac{1}{2}}\eta^m_{\partial(\mathrm{displ})}.
$$

It satisfies

$$
X^n \le C\Big[\sum_{m=1}^n(\Delta t)^{\frac{1}{2}}\eta^m_{\partial(\mathrm{displ})} + \|\partial_t(\boldsymbol{f}-\boldsymbol{f}_{h\tau})\|_{L^1(0,t;L^2(\Omega))} + \|\partial_t(\boldsymbol{t}_N-\boldsymbol{t}_{N,h\tau})\|_{L^1(0,t;(H^{\frac{1}{2}}_{00}(\Gamma_N))')}\Big]. \tag{5.52}
$$

Then, for any $\delta_1 > 0$,

$$
\mathcal{K}X^n\|\boldsymbol{\varepsilon}(\boldsymbol{u}-\boldsymbol{u}_{h\tau})\|_{L^\infty(0,t;L^2(\Omega))} \le \frac{1}{2}\Big(\delta_1\|\boldsymbol{\varepsilon}(\boldsymbol{u}-\boldsymbol{u}_{h\tau})\|^2_{L^\infty(0,t;L^2(\Omega))} + \frac{\mathcal{K}^2}{\delta_1}\big(X^n\big)^2\Big).
$$

By substituting (5.51) and (5.52), this inequality becomes

$$
\begin{aligned}
\mathcal{K}X^n\|\boldsymbol{\varepsilon}(\boldsymbol{u}-\boldsymbol{u}_{h\tau})\|_{L^\infty(0,t;L^2(\Omega))} \le & \frac{\delta_1\alpha^2}{8\lambda G}\|p-p_{h\tau}\|^2_{L^\infty(0,t;L^2(\Omega_1))} \\
& + C\delta_1\Big[\sup_{m\le n}\big(\eta^m_{\mathrm{displ}}\big)^2 + \|\boldsymbol{f}-\boldsymbol{f}_{h\tau}\|^2_{L^\infty(0,t;L^2(\Omega))} + \|\boldsymbol{t}_N-\boldsymbol{t}_{N,h\tau}\|^2_{L^\infty(0,t;(H^{\frac{1}{2}}_{00}(\Gamma_N))')}\Big] \\
& + \frac{C}{\delta_1}\Big[\|\partial_t(\boldsymbol{f}-\boldsymbol{f}_{h\tau})\|^2_{L^1(0,t;L^2(\Omega))} + \|\partial_t(\boldsymbol{t}_N-\boldsymbol{t}_{N,h\tau})\|^2_{L^1(0,t;(H^{\frac{1}{2}}_{00}(\Gamma_N))')} + \Big(\sum_{m=1}^n(\Delta t)^{\frac{1}{2}}\eta^m_{\partial\mathrm{displ}}\Big)^2\Big].
\end{aligned} \tag{5.53}
$$

By substituting (5.49) and (5.53) into (5.46), and applying once again Young's inequality to the remaining product involving $\|p-p_{h\tau}\|_{L^\infty(0,t;L^2(\Omega_1))}$ we derive an inequality where the factor of $\|p-p_{h\tau}\|^2_{L^\infty(0,t;L^2(\Omega_1))}$ in the right-hand side is $\frac{\delta_2}{2}+\frac{\delta_1\alpha^2}{8\lambda G}$. Then (5.47) follows by choosing δ_1 and δ_2 such that $\delta_2+\frac{\delta_1\alpha^2}{4\lambda G}=\frac{1}{2M}$. $\square$

As announced previously, Lemma 5 does not yet induce an upper bound for the error, because we have no control over the error on the velocities divergence. This is the object of the next section.

6. Further a posteriori analysis

Let us derive additional error equalities and inequalities to estimate the divergence of the velocity.

6.1. The divergence of velocity term

Let us reproduce the stability steps when ℓ is chosen to reach convergence. We begin by testing (5.8) with $\theta=\nabla\cdot(z-z^n_{h\tau})$, and θ_h its L^2 projection on M_h. This gives

$$\|\nabla\cdot(z-z^n_{h\tau})\|^2_{L^2(\Omega_1)}=-\Big(\partial_t\big(\frac{1}{M}(p-p^n_{h\tau})+\alpha\nabla\cdot(\boldsymbol{u}-\boldsymbol{u}^n_{h\tau})\big),\nabla\cdot(z-z^n_{h\tau})\Big)_{\Omega_1}+(q-q^n_h,\nabla\cdot(z-z^n_{h\tau}))_{\Omega_1}$$
$$+\big(R^n_{\text{time}},\nabla\cdot(z-z^n_{h\tau})\big)_{\Omega_1}-\frac{\alpha}{K_b}\big(\partial_t(\bar\sigma^{n,\ell}_{h\tau}-\bar\sigma^{n,\ell-1}_{h\tau}),\theta_h\big)_{\Omega_1}-\sum_{E\subset\overline{\Omega}_1}\big(R^n_{\text{flow}},\nabla\cdot(z-z^n_{h\tau})-\theta_h\big)_E,$$

from which we deduce the bound

$$\|\nabla\cdot(z-z^n_{h\tau})\|_{L^2(\Omega_1)}\le\|\frac{1}{M}\partial_t(p-p^n_{h\tau})\|_{L^2(\Omega_1)}+\alpha\|\nabla\cdot\partial_t(\boldsymbol{u}-\boldsymbol{u}^n_{h\tau})\|_{L^2(\Omega_1)}$$
$$+\|q-q^n_h\|_{L^2(\Omega_1)}+\|R^n_{\text{time}}\|_{L^2(\Omega_1)}+\frac{\alpha}{K_b}\|R^{n,\ell}_{\text{alg}}\|_{L^2(\Omega_1)}+\Big(\sum_{E\subset\overline{\Omega}_1}\|R^n_{\text{flow}}\|^2_{L^2(E)/\mathbb{P}_k}\Big)^{\frac12}. \tag{6.1}$$

As expected, we must find an estimate for the time derivative of the pressure error and of the divergence of the displacement error.

6.2. The time derivative of the pressure and displacement

We shall need below three additional indicators:

- the time derivative of the first velocity error in space on each element $E\subset\overline{\Omega}_1$,

$$\eta^{n,\ell}_{E,\partial\text{vel}}:=(\Delta t)^{\frac12}h_E\big\|\partial_t R^{n,\ell}_{E,\text{vel}}\big\|_{L^2(E)}=(\Delta t)^{\frac12}h_E\big\|\partial_t\big(\mu_f\boldsymbol{\kappa}^{-1}z^{n,\ell}_{h\tau}+\nabla p^{n,\ell}_{h\tau}\big)\big\|_{L^2(E)}, \tag{6.2}$$

- the time derivative of the second velocity error in space on each element $E\subset\overline{\Omega}_1$,

$$\overline{\eta}^{n,\ell}_{E,\partial\text{vel}}:=(\Delta t)^{\frac12}\big\|\partial_t\overline{R}^{n,\ell}_{E,\text{vel}}\big\|_{L^2(E)}=(\Delta t)^{\frac12}\big\|\partial_t\big(\mu_f\boldsymbol{\kappa}^{-1}z^{n,\ell}_{h\tau}+\nabla R_h(p^{n,\ell}_{h\tau})\big)\big\|_{L^2(E)}, \tag{6.3}$$

- the time derivative of the pressure's interface jump at each face $e\in\mathcal{E}^1_h$,

$$\eta^{n,\ell}_{e,\partial\text{p}}:=(\Delta t)^{\frac12}h_e^{\frac12}\big\|[\partial_t p^{n,\ell}_{h\tau}]\big\|_{L^2(e)}, \tag{6.4}$$

and their sums in time and space

$$\eta^n_{\partial\text{vel}}=\Big(\sum_{m=1}^n\sum_{E\subset\overline{\Omega}_1}\big(\eta^m_{E,\partial\text{vel}}\big)^2\Big)^{\frac12},\quad \overline{\eta}^n_{\partial\text{vel}}=\Big(\sum_{m=1}^n\sum_{E\subset\overline{\Omega}_1}\big(\overline{\eta}^m_{E,\partial\text{vel}}\big)^2\Big)^{\frac12},\quad \eta^n_{J,\partial\text{p}}=\Big(\sum_{m=1}^n\sum_{e\in\mathcal{E}^1_h}\big(\overline{\eta}^m_{e,\partial\text{p}}\big)^2\Big)^{\frac12}. \tag{6.5}$$

Now, let us test (5.8) with $\theta=\partial_t(p-p^n_{h\tau})$ and θ_h its L^2 projection on M_h,

$$\frac{1}{M}\|\partial_t(p-p^n_{h\tau})\|^2_{L^2(\Omega_1)}=-\alpha\big(\nabla\cdot\partial_t(\boldsymbol{u}-\boldsymbol{u}^n_{h\tau}),\partial_t(p-p^n_{h\tau})\big)_{\Omega_1}-\big(\nabla\cdot(z-z^n_{h\tau}),\partial_t(p-p^n_{h\tau})\big)_{\Omega_1}$$
$$+(q-q^n_h,\partial_t(p-p^n_{h\tau}))_{\Omega_1}+\big(R^n_{\text{time}},\partial_t(p-p^n_{h\tau})\big)_{\Omega_1}-\frac{\alpha}{K_b}\big(\partial_t(\bar\sigma^{n,\ell}_{h\tau}-\bar\sigma^{n,\ell-1}_{h\tau}),\theta_h\big)_{\Omega_1}$$
$$-\sum_{E\subset\overline{\Omega}_1}\big(R^n_{\text{flow}},\partial_t(p-p^n_{h\tau})-\theta_h\big)_E. \tag{6.6}$$

For the first term in the right-hand side of (6.6), (5.10) is tested with $\partial_t(\boldsymbol{u} - \boldsymbol{u}^n_{h\tau})$ and arbitrary $\boldsymbol{v}_h$. We obtain

$$\begin{aligned}\alpha\big(\partial_t(p - p^n_{h\tau}), \nabla\cdot\partial_t(\boldsymbol{u} - \boldsymbol{u}^n_{h\tau})\big)_{\Omega_1} &= 2G\|\partial_t\boldsymbol{\varepsilon}(\boldsymbol{u} - \boldsymbol{u}^n_{h\tau})\|^2_{L^2(\Omega)} + \lambda\|\partial_t\nabla\cdot(\boldsymbol{u} - \boldsymbol{u}^n_{h\tau})\|^2_{L^2(\Omega)}\\ &- \big(\partial_t(\boldsymbol{f} - \boldsymbol{f}^n_{h\tau}), \partial_t(\boldsymbol{u} - \boldsymbol{u}^n_{h\tau})\big)_\Omega - \big\langle\partial_t(\boldsymbol{t}_N - \boldsymbol{t}^n_{N,h\tau}), \partial_t(\boldsymbol{u} - \boldsymbol{u}^n_{h\tau})\big\rangle_{\Gamma_N}\\ &- \sum_{E\subset\overline{\Omega}}\big(\partial_t R^n_{E,\mathrm{displ}}, \partial_t(\boldsymbol{u} - \boldsymbol{u}^n_{h\tau} - \boldsymbol{v}_h)\big)_E + \sum_{e\in\mathcal{E}_h}\big(\partial_t R^n_{J,\boldsymbol{\sigma}}, \partial_t(\boldsymbol{u} - \boldsymbol{u}^n_{h\tau} - \boldsymbol{v}_h)\big)_e\\ &+ \big(\partial_t R^n_{\mathrm{tract}}, \partial_t(\boldsymbol{u} - \boldsymbol{u}^n_{h\tau} - \boldsymbol{v}_h)\big)_{\Gamma_N}.\end{aligned}$$

Hence, for $\theta_h = P_h(p - p^n_{h\tau})$,

$$\begin{aligned}&\frac{1}{M}\|\partial_t(p - p^n_{h\tau})\|^2_{L^2(\Omega_1)} + 2G\|\partial_t\boldsymbol{\varepsilon}(\boldsymbol{u} - \boldsymbol{u}^n_{h\tau})\|^2_{L^2(\Omega)} + \lambda\|\partial_t\nabla\cdot(\boldsymbol{u} - \boldsymbol{u}^n_{h\tau})\|^2_{L^2(\Omega)}\\ &= \big(\partial_t(\boldsymbol{f} - \boldsymbol{f}^n_{h\tau}), \partial_t(\boldsymbol{u} - \boldsymbol{u}^n_{h\tau})\big)_\Omega + \big\langle\partial_t(\boldsymbol{t}_N - \boldsymbol{t}^n_{N,h\tau}), \partial_t(\boldsymbol{u} - \boldsymbol{u}^n_{h\tau})\big\rangle_{\Gamma_N}\\ &+ \sum_{E\subset\overline{\Omega}}\big(\partial_t R^n_{E,\mathrm{displ}}, \partial_t(\boldsymbol{u} - \boldsymbol{u}^n_{h\tau} - \boldsymbol{v}_h)\big)_E - \sum_{e\in\mathcal{E}_h}\big(\partial_t R^n_{J,\boldsymbol{\sigma}}, \partial_t(\boldsymbol{u} - \boldsymbol{u}^n_{h\tau} - \boldsymbol{v}_h)\big)_e\\ &- \sum_{e\subset\Gamma_N}\big(\partial_t R^n_{\mathrm{tract}}, \partial_t(\boldsymbol{u} - \boldsymbol{u}^n_{h\tau} - \boldsymbol{v}_h)\big)_e + (q - q^n_h, \partial_t(p - p^n_{h\tau}))_{\Omega_1} + \big(R^n_{\mathrm{time}}, \partial_t(p - p^n_{h\tau})\big)_{\Omega_1}\\ &- \frac{\alpha}{K_b}\big(\partial_t(\bar{\sigma}^{n,\ell}_{h\tau} - \bar{\sigma}^{n,\ell-1}_{h\tau}), \theta_h\big)_{\Omega_1} - \big(\nabla\cdot(\boldsymbol{z} - \boldsymbol{z}^n_{h\tau}), \partial_t(p - p^n_{h\tau})\big)_{\Omega_1} - \sum_{E\subset\overline{\Omega}_1}\big(R^n_{\mathrm{flow}}, \partial_t(p - p^n_{h\tau}) - \theta_h\big)_E.\end{aligned}$$

After integration in time, this leads to the next inequality for $1 \le n \le N$, and $t_{n-1} < t \le t_n$,

$$\begin{aligned}&\frac{1}{M}\|\partial_t(p - p_{h\tau})\|^2_{L^2(\Omega_1\times]0,t[)} + 2G\|\partial_t\boldsymbol{\varepsilon}(\boldsymbol{u} - \boldsymbol{u}_{h\tau})\|^2_{L^2(\Omega\times]0,t[)} + \lambda\|\partial_t\nabla\cdot(\boldsymbol{u} - \boldsymbol{u}_{h\tau})\|^2_{L^2(\Omega\times]0,t[)}\\ &\le \mathcal{K}\|\partial_t\boldsymbol{\varepsilon}(\boldsymbol{u} - \boldsymbol{u}_{h\tau})\|_{L^2(\Omega\times]0,t[)}\Big[\mathcal{P}\|\partial_t(\boldsymbol{f} - \boldsymbol{f}_{h\tau})\|_{L^2(\Omega\times]0,t[)} + C_N\|\partial_t(\boldsymbol{t}_N - \boldsymbol{t}_{N,h\tau})\|_{L^2(0,t;(H^{\frac{1}{2}}_{00}(\Gamma_N))')}\\ &+ \hat{C}\Big(\sum_{m=1}^n\sum_{E\subset\overline{\Omega}}(\eta^m_{E,\partial\boldsymbol{u}})^2\Big)^{\frac{1}{2}} + \hat{C}\Big(\sum_{m=1}^n\sum_{e\in\mathcal{E}_h}(\eta^m_{e,\partial\boldsymbol{\sigma}})^2\Big)^{\frac{1}{2}} + \hat{C}C_N\Big(\sum_{m=1}^n\sum_{e\subset\Gamma_N}\big(\eta_{e,\partial\boldsymbol{\sigma},N}\big)^2\Big)^{\frac{1}{2}}\Big]\\ &+ \|\partial_t(p - p_{h\tau})\|_{L^2(\Omega_1\times]0,t[)}\Big[\|q - q_h\|_{L^2(\Omega_1\times]0,t[)} + \frac{2}{\sqrt{3}}\overline{\eta}^n_{\mathrm{time}} + \frac{\alpha}{K_b}\overline{\eta}^{n,\ell}_{\mathrm{fs}}\Big]\\ &- \int_0^t\big(\nabla\cdot(\boldsymbol{z} - \boldsymbol{z}_{h\tau}), \partial_t(p - p_{h\tau})\big)_{\Omega_1}.\end{aligned} \tag{6.7}$$

To treat the last term, (5.15) is differentiated with respect to time,

$$\begin{aligned}&\big(\mu_f\boldsymbol{\kappa}^{-1}\partial_t(\boldsymbol{z} - \boldsymbol{z}_{h\tau}), \boldsymbol{\zeta}\big)_{\Omega_1} - (\partial_t(p - p_{h\tau}), \nabla\cdot\boldsymbol{\zeta})_{\Omega_1} = \sum_{E\in\overline{\Omega}_1}\big(\partial_t(-\mu_f\boldsymbol{\kappa}^{-1}\boldsymbol{z}_{h\tau} + \rho g\nabla\eta - \nabla p_{h\tau}), \boldsymbol{\lambda} - \Pi_h(\boldsymbol{\lambda})\big)_E\\ &+ \sum_{E\in\overline{\Omega}_1}\big(\partial_t(-\mu_f\boldsymbol{\kappa}^{-1}\boldsymbol{z}_{h\tau} + \rho g\nabla\eta + \nabla R_h(p_{h\tau})), \mathbf{curl}(\boldsymbol{\psi} - R_h(\boldsymbol{\psi}))\big)_E + \sum_{e\in\mathcal{E}^1_h}\int_e[\partial_t p_{h\tau}]_e(\boldsymbol{\lambda} - \Pi_h(\boldsymbol{\lambda}))\cdot\boldsymbol{n}_e,\end{aligned}$$

and then tested with $\boldsymbol{\zeta} = \boldsymbol{z} - \boldsymbol{z}_{h\tau}$. This gives

$$\frac{1}{2}\mu_f\frac{d}{dt}\|\boldsymbol{\kappa}^{-\frac{1}{2}}(\boldsymbol{z} - \boldsymbol{z}^{n,\ell}_{h\tau})\|^2_{L^2(\Omega_1)} = \big(\partial_t(p - p^{n,\ell}_{h\tau}), \nabla\cdot(\boldsymbol{z} - \boldsymbol{z}^{n,\ell}_{h\tau})\big)_{\Omega_1} + B_t,$$

where

$$\begin{aligned}|B_t| \le& C\|\nabla\cdot(\boldsymbol{z} - \boldsymbol{z}^{n,\ell}_{h\tau})\|_{L^2(\Omega_1)}\Big[\Big(\sum_{E\subset\overline{\Omega}_1}h^2_E\|\partial_t R^{n,\ell}_{E,\mathrm{vel}}\|^2_{L^2(E)}\Big)^{\frac{1}{2}} + \Big(\sum_{e\in\mathcal{E}^1_h}h_e\|\partial_t R^{n,\ell}_{e,\mathrm{p}}\|^2_{L^2(E)}\Big)^{\frac{1}{2}}\\ &+ \Big(\sum_{E\in\overline{\Omega}_1}\|\partial_t\overline{R}^{n,\ell}_{E,\mathrm{vel}}\|^2_{L^2(E)}\Big)^{\frac{1}{2}}\Big] + C\|\boldsymbol{z} - \boldsymbol{z}^{n,\ell}_{h\tau}\|_{L^2(\Omega_1)}\Big(\sum_{E\in\overline{\Omega}_1}\|\partial_t\overline{R}^{n,\ell}_{E,\mathrm{vel}}\|^2_{L^2(E)}\Big)^{\frac{1}{2}}.\end{aligned}$$

The factor $\|\nabla\cdot(z-z_{h\tau}^{n,\ell})\|_{L^2(\Omega_1)}$ can be eliminated by substituting (6.1) in the above inequality; this leads to

$$\begin{aligned}|B_t| \le& C\Big(\frac{1}{M}\|\partial_t(p-p_{h\tau}^n)\|_{L^2(\Omega_1)}+\alpha\|\nabla\cdot\partial_t(\boldsymbol{u}-\boldsymbol{u}_{h\tau}^n)\|_{L^2(\Omega_1)}+\|q-q_h^n\|_{L^2(\Omega_1)}+\|R_{\text{time}}^n\|_{L^2(\Omega_1)}\\&+\frac{\alpha}{K_b}\|R_{\text{alg}}^{n,\ell}\|_{L^2(\Omega_1)}\Big)\\&\Big[\Big(\sum_{E\subset\overline{\Omega}_1}h_E^2\|\partial_t R_{E,\text{vel}}^{n,\ell}\|_{L^2(E)}^2\Big)^{\frac12}+\Big(\sum_{e\in\mathcal{E}_h^1}h_e\|\partial_t R_{e,\text{p}}^{n,\ell}\|_{L^2(E)}^2\Big)^{\frac12}+\Big(\sum_{E\in\overline{\Omega}_1}\|\partial_t\overline{R}_{E,\text{vel}}^{n,\ell}\|_{L^2(E)}^2\Big)^{\frac12}\Big]\\&+C\|\boldsymbol{\kappa}^{\frac12}\|_{L^\infty(\Omega_1)}\|\boldsymbol{\kappa}^{-\frac12}(z-z_{h\tau})(t)\|_{L^2(\Omega_1)}\Big(\sum_{E\in\overline{\Omega}_1}\|\partial_t\overline{R}_{E,\text{vel}}^{n,\ell}\|_{L^2(E)}^2\Big)^{\frac12}.\end{aligned}\tag{6.8}$$

To simplify, we group the errors into three terms

$$D^n=\|q-q_h\|_{L^2(\Omega_1\times]0,t[)}+\frac{2}{\sqrt3}\overline{\eta}_{\text{time}}^n+\frac{\alpha}{K_b}\overline{\eta}_{\text{fs}}^n,\quad E^n=\eta_{\partial\text{vel}}^n+\eta_{J,\partial\text{p}}^n+\overline{\eta}_{\partial\text{vel}}^n,\tag{6.9}$$

$$\begin{aligned}F^n=&\mathcal{P}\|\partial_t(\boldsymbol{f}-\boldsymbol{f}_{h\tau})\|_{L^2(\Omega\times]0,t[)}+C_N\|\partial_t(\boldsymbol{t}_N-\boldsymbol{t}_{N,h\tau})\|_{L^2(0,t;(H_{00}^{\frac12}(\Gamma_N))')}\\&+\hat C\Big(\sum_{m=1}^n\sum_{E\subset\overline{\Omega}}\big(\eta_{E,\partial\boldsymbol{u}}^m\big)^2\Big)^{\frac12}+\hat C\Big(\sum_{m=1}^n\sum_{e\in\mathcal{E}_h}\big(\eta_{e,\partial\boldsymbol{\sigma}}^m\big)^2\Big)^{\frac12}+\hat C C_N\Big(\sum_{m=1}^n\sum_{e\subset\Gamma_N}\big(\eta_{e,\partial\boldsymbol{\sigma},N}\big)^2\Big)^{\frac12}.\end{aligned}\tag{6.10}$$

Then by integrating in time, combining (6.8) with (6.7), and grouping terms, we obtain

$$\begin{aligned}&\frac1M\|\partial_t(p-p_{h\tau})\|_{L^2(\Omega_1\times]0,t[)}^2+2G\|\partial_t\boldsymbol{\varepsilon}(\boldsymbol{u}-\boldsymbol{u}_{h\tau})\|_{L^2(\Omega\times]0,t[)}^2+\lambda\|\partial_t\nabla\cdot(\boldsymbol{u}-\boldsymbol{u}_{h\tau})\|_{L^2(\Omega\times]0,t[)}^2\\&+\frac12\mu_f\|\boldsymbol{\kappa}^{-\frac12}(z-z_{h\tau})(t)\|_{L^2(\Omega_1)}^2\\&\le\mathcal{K}\|\partial_t\boldsymbol{\varepsilon}(\boldsymbol{u}-\boldsymbol{u}_{h\tau})\|_{L^2(\Omega\times]0,t[)}F^n+\|\partial_t(p-p_{h\tau})\|_{L^2(\Omega_1\times]0,t[)}\Big[D^n+\frac CM E^n\Big]\\&+C\alpha\|\nabla\cdot\partial_t(\boldsymbol{u}-\boldsymbol{u}_{h\tau})\|_{L^2(\Omega_1\times]0,t[)}E^n+CD^nE^n\\&+C\|\boldsymbol{\kappa}^{\frac12}\|_{L^\infty(\Omega_1)}\|\boldsymbol{\kappa}^{-\frac12}(z-z_{h\tau})\|_{L^2(\Omega_1\times]0,t[)}\big(\overline{\eta}_{\partial\text{vel}}^n\big)^2+\frac12\mu_f\|\boldsymbol{\kappa}^{-\frac12}(z-z_h)(0)\|_{L^2(\Omega_1)}^2.\end{aligned}\tag{6.11}$$

This formula, readily yields a bound first for the maximum velocity error in time, next for the time derivative of the pressure and displacement, and finally for the velocity's divergence, in view of (6.1). For the sake of simplicity the constant in the last estimate is not specified. The proof are straightforward and skipped.

Lemma 6. *There exists a constant C, independent of h, n, and Δt, such that for $1\le n\le N$, and $t_{n-1}<t\le t_n$, the following inequalities hold*

$$\begin{aligned}\frac12\mu_f\|\boldsymbol{\kappa}^{-\frac12}(z-z_{h\tau})\|_{L^\infty(0,t;L^2(\Omega_1))}^2\le&\mu_f\|\boldsymbol{\kappa}^{-\frac12}(z-z_h)(0)\|_{L^2(\Omega_1)}^2+\frac{1}{2G}\mathcal{K}^2\big(F^n\big)^2+M\Big[D^n+\frac CM E^n\Big]^2\\&+\frac1\lambda C^2\alpha^2\big(E^n\big)^2+2CD^nE^n+\frac{2}{\mu_f}C^2\|\boldsymbol{\kappa}^{\frac12}\|_{L^\infty(\Omega_1)}^2\big(\overline{\eta}_{\partial\text{vel}}^n\big)^2,\end{aligned}\tag{6.12}$$

$$\begin{aligned}&\frac{1}{2M}\|\partial_t(p-p_{h\tau})\|_{L^2(\Omega_1\times]0,t[)}^2+G\|\partial_t\boldsymbol{\varepsilon}(\boldsymbol{u}-\boldsymbol{u}_{h\tau})\|_{L^2(\Omega\times]0,t[)}^2+\frac\lambda2\|\partial_t\nabla\cdot(\boldsymbol{u}-\boldsymbol{u}_{h\tau})\|_{L^2(\Omega\times]0,t[)}^2\\&\qquad\le\frac{3}{2\mu_f}\|\boldsymbol{\kappa}^{-\frac12}(z-z_h)(0)\|_{L^2(\Omega_1)}^2+\frac{3}{4G}\mathcal{K}^2\big(F^n\big)^2+\frac32M\Big[D^n+\frac CM E^n\Big]^2\\&\qquad+\frac{3}{2\lambda}\alpha^2C^2\big(E^n\big)^2+3CD^nE^n+\frac{5}{2\mu_f}C^2\|\boldsymbol{\kappa}^{\frac12}\|_{L^\infty(\Omega_1)}^2\big(\overline{\eta}_{\partial\text{vel}}^n\big)^2,\end{aligned}\tag{6.13}$$

with D^n, E^n and F^n defined respectively by (6.9) and (6.10).

Theorem 2. *There exists a constant C, independent of h, n, and Δt, such that for $1 \le n \le N$, and $t_{n-1} < t \le t_n$, we have*

$$\|\nabla \cdot (z - z_{h\tau})\|^2_{L^2(\Omega_1 \times]0,t[)} \le C\Big[\|\partial_t(\boldsymbol{f} - \boldsymbol{f}_{h\tau})\|^2_{L^2(\Omega \times]0,t[)} + \|\partial_t(\boldsymbol{t}_N - \boldsymbol{t}_{N,h\tau})\|^2_{L^2(0,t;(H^{\frac{1}{2}}_{00}(\Gamma_N))')} + \|q - q_h\|^2_{L^2(\Omega_1 \times]0,t[)} + \left(\overline{\eta}^n_{\mathrm{time}}\right)^2 + \left(\overline{\eta}^n_{\mathrm{fs}}\right)^2 + \left(\eta^n_{\partial \mathrm{vel}}\right)^2 + \left(\eta^n_{J,\partial \mathrm{p}}\right)^2 + \left(\overline{\eta}^n_{\partial \mathrm{vel}}\right)^2 + \left(\eta^n_{\partial(\mathrm{displ})}\right)^2 + \sum_{m=1}^{n}\left(\eta_{\mathrm{flow}}\right)^2 + \|\boldsymbol{\kappa}^{-\frac{1}{2}}(z - z_h)(0)\|^2_{L^2(\Omega_1)}\Big]. \tag{6.14}$$

Of course, this last estimate closes the bound of Lemma 5.

6.3. Useful inequalities

Some useful inequalities are recalled here. First a local Poincaré inequality in each element E,

$$\forall \theta \in H^1_0(E), \quad \|\theta\|_{L^2(E)} \le \hat{C} h_E |\theta|_{H^1(E)}. \tag{6.15}$$

It extends to the union ω_e of elements adjacent to a face e, with a different constant,

$$\forall \theta \in H^1_0(\omega_e), \quad \|\theta\|_{L^2(\omega_e)} \le \hat{C} h_{\omega_e} |\theta|_{H^1(\omega_e)}, \tag{6.16}$$

where h_{ω_e} is the maximum diameter of the elements sharing e. Next, a trace inequality and a scaling argument gives for any E adjacent to e,

$$\forall \theta \in H^1_0(\omega_e), \quad \|\theta\|_{L^2(e)} \le \hat{C} h_e^{\frac{1}{2}} |\theta|_{H^1(E)}. \tag{6.17}$$

The following local inverse inequalities hold for functions θ in finite dimensional spaces, the dimension being independent of h, e, E. First,

$$|\theta|_{H^1(E)} \le \frac{\hat{C}}{h_E} \|\theta\|_{L^2(E)}. \tag{6.18}$$

Next, we have the inverse trace inequality

$$\|\theta\|_{L^2(e)} \le \frac{\hat{C}}{\sqrt{h_e}} \|\theta\|_{L^2(E)}. \tag{6.19}$$

If, in addition, θ belongs to $H^{1/2}_{00}(e)$,

$$\|\theta\|_{H^{1/2}_{00}(e)} \le \frac{\hat{C}}{\sqrt{h_e}} \|\theta\|_{L^2(e)}. \tag{6.20}$$

The above constants depend only on the dimension of the local spaces.

6.4. Weak residual error terms

We observe that several indicators involve time derivatives or expressions that the left-hand sides of the reliability bounds of Lemma 5 and Theorem 2 do not include. As a consequence, some indicators cannot be bounded by the errors in this lemma and theorem. Thus, when developing these bounds we are led to introduce several *weak residual error* terms, relative to derivation in time, that arise in the subsequent section, namely,

$$\left(\mathcal{E}^{n,\ell_n}_{E,\partial\boldsymbol{\sigma}}\right)^2 = \int_{t_{n-1}}^{t_n} \sup_{\boldsymbol{v} \in H^1_0(E)^3} \frac{1}{|\boldsymbol{v}|^2_{H^1(E)}} \left|\left(\partial_t \boldsymbol{\sigma}(\boldsymbol{u} - \boldsymbol{u}^{n,\ell_n}_{h\tau}), \boldsymbol{\varepsilon}(\boldsymbol{v})\right)_E - \alpha\left(\partial_t(p - p^{n,\ell_n}_{h\tau}), \nabla \cdot \boldsymbol{v}\right)_E - \left(\partial_t(\boldsymbol{f} - \boldsymbol{f}^n_{h\tau}), \boldsymbol{v}\right)_E\right|^2, \tag{6.21}$$

where $E \subset \overline{\Omega}$, and the pressures, exact and discrete, are set to zero in Ω_2,

$$\big(\mathcal{E}^{n,\ell_n}_{\omega_e,\partial\boldsymbol{\sigma}}\big)^2 = \int_{t_{n-1}}^{t_n} \sup_{\boldsymbol{v}\in H^1_0(\omega_e)^3} \frac{1}{|\boldsymbol{v}|^2_{H^1(\omega_e)}} \Big|\big(\partial_t \boldsymbol{\sigma}(\boldsymbol{u}-\boldsymbol{u}^{n,\ell_n}_{h\tau}), \boldsymbol{\varepsilon}(\boldsymbol{v})\big)_{\omega_e} - \alpha\big(\partial_t(p-p^{n,\ell_n}_{h\tau}), \nabla\cdot\boldsymbol{v}\big)_{\omega_e} - \big(\partial_t(\boldsymbol{f}-\boldsymbol{f}^n_{h\tau}), \boldsymbol{v}\big)_{\omega_e}\Big|^2, \tag{6.22}$$

where e is an interior face of Ω, and again the pressures are set to zero in Ω_2,

$$\big(\mathcal{E}^{n,\ell_n}_{e,N,\partial\boldsymbol{\sigma}}\big)^2 = \int_{t_{n-1}}^{t_n} \sup_{\boldsymbol{v}\in H^1_e(E)^3} \frac{1}{|\boldsymbol{v}|^2_{H^1(E)}} \Big|\big(\partial_t \boldsymbol{\sigma}(\boldsymbol{u}-\boldsymbol{u}^{n,\ell_n}_{h\tau}), \boldsymbol{\varepsilon}(\boldsymbol{v})\big)_{E} - \big(\partial_t(\boldsymbol{t}_N-\boldsymbol{t}^n_{N,h\tau}), \boldsymbol{v}\big)_{e} - \big(\partial_t(\boldsymbol{f}-\boldsymbol{f}^n_{h\tau}), \boldsymbol{v}\big)_{E}\Big|^2, \tag{6.23}$$

where e is a face on Γ_N, E is the element adjacent to e, and exceptionally,

$$H^1_e(E) = \{z \in H^1(E);\ z = 0 \text{ on } \partial E \setminus e\},$$

next for all $E \subset \overline{\Omega}_1$,

$$\big(\overline{\mathcal{E}}^{n,\ell_n}_{E,\mathrm{vel}}\big)^2 = \int_{t_{n-1}}^{t_n} \sup_{\boldsymbol{\zeta}\in H_0(\mathrm{div},E)} \frac{1}{\|\boldsymbol{\zeta}\|^2_{H(\mathrm{div};E)}} \Big|\big(\mu_f \boldsymbol{\kappa}^{-1}(\boldsymbol{z}-\boldsymbol{z}^{n,\ell}_{h\tau}), \boldsymbol{\zeta}\big)_E - \big(p - R_h(p^{n,\ell_n}_{h\tau}), \nabla\cdot\boldsymbol{\zeta}\big)_E\Big|^2, \tag{6.24}$$

$$\big(\overline{\mathcal{E}}^{n,\ell_n}_{E,\partial\mathrm{vel}}\big)^2 = \int_{t_{n-1}}^{t_n} \sup_{\boldsymbol{\zeta}\in H_0(\mathrm{div},E)} \frac{1}{\|\boldsymbol{\zeta}\|^2_{H(\mathrm{div};E)}} \Big|\big(\mu_f \boldsymbol{\kappa}^{-1}\partial_t(\boldsymbol{z}-\boldsymbol{z}^{n,\ell}_{h\tau}), \boldsymbol{\zeta}\big)_E - \big(\partial_t(p - R_h(p^{n,\ell_n}_{h\tau})), \nabla\cdot\boldsymbol{\zeta}\big)_E\Big|^2, \tag{6.25}$$

$$\big(\mathcal{E}^{n,\ell_n}_{E,\partial\mathrm{vel}}\big)^2 = \int_{t_{n-1}}^{t_n} \sup_{\boldsymbol{\zeta}\in H^1_0(E)} \frac{1}{|\boldsymbol{\zeta}|^2_{H^1(E)}} \Big|\big(\mu_f \boldsymbol{\kappa}^{-1}\partial_t(\boldsymbol{z}-\boldsymbol{z}^{n,\ell}_{h\tau}), \boldsymbol{\zeta}\big)_E - \big(\partial_t(p - p^{n,\ell_n}_{h\tau}), \nabla\cdot\boldsymbol{\zeta}\big)_E\Big|^2, \tag{6.26}$$

and finally, for all faces e in $\mathcal{E}^1_h$,

$$\big(\mathcal{E}^{n,\ell_n}_{\omega_e,\partial\mathrm{vel}}\big)^2 = \int_{t_{n-1}}^{t_n} \sup_{\boldsymbol{\zeta}\in H^1_0(\omega_e)} \frac{1}{|\boldsymbol{\zeta}|^2_{H^1(\omega_e)}} \Big|\big(\mu_f \boldsymbol{\kappa}^{-1}\partial_t(\boldsymbol{z}-\boldsymbol{z}^{n,\ell}_{h\tau}), \boldsymbol{\zeta}\big)_{\omega_e} - \big(\partial_t(p - p^{n,\ell_n}_{h\tau}), \nabla\cdot\boldsymbol{\zeta}\big)_{\omega_e}\Big|^2. \tag{6.27}$$

Let us estimate these weak residual errors. To simplify, for the moment, we omit the superscript ℓ_n. An upper bound for the three weak residues $\mathcal{E}^n_{E,\partial\boldsymbol{\sigma}}$, $\mathcal{E}^n_{\omega_e,\partial\boldsymbol{\sigma}}$ and $\mathcal{E}^n_{e,N,\partial\boldsymbol{\sigma}}$ are derived by much the same argument, so that we only study the first one. For $\mathcal{E}^n_{E,\partial\boldsymbol{\sigma}}$, (5.10) is tested with $\boldsymbol{v}_h = \boldsymbol{0}$, and $\boldsymbol{v} \in H^1_0(E)^3$; this gives

$$\big(\boldsymbol{\sigma}(\partial_t(\boldsymbol{u}-\boldsymbol{u}^n_{h\tau})), \boldsymbol{\varepsilon}(\boldsymbol{v})\big)_E - \alpha\big(\partial_t(p-p^n_{h\tau}), \nabla\cdot\boldsymbol{v}\big)_E - \big(\partial_t(\boldsymbol{f}-\boldsymbol{f}^n_{h\tau}), \boldsymbol{v}\big)_E = \big(\partial_t \boldsymbol{f}^n_{h\tau} + \nabla\cdot\boldsymbol{\sigma}(\partial_t\boldsymbol{u}^n_{h\tau}) - \alpha\nabla\,\partial_t p^n_{h\tau}, \boldsymbol{v}\big)_E.$$

Then the local Poincaré inequality (6.15) implies,

$$\Big|\big(\boldsymbol{\sigma}(\partial_t(\boldsymbol{u}-\boldsymbol{u}^n_{h\tau})), \boldsymbol{\varepsilon}(\boldsymbol{v})\big)_E - \alpha\big(\partial_t(p-p^n_{h\tau}), \nabla\cdot\boldsymbol{v}\big)_E - \big(\partial_t(\boldsymbol{f}-\boldsymbol{f}^n_{h\tau}), \boldsymbol{v}\big)_E\Big| \le \hat{C}\, h_E \|\partial_t \boldsymbol{f}^n_{h\tau} + \nabla\cdot\boldsymbol{\sigma}(\partial_t\boldsymbol{u}^n_{h\tau}) - \alpha\nabla\,\partial_t p^n_{h\tau}\|_{L^2(E)} |\boldsymbol{v}|_{H^1(E)},$$

and dividing by $|\boldsymbol{v}|_{H^1(E)}$, taking the maximum with respect to $\boldsymbol{v} \in H^1_0(E)^3$, squaring, and integrating in time, we derive a bound for $\mathcal{E}^n_{E,\partial\boldsymbol{\sigma}}$ with the constant $\hat{C}$ of (6.15),

$$\mathcal{E}^n_{E,\partial\boldsymbol{\sigma}} \le \hat{C}\eta^n_{E,\partial\boldsymbol{u}}. \tag{6.28}$$

For $\overline{\mathcal{E}}^n_{E,\mathrm{vel}}$, the error equality (5.13) is tested with $\boldsymbol{\zeta}_h = \boldsymbol{0}$ and any $\boldsymbol{\zeta}$ in $H_0(\mathrm{div}, E)$. Note that $p^n_{h\tau}$ can be eliminated form the resulting equality and replaced by $R_h(p^n_{h\tau}) \in H^1(\Omega_1)$,

$$\big(\mu_f \boldsymbol{\kappa}^{-1}(\boldsymbol{z}-\boldsymbol{z}^n_{h\tau}), \boldsymbol{\zeta}\big)_E - (p - R_h(p^n_{h\tau}), \nabla\cdot\boldsymbol{\zeta})_E = \big(-\mu_f\boldsymbol{\kappa}^{-1}\boldsymbol{z}^n_{h\tau} + \rho g\nabla\eta - \nabla R_h(p^n_{h\tau}), \boldsymbol{\zeta}\big)_E.$$

Hence

$$\big|\big(\mu_f \boldsymbol{\kappa}^{-1}(\boldsymbol{z}-\boldsymbol{z}^n_{h\tau}), \boldsymbol{\zeta}\big)_E - (p - R_h(p^n_{h\tau}), \nabla\cdot\boldsymbol{\zeta})_E\big| \le \|-\mu_f\boldsymbol{\kappa}^{-1}\boldsymbol{z}^n_{h\tau} + \rho g\nabla\eta - \nabla R_h(p^n_{h\tau})\|_{L^2(E)}\|\boldsymbol{\zeta}\|_{L^2(E)},$$

and proceeding as above,

$$\overline{\mathcal{E}}^n_{E,\mathrm{vel}} \le \overline{\eta}^n_{E,\mathrm{vel}}. \tag{6.29}$$

Let us differentiate (5.13) with respect to time,

$$\big(\mu_f \boldsymbol{\kappa}^{-1}\partial_t(\boldsymbol{z}-\boldsymbol{z}^n_{h\tau}), \boldsymbol{\zeta}\big)_{\Omega_1} - (\partial_t(p-p^n_{h\tau}), \nabla\cdot\boldsymbol{\zeta})_{\Omega_1} = \big(-\mu_f\boldsymbol{\kappa}^{-1}\partial_t \boldsymbol{z}^n_{h\tau}, \boldsymbol{\zeta}-\boldsymbol{\zeta}_h\big)_{\Omega_1} + \big(\partial_t p^n_{h\tau}, \nabla\cdot(\boldsymbol{\zeta}-\boldsymbol{\zeta}_h)\big)_{\Omega_1}.$$

By applying the same procedure to this equality, we immediately derive

$$\overline{\mathcal{E}}^n_{E,\partial\text{vel}} \le \overline{\eta}^n_{E,\partial\text{vel}}. \tag{6.30}$$

For $\mathcal{E}^n_{E,\partial\text{vel}}$, the derivative in time of (5.13) is tested with $\boldsymbol{\zeta}_h = \boldsymbol{0}$ and $\boldsymbol{\zeta} \in H^1_0(E)$,

$$\big(\mu_f \boldsymbol{\kappa}^{-1}\partial_t(\boldsymbol{z}-\boldsymbol{z}^n_{h\tau}), \boldsymbol{\zeta}\big)_{E} - (\partial_t(p-p^n_{h\tau}), \nabla\cdot\boldsymbol{\zeta})_{E} = \big(-\mu_f\boldsymbol{\kappa}^{-1}\partial_t \boldsymbol{z}^n_{h\tau} - \nabla\,\partial_t p^n_{h\tau}, \boldsymbol{\zeta}\big)_{E};$$

then (6.15) gives

$$\mathcal{E}^n_{E,\partial\text{vel}} \le \hat{C}\eta^n_{E,\partial\text{vel}}, \tag{6.31}$$

with the constant $\hat{C}$ of (6.15). Finally, with $\boldsymbol{\zeta} \in H^1_0(\omega_e)$ and again $\boldsymbol{\zeta}_h = \boldsymbol{0}$, we have

$$\big(\partial_t p^n_{h\tau}, \nabla\cdot\boldsymbol{\zeta}\big)_{\omega_e} = -\sum_{E\subset\omega_e}\big(\nabla\,\partial_t p^n_{h\tau}, \boldsymbol{\zeta}\big)_E + \big([\partial_t p^n_{h\tau}], \boldsymbol{\zeta}\cdot\boldsymbol{n}_e\big)_e.$$

Hence

$$\begin{aligned}\Big|\big(\mu_f \boldsymbol{\kappa}^{-1}\partial_t(\boldsymbol{z}-\boldsymbol{z}^n_{h\tau}), \boldsymbol{\zeta}\big)_{\omega_e} - (\partial_t(p-p^n_{h\tau}), \nabla\cdot\boldsymbol{\zeta})_{\omega_e}\Big| \le & \sum_{E\subset\omega_e}\|-\mu_f\boldsymbol{\kappa}^{-1}\partial_t \boldsymbol{z}^n_{h\tau} - \nabla\,\partial_t p^n_{h\tau}\|_{L^2(E)}\|\boldsymbol{\zeta}\|_{L^2(E)} \\ & + \|[\partial_t p^n_{h\tau}]\|_{L^2(e)}\|\boldsymbol{\zeta}\cdot\boldsymbol{n}_e\|_{L^2(e)}.\end{aligned}$$

By applying (6.17) and the above argument, we immediately deduce that

$$\mathcal{E}^n_{\omega_e,\partial\text{vel}} \le \hat{C}\sqrt{3}\Big(\sum_{E\subset\omega_e}\big(\eta^n_{E,\partial\text{vel}}\big)^2 + \big(\eta^n_{e,\partial\text{p}}\big)^2\Big)^{\frac{1}{2}}, \tag{6.32}$$

where $\hat{C}$ is the maximum of the constants of (6.16) and (6.17).

7. Efficiency bounds

The object of this section is the investigation of upper bounds for the indicators. They are all written when the iteration counter ℓ_n is the smallest that achieves convergence, and so ℓ_n is omitted except in the algorithmic error just below.

7.1. The algorithmic error $\eta^{n,\ell}_{\text{fs}}$

Let us start with this algorithmic error defined in (5.29),

$$\eta^{n,\ell}_{\text{fs}} = \big(\Delta t\big)^{\frac{1}{2}}\Big\|\frac{1}{\Delta t}\big(\bar{\sigma}^{n,\ell}_h - \bar{\sigma}^{n,\ell-1}_h\big)\Big\|_{L^2(\Omega_1)}.$$

Owing to (3.27), we have

$$\big(\eta^{n,\ell}_{\text{fs}}\big)^2 \le \frac{1}{\Delta t}\Big(\frac{1}{\beta K_b}\Big)^{2\ell-2}\|\bar{\sigma}^{n,1}_h - \bar{\sigma}^{n-1}_h\|^2_{L^2(\Omega_1)}. \tag{7.1}$$

Next, by Proposition 3,

$$\begin{aligned}\frac{1}{\Delta t}\|\bar{\sigma}^{n,1}_h - \bar{\sigma}^{n-1}_h\|^2_{L^2(\Omega_1)} \le & \,\alpha^2\frac{1}{\Delta t}\|p^{n,1}_h - p^{n-1}_h\|^2_{L^2(\Omega_1)} \\ & + \frac{K_b\mathcal{K}^2}{2G}\frac{1}{\Delta t}\Big[\mathcal{P}^2\|\boldsymbol{f}^n - \boldsymbol{f}^{n-1}\|^2_{L^2(\Omega)} + C_N^2\|\boldsymbol{t}^n_N - \boldsymbol{t}^{n-1}_N\|^2_{H^{\frac{1}{2}}_{00}(\Gamma_N)'}\Big].\end{aligned} \tag{7.2}$$

To derive a bound for $\|p^{n,1}_h - p^{n-1}_h\|_{L^2(\Omega_1)}$, we introduce the mean value in time of a given function v

$$m^n_t(v) = \frac{1}{\Delta t}\int_{t_{n-1}}^{t_n} v. \tag{7.3}$$

It stems from the exact flow equation in (2.3) at time t_n, that

$$m_t^n(q) = m_t^n\big(\partial_t(\frac{1}{M}p + \alpha\,\nabla\cdot\boldsymbol{u}) + \nabla\cdot\boldsymbol{z}\big).$$

Thus, in view of (3.16) when $\ell = 1$, we can write

$$\begin{aligned}\big(p_h^{n,1} - p_h^{n-1}, \theta_h\big)_{\Omega_1} = & \frac{\Delta t}{\frac{1}{M} + \frac{\alpha^2}{K_b}}\Big[\big(q^n - m_t^n(q), \theta_h\big)_{\Omega_1} + \big(m_t^n(\partial_t(\frac{1}{M}p + \alpha\,\nabla\cdot\boldsymbol{u})), \theta_h\big)_{\Omega_1} \\ & + \big(m_t^n(\nabla\cdot\boldsymbol{z}) - \nabla\cdot\boldsymbol{z}_h^{n-1}, \theta_h\big)_{\Omega_1} - \big(\nabla\cdot(\boldsymbol{z}_h^{n,1} - \boldsymbol{z}_h^{n-1}), \theta_h\big)_{\Omega_1}\Big].\end{aligned} \tag{7.4}$$

As the natural choice for θ_h is $p_h^{n,1} - p_h^{n-1}$, we invoke the discrete velocity equation (3.17) to control the last term in the right-hand side,

$$\mu_f\|\boldsymbol{\kappa}^{-\frac{1}{2}}(\boldsymbol{z}_h^{n,1} - \boldsymbol{z}_h^{n-1})\|_{L^2(\Omega_1)}^2 = \big(\nabla\cdot(\boldsymbol{z}_h^{n,1} - \boldsymbol{z}_h^{n-1}), p_h^{n,1} - p_h^{n-1}\big)_{\Omega_1}.$$

By substituting this equality into (7.4), we obtain with $\theta_h = p_h^{n,1} - p_h^{n-1}$,

$$\begin{aligned}&\|p_h^{n,1} - p_h^{n-1}\|_{L^2(\Omega_1)}^2 + \mu_f\frac{\Delta t}{\frac{1}{M} + \frac{\alpha^2}{K_b}}\|\boldsymbol{\kappa}^{-\frac{1}{2}}(\boldsymbol{z}_h^{n,1} - \boldsymbol{z}_h^{n-1})\|_{L^2(\Omega_1)}^2 \\ &= \frac{\Delta t}{\frac{1}{M} + \frac{\alpha^2}{K_b}}\Big[\big(q^n - m_t^n(q), \theta_h\big)_{\Omega_1} + \big(m_t^n(\partial_t(\frac{1}{M}p + \alpha\,\nabla\cdot\boldsymbol{u})), \theta_h\big)_{\Omega_1} + \big(m_t^n(\nabla\cdot\boldsymbol{z}) - \nabla\cdot\boldsymbol{z}_h^{n-1}, \theta_h\big)_{\Omega_1}\Big]\end{aligned}$$

Hence

$$\begin{aligned}\|p_h^{n,1} - p_h^{n-1}\|_{L^2(\Omega_1)} \le & \frac{\Delta t}{\frac{1}{M} + \frac{\alpha^2}{K_b}}\Big[\|q^n - m_t^n(q)\|_{L^2(\Omega_1)} + \|m_t^n(\partial_t(\frac{1}{M}p + \alpha\,\nabla\cdot\boldsymbol{u}))\|_{L^2(\Omega_1)} \\ & + \|m_t^n(\nabla\cdot\boldsymbol{z}) - (\nabla\cdot\boldsymbol{z})(t_{n-1}) + \nabla\cdot(\boldsymbol{z}(t_{n-1}) - \boldsymbol{z}_h^{n-1})\|_{L^2(\Omega_1)}\Big].\end{aligned}$$

When substituting this bound into (7.2) and applying (7.1), we derive

$$\begin{aligned}\big(\eta_{\rm fs}^{n,\ell}\big)^2 \le \Big(\frac{1}{\beta K_b}\Big)^{2\ell-2}\Big[&\frac{4\alpha^2\Delta t}{\big(\frac{1}{M} + \frac{\alpha^2}{K_b}\big)^2}\Big(\|q^n - m_t^n(q)\|_{L^2(\Omega_1)}^2 + \|m_t^n(\partial_t(\frac{1}{M}p + \alpha\,\nabla\cdot\boldsymbol{u}))\|_{L^2(\Omega_1)}^2 \\ & + \|m_t^n(\nabla\cdot\boldsymbol{z}) - (\nabla\cdot\boldsymbol{z})(t_{n-1})\|_{L^2(\Omega_1)}^2 + \|\nabla\cdot(\boldsymbol{z}(t_{n-1}) - \boldsymbol{z}_h^{n-1})\|_{L^2(\Omega_1)}^2\Big) \\ & + \frac{K_b\mathcal{K}^2}{2G}\frac{1}{\Delta t}\Big(\mathcal{P}^2\|\boldsymbol{f}^n - \boldsymbol{f}^{n-1}\|_{L^2(\Omega)}^2 + C_N^2\|\boldsymbol{t}_N^n - \boldsymbol{t}_N^{n-1}\|_{H_{00}^{\frac{1}{2}}(\Gamma_N)'}^2\Big)\Big].\end{aligned} \tag{7.5}$$

Assumption (4.16) states that for each n, ℓ_n is large enough so that

$$\Big(\frac{1}{\beta K_b}\Big)^{2\ell_m-1} \le \frac{\Delta t}{2}\big(\beta K_b - 1\big).$$

However, this extra Δt factor is not sufficient to balance the terms on the last line of (7.5), and Assumption (4.16) is strengthened as follows:

$$\Big(\frac{1}{\beta K_b}\Big)^{\ell_m} \le C\,\Delta t. \tag{7.6}$$

For the sake of simplicity, the constant C, independent of h and Δt, is not specified here. This leads to the estimate, when (7.6) holds

$$\begin{aligned}\big(\eta_{\rm fs}^n\big)^2 \le\ & C\big(\Delta t\big)^3\Big(\|q^n - m_t^n(q)\|_{L^2(\Omega_1)}^2 + \|m_t^n(\partial_t(\frac{1}{M}p + \alpha\,\nabla\cdot\boldsymbol{u}))\|_{L^2(\Omega_1)}^2 \\ & + \|m_t^n(\nabla\cdot\boldsymbol{z}) - (\nabla\cdot\boldsymbol{z})(t_{n-1})\|_{L^2(\Omega_1)}^2 + \|\nabla\cdot(\boldsymbol{z}(t_{n-1}) - \boldsymbol{z}_h^{n-1})\|_{L^2(\Omega_1)}^2\Big) \\ & + C\big(\Delta t\big)^2\Big(\|\partial_t\boldsymbol{f}\|_{L^2(\Omega\times]t_{n-1},t_n[)}^2 + \|\partial_t\boldsymbol{t}_N\|_{L^2(t_{n-1},t_n;H_{00}^{\frac{1}{2}}(\Gamma_N)')}^2\Big).\end{aligned} \tag{7.7}$$

7.2. The time error η^n_{time}

The velocity's error in time defined by (5.28) is

$$\eta^n_{\text{time}} = \frac{1}{2}(\Delta t)^{\frac{1}{2}} \left\| \nabla \cdot (z^n_h - z^{n-1}_h) \right\|_{L^2(\Omega_1)}.$$

For estimating this indicator, we introduce the auxiliary residual

$$X = q^n_h - q + \partial_t\Big(\frac{1}{M}(p - p^n_{h\tau}) + \alpha \nabla \cdot (\boldsymbol{u} - \boldsymbol{u}^n_{h\tau})\Big) + \frac{\alpha}{K_b} \partial_t(\bar{\sigma}^n_{h\tau} - \bar{\sigma}^{n,\ell_n - 1}_{h\tau}).$$

On the one hand, it satisfies the bound

$$\|X\|_{L^2(\Omega_1)} \le \|q^n_h - q\|_{L^2(\Omega_1)} + \|\partial_t\Big(\frac{1}{M}(p - p^n_{h\tau}) + \alpha \nabla \cdot (\boldsymbol{u} - \boldsymbol{u}^n_{h\tau})\Big)\|_{L^2(\Omega_1)} + \frac{\alpha}{K_b}\|\partial_t(\bar{\sigma}^n_{h\tau} - \bar{\sigma}^{n,\ell_n-1}_{h\tau})\|_{L^2(\Omega_1)}.$$

On the other hand, from (3.16), we easily derive for any $\theta_h \in M_h$,

$$\big(\nabla \cdot (z^n_h - z^n_{h\tau}), \theta_h\big)_{\Omega_1} = \big(X, \theta_h\big)_{\Omega_1} + \big(\nabla \cdot (z - z^n_{h\tau}), \theta_h\big)_{\Omega_1}.$$

Owing to the compatibility condition (3.6), this equality can be tested with $\theta_h = \nabla \cdot (z^n_h - z^n_{h\tau})$,

$$\|\nabla \cdot (z^n_h - z^n_{h\tau})\|_{L^2(\Omega_1)} \le \|X\|_{L^2(\Omega_1)} + \|\nabla \cdot (z - z^n_{h\tau})\|_{L^2(\Omega_1)}.$$

Thus

$$\begin{aligned}\big(\eta^n_{\text{time}}\big)^2 \le & \frac{3}{2}\Big(\|q_h - q\|^2_{L^2(\Omega_1\times]t_{n-1},t_n[)} + \|\partial_t\Big(\frac{1}{M}(p - p_{h\tau}) + \alpha\nabla \cdot (\boldsymbol{u} - \boldsymbol{u}_{h\tau})\Big)\|^2_{L^2(\Omega_1\times]t_{n-1},t_n[)} + \frac{\alpha^2}{K_b^2}\big(\eta^{n,\ell}_{\text{fs}}\big)^2\Big) \\ & \frac{1}{2}\|\nabla \cdot (z - z_{h\tau})\|^2_{L^2(\Omega_1\times]t_{n-1},t_n[)}.\end{aligned} \tag{7.8}$$

7.3. The first velocity error in space $\eta^n_{E,\text{vel}}$

The first velocity error in space, defined by (5.31) is

$$\eta^n_{E,\text{vel}} = \big(\Delta t\big)^{\frac{1}{2}} h_E \left\| \mu_f \boldsymbol{\kappa}^{-1} z^n_{h\tau} - \rho g \nabla \eta + \nabla p^n_{h\tau} \right\|_{L^2(E)}.$$

It is bounded in each element E by a standard localization procedure. Let b_E denote the bubble function of smallest degree that vanishes on the boundary of E, set

$$\boldsymbol{\zeta} = \big(\mu_f \boldsymbol{\kappa}^{-1} z^n_{h\tau} - \rho g \nabla \eta + \nabla p^n_{h\tau}\big) b_E,$$

a polynomial function (assuming that the components of $\boldsymbol{\kappa}$ are polynomials) in $H^1_0(E)^d$ and test (5.13) with this function $\boldsymbol{\zeta}$ and $\boldsymbol{\zeta}_h = \boldsymbol{0}$. By Green's formula, (5.13) becomes

$$\big(\mu_f \boldsymbol{\kappa}^{-1}(z - z^n_{h\tau}), \boldsymbol{\zeta}\big)_E - (p - p^n_{h\tau}, \nabla \cdot \boldsymbol{\zeta})_E = \big(-\mu_f \boldsymbol{\kappa}^{-1} z^n_{h\tau} + \rho g \nabla \eta - \nabla p^n_{h\tau}, \boldsymbol{\zeta}\big)_E.$$

By a standard equivalence of norms in finite dimensions, we can write

$$\begin{aligned}\| - \mu_f \boldsymbol{\kappa}^{-1} z^n_{h\tau} + \rho g \nabla \eta - \nabla p^n_{h\tau}\|^2_{L^2(E)} &\le \hat{c} \int_E | - \mu_f \boldsymbol{\kappa}^{-1} z^n_{h\tau} + \rho g \nabla \eta - \nabla p^n_{h\tau}|^2 b_E \\ &= \int_E \big(-\mu_f \boldsymbol{\kappa}^{-1} z^n_{h\tau} + \rho g \nabla \eta - \nabla p^n_{h\tau}\big) \cdot \boldsymbol{\zeta} \\ &= \big(\mu_f \boldsymbol{\kappa}^{-1}(z - z^n_{h\tau}), \boldsymbol{\zeta}\big)_E - (p - p^n_{h\tau}, \nabla \cdot \boldsymbol{\zeta})_E.\end{aligned}$$

Then, by the local inverse inequality (6.18)

$$\| - \mu_f \boldsymbol{\kappa}^{-1} z^n_{h\tau} + \rho g \nabla \eta - \nabla p^n_{h\tau}\|^2_{L^2(E)} \le \hat{c}\Big(\|\mu_f \boldsymbol{\kappa}^{-1}(z - z^n_{h\tau})\|_{L^2(E)} + \frac{1}{h_E}\|p - p^n_{h\tau}\|_{L^2(E)}\Big)\|\boldsymbol{\zeta}\|_{L^2(E)}.$$

Finally, by multiplying both sides by h_E, squaring, and integrating in time on $]t_{n-1}, t_n[$, we infer

$$\big(\eta^n_{E,\text{vel}}\big)^2 \le \hat{c}\Big(\|\mu_f \boldsymbol{\kappa}^{-\frac{1}{2}}(z - z_{h\tau})\|^2_{L^2(E\times]t_{n-1},t_n[)} + \|p - p_{h\tau}\|^2_{L^2(E\times]t_{n-1},t_n[)}\Big). \tag{7.9}$$

7.4. The pressure's interface jump

The pressure's interface jump at each face $e \in \mathcal{E}_h^1$, defined by (5.33) is

$$\eta_{e,\mathrm{p}}^n = (\Delta t)^{\frac{1}{2}} h_e^{\frac{1}{2}} \| [p_{h\tau}^n] \|_{L^2(e)}.$$

It is bounded via a classical argument on each face $e \in \mathcal{E}_h^1$. Let b_e be a unit bubble polynomial function of the lowest degree that vanishes on ∂e. Let $\hat{e}$ be a reference unit face and $\hat{\omega}_{\hat{e}}$ the union of two reference unit elements that share $\hat{e}$. By working first on $\hat{\omega}_{\hat{e}}$ and then switching to ω_e by a suitable transformation, we can construct an extension operator $\mathcal{G}$, linear from $H_{00}^{\frac{1}{2}}(e)$ into $H_0^1(\omega_e)$ and uniformly continuous with respect to e and h, i.e.,

$$\forall f \in H_{00}^{\frac{1}{2}}(e), \quad |\mathcal{G}(f)|_{H^1(\omega_e)} \le C |f|_{H_{00}^{\frac{1}{2}}(e)}, \tag{7.10}$$

with C independent of h, e, and ω_e. The error equality (5.13) is tested with $\boldsymbol{\zeta}_h = \mathbf{0}$ and

$$\boldsymbol{\zeta} = \mathcal{G}([p_{h\tau}^n] b_e) \boldsymbol{n}_e,$$

a vector valued function that belongs to $H_0^1(\omega_e)^d$. With this choice, Green's formula applied in each of the two elements sharing e results in

$$\begin{aligned}\int_e |[p_{h\tau}^n]|^2 b_e &= \sum_{E\subset\omega_e} \Big(\big(\mu_f \boldsymbol{\kappa}^{-1}(\boldsymbol{z} - \boldsymbol{z}_{h\tau}^n), \boldsymbol{\zeta} \big)_E - \big(p - p_{h\tau}^n, \nabla\cdot\boldsymbol{\zeta} \big)_E \Big) \\ &\quad - \sum_{E\subset\omega_e} \big(-\mu_f \boldsymbol{\kappa}^{-1} \boldsymbol{z}_{h\tau}^n + \rho g \nabla \eta - \nabla p_{h\tau}^n, \boldsymbol{\zeta} \big)_E \\ &\le \|\mu_f \boldsymbol{\kappa}^{-1}(\boldsymbol{z} - \boldsymbol{z}_{h\tau}^n)\|_{L^2(\omega_e)} \|\boldsymbol{\zeta}\|_{L^2(\omega_e)} + \|p - p_{h\tau}^n\|_{L^2(\omega_e)} \|\nabla\cdot\boldsymbol{\zeta}\|_{L^2(\omega_e)} \\ &\quad + \sum_{E\subset\omega_e} \| -\mu_f \boldsymbol{\kappa}^{-1} \boldsymbol{z}_{h\tau}^n + \rho g \nabla \eta - \nabla p_{h\tau}^n \|_{L^2(E)} \|\boldsymbol{\zeta}\|_{L^2(E)}.\end{aligned}$$

Now, by (6.16), (7.10), (6.20) (owing that $[p_{h\tau}^n] b_e$ belongs to a finite dimensional space), the regularity of the mesh, and the local inverse inequality (6.18)

$$\|\boldsymbol{\zeta}\|_{L^2(\omega_e)} \le \hat{C} h_{\omega_e} |\boldsymbol{\zeta}|_{H^1(\omega_e)} \le \hat{C} h_{\omega_e} |[p_{h\tau}^n] b_e|_{H_{00}^{\frac{1}{2}}(e)} \le \hat{C} h_e^{\frac{1}{2}} \|[p_{h\tau}^n]\|_{L^2(e)}, \quad \|\nabla\cdot\boldsymbol{\zeta}\|_{L^2(\omega_e)} \le \frac{\hat{C}}{h_e^{\frac{1}{2}}} \|[p_{h\tau}^n]\|_{L^2(e)}. \tag{7.11}$$

Finally, by the construction of $\mathcal{G}$ and the fact that the restriction of $\boldsymbol{\zeta}$ to e belongs to a finite dimensional space, we obtain

$$\begin{aligned}\|[p_{h\tau}^n]\|_{L^2(e)} \le \hat{C} \Big(&\sum_{E\subset\omega_e} h_e^{\frac{1}{2}} \|\mu_f \boldsymbol{\kappa}^{-1}(\boldsymbol{z} - \boldsymbol{z}_{h\tau}^n)\|_{L^2(E)} + \sum_{E\subset\omega_e} \frac{1}{h_e^{\frac{1}{2}}} \|p - p_{h\tau}^n\|_{L^2(E)} \\ &+ \sum_{E\subset\omega_e} h_e^{\frac{1}{2}} \| -\mu_f \boldsymbol{\kappa}^{-1} \boldsymbol{z}_{h\tau}^n + \rho g \nabla \eta - \nabla p_{h\tau}^n \|_{L^2(E)} \Big).\end{aligned}$$

By multiplying both sides with $h_e^{\frac{1}{2}}$, squaring, and integrating in time, we conclude

$$\big(\eta_{e,\mathrm{p}}^n\big)^2 \le \hat{C} \Big(\|p - p_{h\tau}\|_{L^2(\omega_e \times]t_{n-1}, t_n[)}^2 + \sum_{E\subset\omega_e} h_E^2 \|\mu_f \boldsymbol{\kappa}^{-1}(\boldsymbol{z} - \boldsymbol{z}_{h\tau})\|_{L^2(E\times]t_{n-1}, t_n[)}^2 + \sum_{E\subset\omega_e} \big(\eta_{E,\mathrm{vel}}^n\big)^2 \Big). \tag{7.12}$$

7.5. The second velocity error in space $\overline{\eta}_{E,\mathrm{vel}}^n$

The second velocity error in space, defined by (6.3) is

$$\overline{\eta}_{E,\mathrm{vel}}^n = (\Delta t)^{\frac{1}{2}} \big\| \mu_f \boldsymbol{\kappa}^{-1} \boldsymbol{z}_{h\tau}^n - \rho g \nabla \eta + \nabla (R_h(p_{h\tau}^n)) \big\|_{L^2(E)}.$$

Its bound is derived first as in Section 7.3; the equality (5.13) is tested with $\boldsymbol{\zeta}_h = \mathbf{0}$ and

$$\boldsymbol{\zeta} = \big(\mu_f \boldsymbol{\kappa}^{-1} z^n_{h\tau} - \rho g \nabla \eta + \nabla(R_h(p^n_{h\tau}))\big) b_E.$$

After cancelling some terms, this gives

$$\int_E \big|\mu_f \boldsymbol{\kappa}^{-1} z^n_{h\tau} - \rho g \nabla \eta + \nabla(R_h(p^n_{h\tau}))\big|^2 b_E = \big(\mu_f \boldsymbol{\kappa}^{-1}(z - z^n_{h\tau}), \boldsymbol{\zeta}\big)_E - (p - R_h(p^n_{h\tau}), \nabla \cdot \boldsymbol{\zeta})_E$$
$$\le \sup_{\boldsymbol{\zeta} \in H_0(\mathrm{div}; E)} \frac{1}{\|\boldsymbol{\zeta}\|_{H(\mathrm{div};E)}} \big|\big(\mu_f \boldsymbol{\kappa}^{-1}(z - z^n_{h\tau}), \boldsymbol{\zeta}\big)_E - \big(p - R_h(p^n_{h\tau}), \nabla \cdot \boldsymbol{\zeta}\big)_E\big| \|\boldsymbol{\zeta}\|_{H(\mathrm{div};E)}.$$

Then the local inverse inequality (6.18) implies

$$\overline{\eta}^n_{E,\mathrm{vel}} \le \frac{\hat{C}}{h_E} \overline{\mathcal{E}}^n_{E,\mathrm{vel}}. \tag{7.13}$$

Remark 4. *Of course, the bound (7.13) is not optimal; it is the price to pay for using a simpler indicator that does not invoke the curl and tangential components as in Refs. [9,10].*

7.6. The flow error $\eta^n_{E,\mathrm{flow}}$

The flow error in each element E contained in Ω_1 is

$$\eta^n_{E,\mathrm{flow}} = (\Delta t)^{\frac{1}{2}} \Big\| q^n_h - \frac{1}{\Delta t}\Big(\frac{1}{M}(p^n_h - p^{n-1}_h) + \alpha \nabla \cdot (\boldsymbol{u}^n_h - \boldsymbol{u}^{n-1}_h)\Big) - \nabla \cdot z^n_h \Big\|_{L^2(E)/M_h},$$

where the quotient with respect to M_h is done independently in each element, since the functions of M_h are defined independently in each element. In the case of simplices, and when the divergence of the displacement is locally in M_h, this quotient is zero, but not in the case of bricks, because $\nabla \cdot \boldsymbol{u}_h$ does not have the same degree as p_h, although intuitively the quotient is small. But it does not seem possible to prove mathematically that it is small. It can bounded in each element E by the same localization procedure as in Section 7.3, but this process loses the quotient norm. Indeed, let b_E be the above bubble function, and test Eq. (5.7) with $\theta_h = 0$ and

$$\theta = \Big(q^n_h - \frac{1}{\Delta t}\Big(\frac{1}{M}(p^n_h - p^{n-1}_h) + \alpha \nabla \cdot (\boldsymbol{u}^n_h - \boldsymbol{u}^{n-1}_h)\Big) - \nabla \cdot z^n_h\Big) b_E,$$

that is a polynomial quantity. This gives

$$\int_E \big|q^n_h - \partial_t\big(\frac{1}{M} p^n_{h\tau} + \alpha \nabla \cdot \boldsymbol{u}^n_{h\tau}\big) - \nabla \cdot z^n_h\big|^2 b_E = \Big(\partial_t\big(\frac{1}{M}(p - p^n_{h\tau}) + \alpha \nabla \cdot (\boldsymbol{u} - \boldsymbol{u}^n_{h\tau})\big), \theta\Big)_E$$
$$+ \big(\nabla \cdot (z - z^n_{h\tau}), \theta\big)_E - (q - q^n_h, \theta)_E - \big(\nabla \cdot (z^n_h - z^n_{h\tau}), \theta\big)_E.$$

A standard equivalence of norms in finite dimensions yields

$$\begin{aligned}\big(\eta^n_{E,\mathrm{flow}}\big)^2 \le \hat{c}\Big(&\|\partial_t\big(\frac{1}{M}(p - p_{h\tau}) + \alpha \nabla \cdot (\boldsymbol{u} - \boldsymbol{u}_{h\tau})\big)\|^2_{L^2(E\times]t_{n-1},t_n[)} + \|\nabla \cdot (z - z_{h\tau})\|^2_{L^2(E\times]t_{n-1},t_n[)}\\ &+ \|q - q_h\|^2_{L^2(E\times]t_{n-1},t_n[)} + \|\nabla \cdot (z_h - z_{h\tau})\|^2_{L^2(E\times]t_{n-1},t_n[)}\Big).\end{aligned} \tag{7.14}$$

7.7. The remaining indicators

The upper bounds for the remaining indicators are derived by repeating the above arguments. They lead to

$$\eta^n_{E,\boldsymbol{u}} \le C\Big(h_E \|\boldsymbol{f}(t_n) - \boldsymbol{f}^n_h\|_{H^{-1}(E)} + 2G\|\boldsymbol{\varepsilon}(\boldsymbol{u}(t_n) - \boldsymbol{u}^n_h)\|_{L^2(E)} + \lambda\|\nabla \cdot (\boldsymbol{u}(t_n) - \boldsymbol{u}^n_h)\|_{L^2(E)} + \alpha\|p(t_n) - p^n_h\|_{L^2(E)}\Big), \tag{7.15}$$

$$\begin{aligned}\eta^n_{e,\boldsymbol{\sigma}} \le \hat{C}\Big(&2G\|\boldsymbol{\varepsilon}(\boldsymbol{u}(t_n) - \boldsymbol{u}^n_h)\|_{L^2(\omega_e)} + \lambda\|\nabla \cdot (\boldsymbol{u}(t_n) - \boldsymbol{u}^n_h)\|_{L^2(\omega_e)} + \alpha\|p(t_n) - p^n_h\|_{L^2(\omega_e)} + \|\boldsymbol{f}(t_n) - \boldsymbol{f}^n_h\|_{H^{-1}(\omega_e)}\\ &+ \Big(\sum_{E\subset\omega_e} (\eta^n_{E,\boldsymbol{u}})^2\Big)^{\frac{1}{2}}\Big),\end{aligned} \tag{7.16}$$

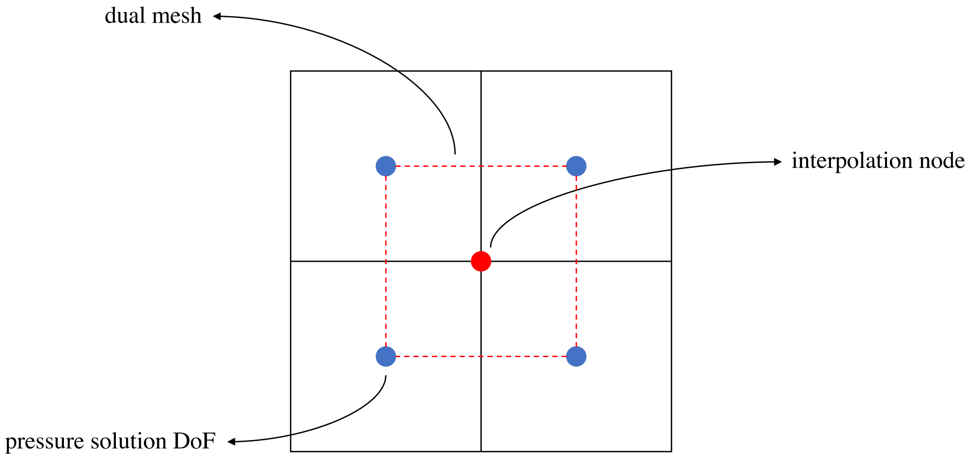

Fig. 1. Postprocess pressure using local interpolation.

$$\eta^n_{e,\boldsymbol{\sigma},N} \leq \hat{C}\Big(2G\|\boldsymbol{\varepsilon}(\boldsymbol{u}(t_n)-\boldsymbol{u}^n_h)\|_{L^2(E_e)} + \lambda\|\nabla\cdot(\boldsymbol{u}(t_n)-\boldsymbol{u}^n_h)\|_{L^2(E_e)} + \|\boldsymbol{f}(t_n)-\boldsymbol{f}^n_h\|_{H^{-1}(E_e)} + \|\boldsymbol{t}_N(t_n)-\boldsymbol{t}^n_{N,h}\|_{H^{-\frac{1}{2}}(e)} + \eta^n_{E_e,\boldsymbol{u}}\Big), \tag{7.17}$$

$$\eta^n_{E,\partial\text{vel}} \leq \hat{C}\mathcal{E}^n_{E,\partial\text{vel}}, \tag{7.18}$$

$$\overline{\eta}^n_{E,\partial\text{vel}} \leq \frac{\hat{C}}{h_E}\overline{\mathcal{E}}^n_{E,\partial\text{vel}}, \tag{7.19}$$

a suboptimal bound, as was the case of $\overline{\eta}^n_{E,\text{vel}}$, for the same reason,

$$\eta^n_{e,\partial\text{p}} \leq \hat{C}\Big(\big(\mathcal{E}^n_{\omega_e,\partial\text{vel}}\big)^2 + \sum_{E\subset\omega_e}\big(\eta^n_{E,\partial\text{vel}}\big)^2\Big)^{\frac{1}{2}}, \tag{7.20}$$

$$\eta^n_{E,\partial\boldsymbol{u}} \leq \hat{C}\mathcal{E}^n_{E,\partial\boldsymbol{\sigma}}, \tag{7.21}$$

with similar upper bounds for $\eta^n_{e,\partial\boldsymbol{\sigma}}$ and $\eta^n_{e,\partial\boldsymbol{\sigma},N}$.

8. Numerical results

In this section, we first present numerical results that validate the theoretical analysis. Then we demonstrate the improvement made on the algorithm performance based upon the a posteriori error indicators. The code that produces the examples is constructed using the open-source finite element library deal.II [19]. The experiment setup are mostly kept consistent with the previous study where the flow is solved by Enriched Galerkin method [5].

8.1. Pressure post processing

The error indicators $\bar{\eta}_{vel}$ and $\bar{\eta}_{\partial vel}$ involve a reconstructed pressure $R_h(p_h)$ in $H^1(\Omega)$ derived from the piecewise constant pressure obtained by solving the mixed formulation. In this section, we introduce a cheap post processing procedure that does not require solving a local problem. The reconstruction is depicted using quadrilaterals but can be easily adapted to triangles.

As illustrated in Fig. 1, for each interpolation node, we construct a dual mesh E^* by connecting the centroid of the elements adjacent to it. Let z_h be the discrete velocity and let $\tilde{p}_h = R_h(p_h)$ be the reconstructed pressure in $H^1(\Omega)$; we denote by $\tilde{z}_h$ the quantity defined at the interpolation node by

$$\tilde{z}_h = -\frac{\boldsymbol{\kappa}}{\mu_f}\frac{\tilde{p}_h - p_h}{\Delta x}, \tag{8.1}$$

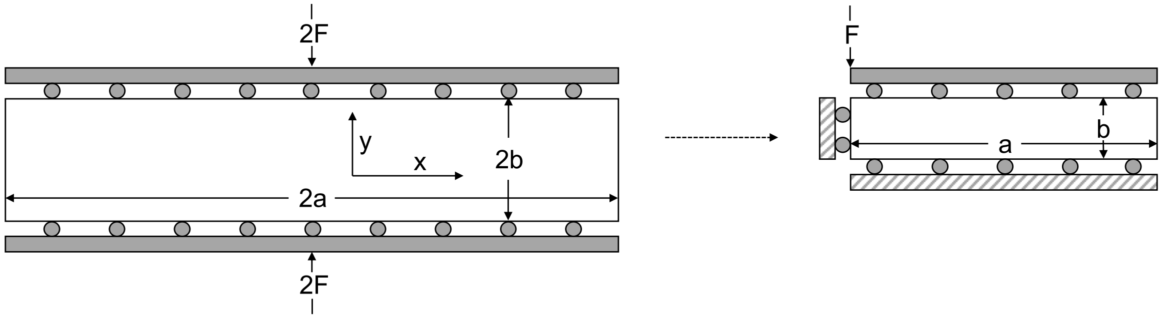

Fig. 2. The physical (left) and computational (right) domain of Mandel's problem.

where Δx is the distance between the interpolation node and the adjacent pressure degree of freedom (DoF). Then the nodal pressure interpolation is computed such that for every element E_k that intersects the dual element E^*,

$$\sum_k \int_{\partial(E_k \cap E^*)} \tilde{z}_h \cdot \boldsymbol{n}_e = \sum_k \int_{\partial(E_k \cap E^*)} z_h \cdot \boldsymbol{n}_e. \tag{8.2}$$

8.2. The Mandel problem

We use Mandel's problem [20] to benchmark our numerical solution and investigate the effectivity of the a posteriori error indicators. Consider a poroelastic slab with $2a$ in the x-direction and $2b$ in the y-direction sandwiched between two frictionless rigid plates. At $t = 0^+$, both plates are loaded instantaneously by a constant force $2F$. Due to the bi-axial symmetry of the physical problem, we reduce the computational domain to a quarter of the physical domain as shown in Fig. 2. Such problem setup can be described by the Biot model without gravity as follows:

$$\begin{aligned} -\nabla \cdot (\lambda(\nabla \cdot u)\boldsymbol{I} + 2G\boldsymbol{\varepsilon}(\boldsymbol{u}) - \alpha p \boldsymbol{I}) = \boldsymbol{0} \quad &\text{in } \Omega \times]0, T[, \\ \partial_t \left(\frac{1}{M} p + \alpha \nabla \cdot \boldsymbol{u} \right) - \frac{1}{\mu_f} \nabla \cdot (\boldsymbol{\kappa} \nabla p) = 0 \quad &\text{in } \Omega \times]0, T[, \end{aligned} \tag{8.3}$$

with $\Omega =]0, a[\times]0, b[$ being the computational domain. The boundary and initial conditions are:

$$\begin{aligned} \boldsymbol{z} \cdot \boldsymbol{n} = 0, \quad \boldsymbol{u}_x = 0, \quad \sigma_{xy} = 0 \quad &\text{on } x = 0, \\ p = 0, \quad \boldsymbol{\sigma} \cdot \boldsymbol{n} = \boldsymbol{0} \quad &\text{on } x = a, \\ \boldsymbol{z} \cdot \boldsymbol{n} = 0, \quad \boldsymbol{u}_y = 0, \quad \sigma_{xy} = 0 \quad &\text{on } y = 0, \\ \boldsymbol{z} \cdot \boldsymbol{n} = 0, \quad \boldsymbol{u}_y = U_y(b, t), \quad \sigma_{xy} = 0 \quad &\text{on } y = b, \\ p|_{t=t_0} = P_{t_0}(x, y). & \end{aligned} \tag{8.4}$$

Here $U_y(b, t)$ is the analytical solution of the y-displacement at $y = b$. Since the solution to Mandel's problem at early time lacks regularity [21], the benchmark problem is usually initialized with the pressure's analytical solution at a later time $t_0 > 0$. The analytical solutions for the pressure, displacement, and stress are provided by infinite series as described in [22]. Note that the velocity's analytical solution can be derived from that of the pressure and there is no shear stress in such problem setup.

The parameters used in the numerical experiment are listed in Table 1. To benchmark the solution algorithm, we measure the numerical convergence of the pressure/velocity and displacement solution under spatial refinement by the L^2 and energy norm of their respective error, defined by

$$\|\boldsymbol{u} - \boldsymbol{u}_h\|_e := \left(2G \|\boldsymbol{\varepsilon}(\boldsymbol{u} - \boldsymbol{u}_h)\|^2_{L^2(\Omega)} + \lambda \|\nabla \cdot (\boldsymbol{u} - \boldsymbol{u}_h)\|^2_{L^2(\Omega)} \right)^{\frac{1}{2}}. \tag{8.5}$$

The simulations are run within the time interval [0.01 s, 0.0101 s]. A small time step $\Delta t = 10^{-6}$ s and fixed-stress convergence tolerance $\varepsilon = 10^{-6}$ are employed to minimize the error caused by temporal discretization and fixed-stress split algorithm. The numerical errors calculated at final time are summarized in Table 2. We observe first

Table 1
Parameters for the Mandel problem.

Parameter	Quantity	Value	Unit
a	x dimension	1.0	m
b	y dimension	1.0	m
κ	Permeability	1e−2	m^2
μ_f	Fluid viscosity	1.0	Pa s
F	Point load intensity	2.0×10^3	N
E	Young's modulus	1.0×10^4	Pa
ν	Poisson's ratio	0.2	–
α	Biot's coefficient	1.0	–
M	Biot's modulus	1.0×10^4	Pa

Table 2
Convergence of pressure/velocity and displacement solutions under spatial refinement.

$\mathcal{T}_h$	$\\|M^{-\frac{1}{2}}(p^N - p_h^N)\\|_{L^2(\Omega)}$	Rate	$\\|\boldsymbol{\kappa}^{-\frac{1}{2}}(\boldsymbol{z}^N - \boldsymbol{z}_h^N)\\|_{L^2(\Omega)}$	Rate	$\\|\boldsymbol{u}^N - \boldsymbol{u}_h^N\\|_e$	Rate
32 × 32	2.7137e−02	–	5.3619e−03	–	2.5745e−02	–
64 × 64	1.3568e−02	1.0000	1.3243e−03	2.0175	1.2872e−02	1.0000
128 × 128	6.7842e−03	1.0000	3.1519e−04	2.0710	6.4360e−03	1.0000
256 × 256	3.9063e−03	1.0000	6.4319e−05	2.2929	3.2180e−03	1.0000

order convergence for the pressure and displacement and second order convergence for the velocity, as predicted by the theoretical estimates.

We then test the effectivity of the error indicators in (5.42)–(5.45) and (6.2)–(6.5). With our problem setup, the local error indicators on the interface of pay-zone and nonpay-zone $\mathcal{E}_h^{12}$, the faces in the nonpay-zone $\mathcal{E}_h^2$, and the elements in the nonpay-zone $\mathcal{T}_h^2$ are excluded. Since the traction boundary is applied on part of the pay-zone boundary, the corresponding error indicators related to the stress tensor include the contribution from the pore pressure $-\alpha p\boldsymbol{I}$. We group the indicators into flow and mechanics part with the additional error indicators regarding the time derivative of velocity residuals and pressure jump absorbed by mechanics as follow:

$$\eta_{FLOW} := \left(\eta_{fs}^2 + \eta_{time}^2 + \eta_{flow}^2 + \eta_{vel}^2 + \bar{\eta}_{vel}^2 + \eta_{J,p}^2\right)^{\frac{1}{2}}, \tag{8.6}$$

$$\eta_{MECH} := \left(\eta_{displ}^2 + \eta_{\partial(displ)}^2 + \eta_{\partial vel}^2 + \bar{\eta}_{\partial vel}^2 + \eta_{J,\partial p}^2\right)^{\frac{1}{2}}. \tag{8.7}$$

We associate η_{FLOW} and η_{MECH} with the error norms

$$|||(p,\boldsymbol{u}) - (p_h,\boldsymbol{u}_h)|||_1 := \left(\frac{1}{M}\|p - p_h\|_{L^2(\Omega)}^2 + \|\boldsymbol{u} - \boldsymbol{u}_h\|_e^2 + \mu_f\|\boldsymbol{\kappa}^{-\frac{1}{2}}(\boldsymbol{z} - \boldsymbol{z}_h)\|_{\Omega\times]t_0,T[}\right)^{\frac{1}{2}}, \tag{8.8}$$

$$|||(p,\boldsymbol{u}) - (p_h,\boldsymbol{u}_h)|||_2 := 2G\|\boldsymbol{\varepsilon}(\boldsymbol{u} - \boldsymbol{u}_h)\|_{L^2(\Omega)} + \lambda\|\nabla\cdot(\boldsymbol{u} - \boldsymbol{u}_h)\|_{L^2(\Omega)} + \alpha\|p - p_h\|_{L^2(\Omega)}. \tag{8.9}$$

These error norms are adopted from the left hand side of the posteriori error analysis. Then the effectivity indices are defined as

$$\mathcal{I}_{eff,\ FLOW} = \frac{\eta_{FLOW}}{|||(p,\boldsymbol{u}) - (p_h,\boldsymbol{u}_h)|||_1}, \quad \mathcal{I}_{eff,\ MECH} = \frac{\eta_{MECH}}{|||(p,\boldsymbol{u}) - (p_h,\boldsymbol{u}_h)|||_2}. \tag{8.10}$$

With two groups of convergence tests, we study the effectivity of the a posteriori error indicators under simultaneous spatial and temporal refinements. The first group of simulations run from 0.01 s to 0.02 s with a fixed-stress convergence tolerance of $\varepsilon = 10^{-6}$. Note that the flow indicator η_{flow} is a quotient norm up to polynomials of order k, with $k = 0$ in our case. Since $\nabla\cdot\boldsymbol{u}_h$ is a constant for piecewise linear elements, then the flow indicator has value zero throughout the computational domain and therefore is omitted from the table. The convergence behavior of each error indicator and the overall effectivity index are summarized in Tables 3 and 4. The fixed-stress algorithm indicator η_{fs} is directly affected by the tight tolerance we set on the simulation and therefore remains small. Other indicators mainly exhibit first order convergence except η_{displ} and $\eta_{\partial(displ)}$, which indicate one and

Table 3
Convergence of individual a posteriori error indicators under simultaneous spatial and temporal refinement with simulations from 0.01 s to 0.02 s.

Δt, $\mathcal{T}_h$	η_{fs}	η_{time}	Rate	η_{vel}	Rate	$\bar{\eta}_{vel}$	Rate	$\eta_{J,p}$	Rate
$1e{-}3$, 32×32	$3.1281e{-}09$	$1.5723e{-}02$	–	$5.9467e{-}01$	–	$2.7107e{-}01$	–	$4.2041e{-}01$	–
$5e{-}4$, 64×64	$1.7699e{-}08$	$8.0073e{-}03$	0.9735	$3.0189e{-}01$	0.9781	$1.3753e{-}01$	0.9789	$2.1346e{-}01$	0.9778
$2.5e{-}4$, 128×128	$9.3120e{-}08$	$4.0410e{-}03$	0.9866	$1.5212e{-}01$	0.9888	$6.9284e{-}02$	0.9891	$1.0756e{-}01$	0.9888
$1.25e{-}4$, 256×256	$5.3185e{-}07$	$2.0295e{-}03$	0.9936	$7.6368e{-}02$	0.9942	$3.4779e{-}02$	0.9943	$5.4000e{-}02$	0.9942

Δt, $\mathcal{T}_h$	η_{displ}	Rate	$\eta_{\partial(displ)}$	Rate	$\eta_{\partial vel}$	Rate	$\bar{\eta}_{\partial vel}$	Rate	$\eta_{J,\partial p}$	Rate
$1e{-}3$, 32×32	$5.3517e{-}01$	–	$6.0452e{-}01$	–	$6.2292e{+}01$	–	$2.8385e{+}01$	–	$4.4039e{+}01$	–
$5e{-}4$, 64×64	$1.9498e{-}01$	1.4566	$2.1972e{-}01$	1.4601	$3.1725e{+}01$	0.9734	$1.4450e{+}01$	0.9741	$2.2432e{+}01$	0.9732
$2.5e{-}4$, 128×128	$7.1595e{-}02$	1.4454	$7.9704e{-}02$	1.4630	$1.6010e{+}01$	0.9866	$7.2914e{+}00$	0.9868	$1.1321e{+}01$	0.9866
$1.25e{-}4$, 256×256	$2.8524e{-}02$	1.3277	$3.1185e{-}02$	1.3538	$8.0404e{+}00$	0.9937	$3.6617e{+}00$	0.9937	$5.6854e{+}00$	0.9936

Table 4
Effectivity indices under simultaneous spatial and temporal refinement with simulations from 0.01 s to 0.02 s.

Δt, $\mathcal{T}_h$	η_{FLOW}	Rate	$\lVert(p,\boldsymbol{u})-(p_h,\boldsymbol{u}_h)\rVert_1$	Rate	$\mathcal{I}_{eff,FLOW}$
$1e{-}3$, 32×32	$7.7724e{-}01$	–	$7.5937e{-}02$	–	10.2353
$5e{-}4$, 64×64	$3.9456e{-}01$	0.9781	$3.8937e{-}02$	0.9637	10.1333
$2.5e{-}4$, 128×128	$1.9882e{-}01$	0.9888	$2.0128e{-}02$	0.9520	9.8777
$1.25e{-}4$, 256×256	$9.9808e{-}02$	0.9942	$1.1259e{-}03$	0.8381	8.8648

Δt, $\mathcal{T}_h$	η_{MECH}	Rate	$\lVert(p,\boldsymbol{u})-(p_h,\boldsymbol{u}_h)\rVert_2$	Rate	$\mathcal{I}_{eff,MECH}$
$1e{-}3$, 32×32	$8.1401e{+}01$	–	$8.0730e{+}00$	–	10.0830
$5e{-}4$, 64×64	$4.1455e{+}01$	0.9735	$4.1597e{+}00$	0.9566	9.9660
$2.5e{-}4$, 128×128	$2.0920e{+}01$	0.9866	$2.1600e{+}00$	0.9454	9.6853
$1.25e{-}4$, 256×256	$1.0506e{+}01$	0.9937	$1.2170e{+}00$	0.8277	8.6326

a half order convergence. Consequently, the summation indicator η_{FLOW} for flow reveals first order convergence. Meanwhile, the displacement indicators with one and a half order convergence are overshadowed by error indicators regarding the time derivative of velocity residuals and pressure jump. Therefore, the summation indicator η_{MECH} for mechanics also indicate first order convergence. With $\lVert(p,\boldsymbol{u})-(p_h,\boldsymbol{u}_h)\rVert_1$ and $\lVert(p,\boldsymbol{u})-(p_h,\boldsymbol{u}_h)\rVert_2$ having the same convergence behavior, $\mathcal{I}_{eff,\ FLOW}$ and $\mathcal{I}_{eff,\ MECH}$ demonstrates converging trend towards values around 8.9 and 8.6, respectively. We observe a larger effectivity index as compared to the previous study with flow solved by Enriched Galerkin. This is because the error indicators derived for mixed methods involve bounds for $\|\partial_t(p-p_h)\|_{L^2(\Omega\times]0,T[)}$, $\|\partial_t(\boldsymbol{z}-\boldsymbol{z}_h)\|_{L^2(\Omega\times]0,T[)}$, $\|\nabla\cdot(\boldsymbol{z}-\boldsymbol{z}_h)\|_{L^2(\Omega\times]0,T[)}$, and $\|\partial_t(\boldsymbol{u}-\boldsymbol{u}_h)\|_e$. However it is not possible to calculate the exact errors on these quantities because in this example, the formula for the exact solution is not known. Therefore we find an artificially large effectivity index because the error definitions in (8.8) and (8.9) do not include these quantities.

The other group of simulations run from 0.001 s to 0.002 s with time steps one order of magnitude smaller than the ones from the previous group. The convergence behavior of each error indicator and the overall effectivity index are summarized in Tables 5 and 6. We observe a similar convergence behavior on the individual indicators and effectivity indices while $\mathcal{I}_{eff,\ FLOW}$ and $\mathcal{I}_{eff,\ MECH}$ stay fairly constant around 10.8 and 28.2, respectively. The results from the two groups of tests suggest that the error indicators and effectivity indices depend upon initial/final condition, spatial mesh size, and time step size.

8.3. Dynamic mesh adaptivity guided by the a posteriori error indicators

Geomechanical effects play a significant role in unconventional reservoir development and carbon sequestration by affecting the flow behavior around fractures and faults. In this section, we describe an example where a posteriori error indicators are used to guide dynamic mesh adaptivity for improving computational efficiency of simulations on fractured reservoirs. The permeability distribution and boundary conditions of the model are illustrated in Fig. 3. The domain size is $[0, 1] \times [0, 1]$ m^2. The fracture width is $1/64$ m with a permeability of 10^{-11} m^2 while the

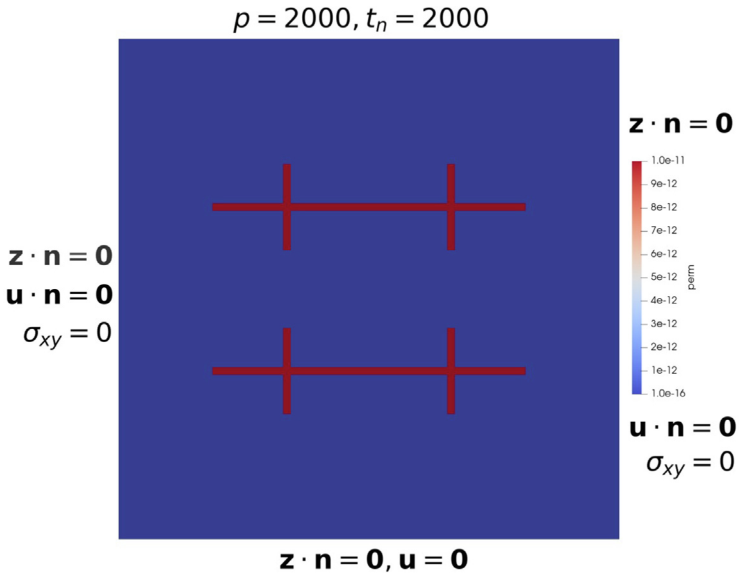

Fig. 3. Permeability distribution and boundary conditions for fractured porous media example.

Table 5
Convergence of individual a posteriori error indicators under simultaneous spatial and temporal refinement with simulations from 0.001 s to 0.002 s.

$\Delta t,\ \mathcal{T}_h$	η_{fs}	η_{time}	Rate	η_{vel}	Rate	$\bar{\eta}_{vel}$	Rate	$\eta_{J,p}$	Rate
$1e{-}4,\ 32\times 32$	$9.4623e{-}09$	$1.4894e{-}02$	–	$7.5062e{-}01$	–	$4.1138e{-}01$	–	$5.3061e{-}01$	–
$5e{-}5,\ 64\times 64$	$5.4140e{-}08$	$7.5924e{-}03$	0.9721	$3.7655e{-}01$	0.9952	$2.0698e{-}01$	0.9910	$2.6624e{-}01$	0.9949
$2.5e{-}5,\ 128\times 128$	$2.8569e{-}08$	$3.8330e{-}03$	0.9861	$1.8858e{-}01$	0.9976	$1.0384e{-}01$	0.9950	$1.3335e{-}01$	0.9976
$1.25e{-}5,\ 256\times 256$	$1.6396e{-}06$	$1.9252e{-}03$	0.9935	$9.4370e{-}02$	0.9988	$5.2021e{-}02$	0.9972	$6.6730e{-}02$	0.9988

$\Delta t,\ \mathcal{T}_h$	η_{displ}	Rate	$\eta_{\partial(displ)}$	Rate	$\eta_{\partial vel}$	Rate	$\bar{\eta}_{\partial vel}$	Rate	$\eta_{J,\partial p}$	Rate
$1e{-}4,\ 32\times 32$	$8.6435e{-}01$	–	$3.0755e{-}01$	–	$2.0153e{+}02$	–	$2.6988e{+}02$	–	$1.4226e{+}02$	–
$5e{-}5,\ 64\times 64$	$3.0634e{-}01$	1.4965	$1.1058e{-}01$	1.4757	$1.0248e{+}02$	0.9757	$1.3714e{+}02$	0.9767	$7.2430e{+}01$	0.9739
$2.5e{-}5,\ 128\times 128$	$1.0892e{-}01$	1.4919	$4.0914e{-}02$	1.4345	$5.1654e{+}01$	0.9883	$6.9176e{+}01$	0.9873	$3.6521e{+}01$	0.9879
$1.25e{-}5,\ 256\times 256$	$3.9125e{-}02$	1.4771	$1.6572e{-}02$	1.3039	$2.5921e{+}01$	0.9947	$3.4737e{+}01$	0.9938	$1.8329e{+}01$	0.9946

Table 6
Effectivity indices under simultaneous spatial and temporal refinement with simulations from 0.001 s to 0.002 s.

$\Delta t,\ \mathcal{T}_h$	η_{FLOW}	Rate	$\vert\!\vert\!\vert(p,\boldsymbol{u})-(p_h,\boldsymbol{u}_h)\vert\!\vert\!\vert_1$	Rate	$\mathcal{I}_{eff,FLOW}$
$1e{-}4,\ 32\times 32$	$1.0072e{+}00$	–	$9.0951e{-}02$	–	11.0740
$5e{-}5,\ 64\times 64$	$5.0554e{-}01$	0.9944	$4.5661e{-}02$	0.9941	11.0716
$2.5e{-}5,\ 128\times 128$	$2.5326e{-}01$	0.9972	$2.3018e{-}02$	0.9882	11.0029
$1.25e{-}5,\ 256\times 256$	$1.2676e{-}01$	0.9985	$1.1778e{-}03$	0.9666	10.7622

$\Delta t,\ \mathcal{T}_h$	η_{MECH}	Rate	$\vert\!\vert\!\vert(p,\boldsymbol{u})-(p_h,\boldsymbol{u}_h)\vert\!\vert\!\vert_2$	Rate	$\mathcal{I}_{eff,MECH}$
$1e{-}4,\ 32\times 32$	$3.6554e{+}02$	–	$1.3039e{+}01$	–	28.0428
$5e{-}5,\ 64\times 64$	$1.8589e{+}02$	0.9760	$6.5353e{+}00$	0.9965	28.4426
$2.5e{-}5,\ 128\times 128$	$9.3740e{+}01$	0.9877	$3.2930e{+}00$	0.9889	28.4668
$1.25e{-}5,\ 256\times 256$	$4.7058e{+}01$	0.9942	$1.6693e{+}00$	0.9801	28.1901

matrix permeability is 10^{-16} m^2. The fluid density is 1 kg/m^3 and its viscosity is 10^{-3} Pa s. The Young's modulus is 5×10^6 Pa and 1×10^4 Pa for the matrix and fracture, respectively. There is one well located at the center of each horizontal fracture, producing at 2×10^{-6} m^3/s. The simulation runs in time interval [0, 500 s] with a uniform time step of 20 s.

Table 7
Comparison of system sizes between the adaptive and fine scale mesh.

Physical system	Fine scale mesh 256 × 256	Adaptive mesh $t = 100$ s	Adaptive mesh $t = 500$ s
Flow (pressure + velocity)	197 120 (65 536 + 131 584)	27 253 (8209 + 19 044, 13.8%)	41 525 (12 256 + 29 269, 21.1%)
Mechanics	132 098	18 298 (13.9%)	27 826 (21.1%)

We first group the local error indicators into the flow and mechanics part to measure their respective error as follow:

$$\eta_{E,displ} = \left(\eta^2_{E,\boldsymbol{u}} + \sum_{e\in\partial E}\eta^2_{e,\boldsymbol{\sigma}}\right)^{\frac{1}{2}}, \quad \eta_{E,\partial(displ)} = \left(\eta_{E,\partial\boldsymbol{u}} + \sum_{e\in\partial E}\eta^2_{e,\partial\boldsymbol{\sigma}}\right)^{\frac{1}{2}}, \tag{8.11}$$

$$\eta_{E,FLOW} := \left(\eta^2_{E,fs} + \eta^2_{E,time} + \eta^2_{E,flow} + \eta^2_{E,vel} + \bar{\eta}^2_{E,vel} + \sum_{e\in\partial E}\eta^2_{J,p}\right)^{\frac{1}{2}}, \tag{8.12}$$

$$\eta_{E,MECH} := \left(\eta^2_{E,displ} + \eta^2_{E,\partial(displ)} + \eta_{E,\partial vel} + \bar{\eta}_{E,\partial vel} + \sum_{e\in\partial E}\eta^2_{J,\partial p}\right)^{\frac{1}{2}}. \tag{8.13}$$

Then each local indicator is normalized and summed to form the refinement indicator as

$$\eta_{E,refine} := \frac{\eta_{E,FLOW}}{\|\eta_{E,FLOW}\|_{l_\infty(\mathcal{T}_h)}} + \frac{\eta_{E,MECH}}{\|\eta_{E,MECH}\|_{l_\infty(\mathcal{T}_h)}}. \tag{8.14}$$

The initial mesh is 64 × 64 uniform squares. For every time step $]t_{n-1}, t_n[$, the local refinement indicators are calculated on each element $E \in \mathcal{T}_h$. Elements with top 10% indicator values are refined while the bottom 20% are coarsened. The minimum and maximum element size constraints are set to $h = 1/8$ m and $h = 1/512$ m respectively. The adaptive mesh and its corresponding solution are illustrated in Fig. 4. We observe that most refinements occur around the well and along the fracture boundary with noticeable pressure disturbance, due to the flow error. Numerous refinements are also applied at fracture tips to capture the special behavior of displacement caused by dramatically changing mechanical properties.

We confirm the accuracy of the adaptive solution by comparing its values for pressure and volumetric strain against the ones from the 256 × 256 fine scale solution along $y = 86/128$, which slices through the well in the upper horizontal fracture. The results for $t = 100$ s and $t = 500$ s are plotted in Fig. 5. We observe that the solutions for pressure and volumetric strain are well aligned with each other. While achieving exceptional accuracy, the dynamic adaptive mesh provides significant improvement on computational efficiency by reducing the size of the system. We compare the number of degree of freedoms (DoFs) between the adaptive and fine scale solution. The result is summarized in Table 7. The number of DoFs for the adaptive mesh increases as time progresses. However, the overall system size is around 20% of the fine scale system. Note that although the mixed method results in a large block matrix, such matrix can be condensed to the pressure system by applying a proper preconditioner.

8.4. Novel stopping criterion for the fixed-stress split algorithm

One has to set the convergence threshold ε to solve the Biot system with the fixed-stress iterative coupling algorithm. Two stopping criteria are widely accepted as

criterion 1

$$\left\|\bar{\sigma}_h^{n,l} - \bar{\sigma}_h^{n,l-1}\right\|_{L^\infty(\Omega)} \le \varepsilon, \tag{8.15}$$

criterion 2

$$\left\|\frac{\bar{\sigma}_h^{n,l} - \bar{\sigma}_h^{n,l-1}}{\bar{\sigma}_h^{n,l}}\right\|_{L^\infty(\Omega)} \le \varepsilon. \tag{8.16}$$

The value for such threshold is either subjectively based on one's experience or finely tuned for specific simulations. A new novel stopping criterion was proposed in the previous work [5] to avoid such subjectivity by balancing the algorithmic error with the discretization error:

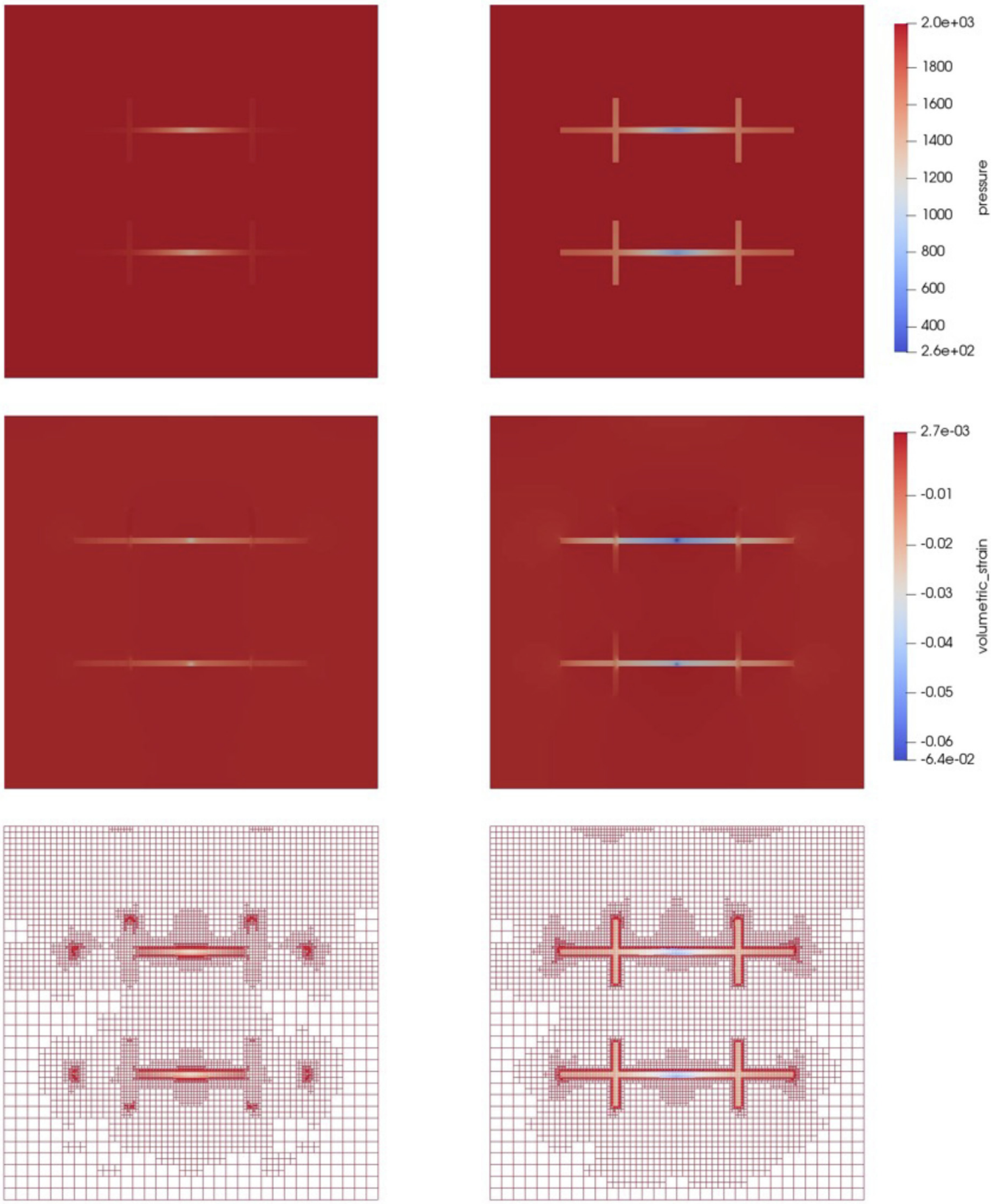

Fig. 4. Dynamic mesh adaptivity for fractured porous media guided by the a posteriori error indicators: pressure (top), volumetric strain (middle), adaptive mesh (bottom).

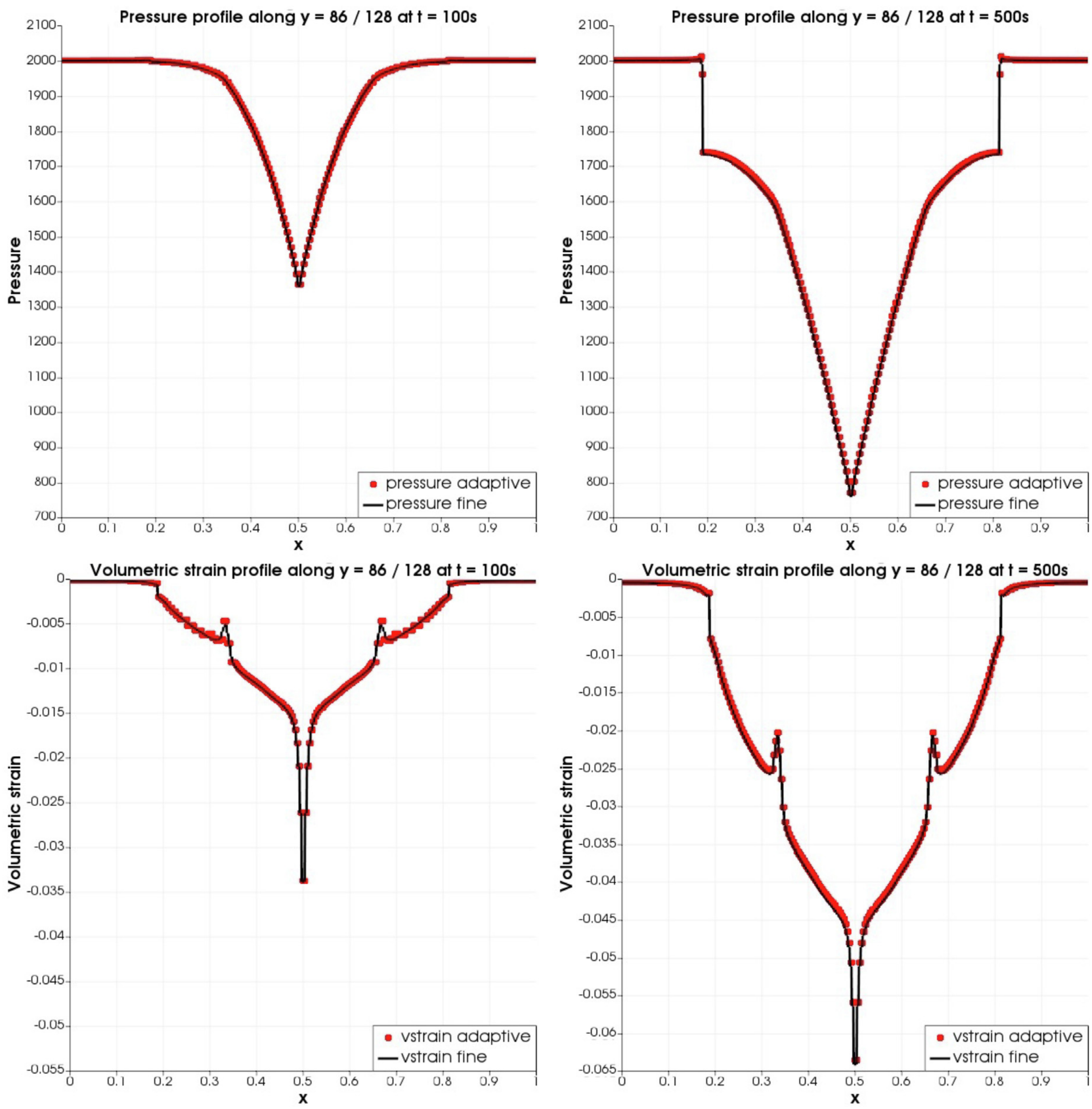

Fig. 5. Comparison between solutions on a dynamic adaptive mesh and an uniform 256 × 256 fine scale mesh along $y = 86/128$: pressure(top), volumetric strain(bottom).

novel criterion

$$\eta_{fs}^{n,l} \leq \delta(\eta_{flow}^{n,l} + \eta_{time}^{n,l} + \eta_{vel}^{n,l} + \bar{\eta}_{vel}^{n,l} + \eta_{J,p}^{n,l} + \eta_{displ}^{n,l} + \eta_{\partial(displ)}^{n,l} + \eta_{\partial vel}^{n,l} + \bar{\eta}_{\partial vel}^{n,l} + \eta_{J,\partial p}^{n,l}). \tag{8.17}$$

The algorithm is considered to achieve convergence when the fixed-stress algorithmic error is one order of magnitude smaller than the sum of discretization errors ($\delta = 0.1$). We demonstrate the validity of this approach with error indicators derived for flow solved by a mixed finite element method.

We first test the novel stopping criterion with Mandel's problem and the model parameters in Table 1. The simulations run from 0 s to 1 s with a time step of 0.1 s on a uniform 64 × 64 mesh. The threshold for criterion 1 and criterion 2 are set to 10^{-6}. The convergence behavior and solution errors from the novel criterion are compared

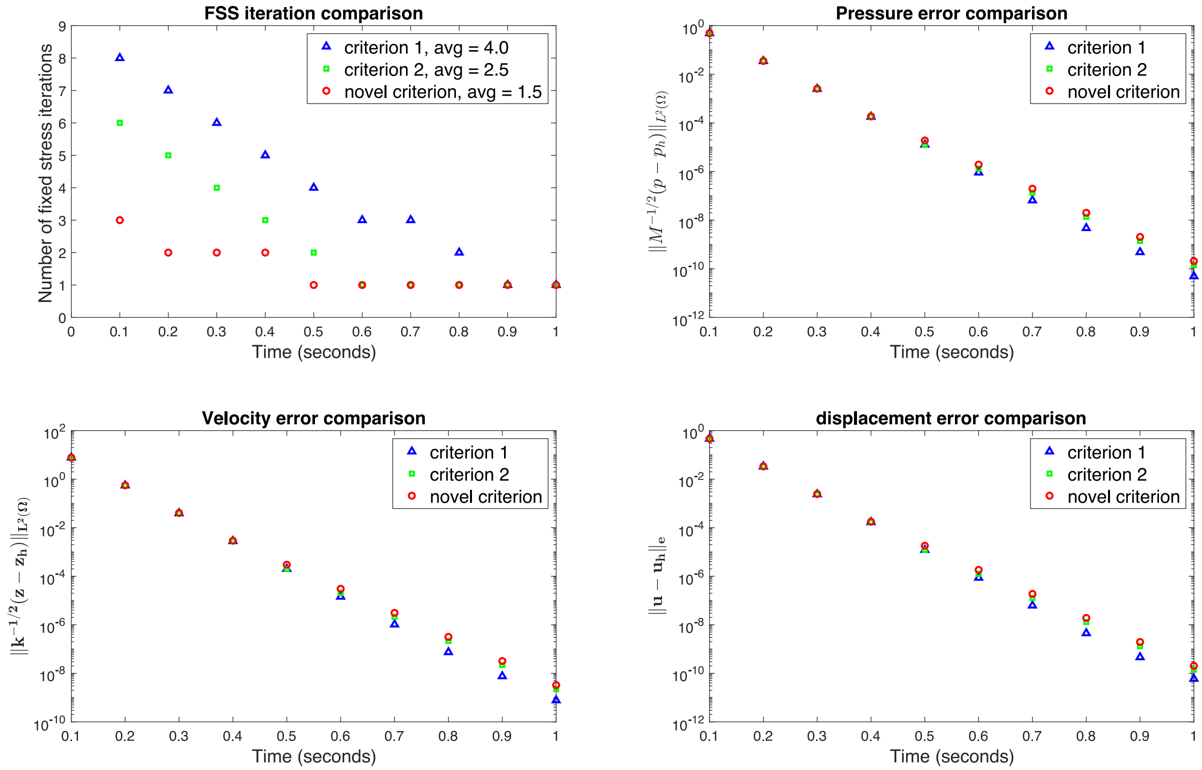

Fig. 6. Comparison of fixed stress iteration number and solution error between different stopping criterion for the Mandel's problem.

Table 8
Comparison of average number of iterations per timestep using different stopping criteria for the fractured porous media.

Criterion	Average number of fixed-stress iterations
Criterion 1, $\varepsilon = 1e{-}3$	3.7
Criterion 2, $\varepsilon = 1e{-}3$	3.5
Novel criterion, $\delta = 0.1$	2.9

versus the ones from the other two criteria as illustrated in Fig. 6. We observe that the number of iterations required for convergence when using the novel criterion is significantly less than the ones using criterion 1 and 2. The novel criterion achieves convergence in an average of 1.5 iterations. Meanwhile, criteria 1 and 2 require 4.0 and 2.5 iterations, respectively. While reducing the number of fixed-stress iterations, the solution computed by using the novel criterion achieves a similar accuracy as with criteria 1 and 2.

The second test is done when using the fractured reservoir example. The simulations run from 0 s to 500 s with a time step of 20 s on a uniform 128 × 128 mesh. The average number of iterations taken for each convergence criterion is summarized in Table 8. The result indicates that the novel criterion also reduces the average number of iterations for convergence. The solutions for the pressure and volumetric strain along the top horizontal fracture using different criteria are plotted in Fig. 7. The solution obtained by the novel criterion achieves similar accuracy compared to that obtained with the other two. The results indicate that the approach proposed in [5] is still valid with the set of estimators used in mixed discretization for the flow.

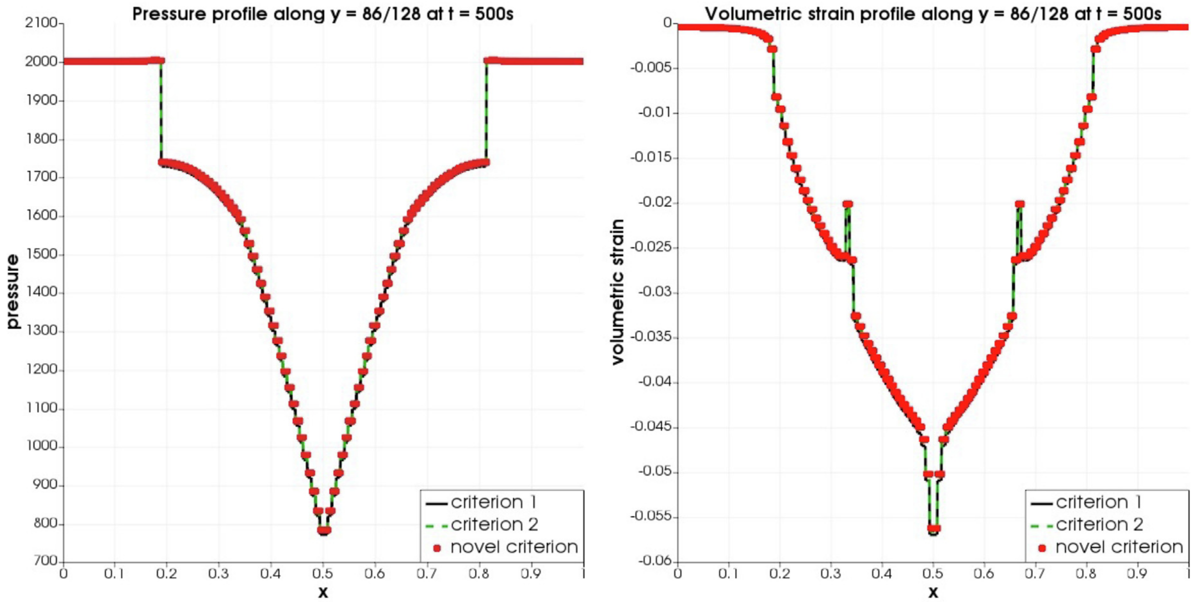

Fig. 7. Comparison of pressure and volumetric strain between different stopping criterion for the fractured reservoir example.

Declaration of competing interest

The authors declare that they have no known competing financial interests or personal relationships that could have appeared to influence the work reported in this paper.

Acknowledgments

Hanyu Li and Mary F. Wheeler have been supported under the Center for Subsurface Modeling Affiliates Program, United States of America and the National Science Foundation, United States of America grant 1911320 (Collaborative Research: High-Fidelity Modeling of Poromechanics with Strong Discontinuities). Vivette Girault has been partially support under the CSM Affiliates program and the J.T. Oden Visitors Program.

References

[1] A. Settari, F.M. Mourits, Coupling of geomechanics and reservoir simulation models, in: Siriwardane, Zema (Eds.), Comp. Methods and Advances in Geomech., Balkema, Rotterdam, 1994, pp. 2151–2158.
[2] A. Settari, D.A. Walters, Advances in coupled geomechanics and reservoir modeling with applications to reservoir compaction, in: The SPE Reservoir Simulation Symposium, Houston, Texas, 1999.
[3] A. Settari, D.A. Walters, Advances in coupled geomechanical and reservoir modeling with applications to reservoir compaction, SPE J. 6 (03) (2001) 334–342.
[4] A. Mikelić, M.F. Wheeler, Convergence of iterative coupling for coupled flow and geomechanics, Comput. Geosci. 17 (3) (2013) 455–461.
[5] V. Girault, X. Lu, M.F. Wheeler, A posteriori error estimates for Biot system using Enriched Galerkin for flow, Comput. Methods Appl. Meth. Engrg. 369 (2020) 113185.
[6] M. Ainsworth, J. Oden, A Posteriori Error Estimation in Finite Element Analysis, John Wiley and Sons Inc., New York, 2000.
[7] T. Arbogast, M.F. Wheeler, I. Yotov, Mixed finite elements for elliptic problems with tensor coefficients as cell-centered finite differences, SIAM J. Numer. Anal. 34 (2) (1997) 828–852.
[8] M. Ainsworth, J.T. Oden, A posteriori error estimation in finite element analysis, Comput. Methods Appl. Mech. Engrg. 142 (1–2) (1997) 1–88.
[9] A. Demlow, A.N. Hirani, A posteriori error estimates for finite element exterior calculus: the de Rham complex, Found. Comput. Math. 14 (2014) 1337–1371.
[10] Y. Li, L. Zikatanov, Residual-based a posteriori error estimates of mixed methods for a three-field Biot's consolidation model, IMA J. Numer. Anal. 42 (1) (2022) 620–648.
[11] R.A. Adams, J.J. Fournier, Sobolev Spaces, Vol. 140, Elsevier, 2003.

[12] J. Nečas, Les Méthodes Directes en Théorie des Équations Elliptiques, Masson, Paris, 1967, p. 351.
[13] J.-L.L.E. Magenes, Non-Homogeneous Boundary Value Problems and Applications. Vol. I, Springer-Verlag, New York, 1972, p. xvi+357.
[14] P. Grisvard, Elliptic Problems in Nonsmooth Domains, in: Monographs and Studies in Mathematics, vol. 24, Pitman, Boston, MA, 1985, p. xiv+410.
[15] V. Girault, P.A. Raviart, Finite Element Methods for Navier-Stokes Equations: Theory and Algorithms, in: Springer Series in Computational Mathematics, vol. 5, Springer-Verlag, Berlin, 1986, p. x+374.
[16] P.G. Ciarlet, Basic error estimates for elliptic problems, in: Handbook of Numerical Analysis, Vol. II, North-Holland, Amsterdam, 1991, pp. 17–351.
[17] J. Roberts, J.-M. Thomas, Mixed and hybrid methods, in: Handbook of Numerical Analysis, Vol. II, North-Holland, Amsterdam, 1991, pp. 523–639.
[18] L.R. Scott, S. Zhang, Finite element interpolation of non-smooth functions satisfying boundary conditions, Math. Comp. 54 (1990) 483–493.
[19] G. Alzetta, D. Arndt, W. Bangerth, V. Boddu, B. Brands, D. Davydov, R. Gassmoeller, T. Heister, L. Heltai, K. Kormann, M. Kronbichler, M. Maier, J.-P. Pelteret, B. Turcksin, D. Wells, The `deal.ii` library, version 9.0, J. Numer. Math. 26 (4) (2018) 173–183.
[20] J. Mandel, Consolidation des sols (étude mathématique), Géotechnique 30 (1953) 287–299.
[21] P.J. Phillips, Finite Element Methods in Linear Poroelasticity: Theoretical and Computational Results (Ph.D. thesis), 2005.
[22] Y. Abousleiman, A.D. Cheng, L. Cui, E. Detournay, J. Roegiers, Mandel's problem revisited, Géotechnique 46 (1996) 187–195.